2017-05-24

Inhibiting Axon Degeneration in a Mouse Model of Acute Brain Injury Through Deletion of Sarm1

Nils Henninger
University of Massachusetts Medical School

INHIBITING AXON DEGENERATION IN A MOUSE MODEL OF ACUTE BRAIN INJURY THROUGH DELETION OF SARM1

A Dissertation Presented

By

NILS HENNINGER

Submitted to the Faculty of the
University of Massachusetts Graduate School of Biomedical Sciences, Worcester
in partial fulfillment of the requirements for the degree of

DOCTOR OF PHILOSOPHY

May 24th, 2017

BIOMEDICAL SCIENCES

INHIBITING AXON DEGENERATION IN A MOUSE MODEL OF ACUTE BRAIN INJURY THROUGH DELETION OF SARM1

A Dissertation Presented

By

NILS HENNINGER

This work was undertaken in the Graduate School of Biomedical Sciences

Millennium PhD Program

The signature of the Thesis Advisor signifies validation of Dissertation content.

_____

Robert H. Brown, Jr., M.D., D.Phil., Thesis Advisor

The signatures of the Dissertation Defense Committee signify completion and approval as to style and content of the Dissertation,

_____

Jean A. King, Ph.D., Member of Committee

_____

William J. Schwartz, M.D., Member of Committee

_____

David R. Weaver, Ph.D., Member of Committee

_____

Cenk Ayata, M.D., External Member of Committee

The signature of the Chair of the Committee signifies that the written dissertation meets the requirements of the Dissertation Committee.

_____

Eric H. Baehrecke, Ph.D., Chair of Committee

The signature of the Dean of the Graduate School of Biomedical Sciences signifies that the student has met all graduation requirements of the School.

_____

Anthony Carruthers, Ph.D., Dean of the Graduate School of Biomedical Sciences

May 24, 2017

Dedication

I dedicate this dissertation to my wife Tanja who has been providing me with love, friendship, and support and without whom my life is incomplete.

Acknowledgements

I would like to thank my thesis advisor, Robert H. Brown Jr., for the opportunities and guidance he gave me during the past several years.

I am very grateful to Dr. William “Bill” Schwartz for numerous engaging discussions, his kind and generous support, as well as the gentle, but persistent, guidance he has given me since I started as a junior resident in Neurology.

Thanks to the members of my Research Advisory and Dissertation Exam Committee for advice to improve the quality of my research and this dissertation: Marc R. Freeman, Jean A. King, Eric H. Baehrecke, David R. Weaver, and Cenk Ayata.

I would also like to acknowledge the support of the Millennium PhD Program of the University of Massachusetts. This program provided me with the structure, rigor, peer review, and feedback to facilitate reaching my goals to learn critical skills in axonal biology in the context of mammalian brain trauma.

My thanks also goes to James Bouley for his aid with animal surgery, behavioral testing, and laboratory maintenance, Elif M. Sikoglu and Constance M. Moore for their invaluable assistance with the mouse MRI, Laura Strittmatter for help with histology, as well as Jiyan An and Robert Bowser for their help with plasma neurofilament assays.

This research would also not have been possible without the generous support of the Department of Neurology. This research was in part supported by grant K08-NS091499 from the National Institute of Neurological Disorders and Stroke of the National Institutes of Health.

Abstract

Traumatic brain injury (TBI) is a leading cause of disability worldwide. Annually, 150 to 200/1,000,000 people become disabled as a result of brain trauma. Axonal degeneration is a critical, early event following TBI of all severities but whether axon degeneration is a driver of TBI remains unclear. Molecular pathways underlying the pathology of TBI have not been defined and there is no efficacious treatment for TBI.

Despite this significant societal impact, surprisingly little is known about the molecular mechanisms that actively drive axon degeneration in any context and particularly following TBI. Although severe brain injury may cause immediate disruption of axons (primary axotomy), it is now recognized that the most frequent form of traumatic axonal injury (TAI) is mediated by a cascade of events that ultimately result in secondary axonal disconnection (secondary axotomy) within hours to days.

Proposed mechanisms include immediate post-traumatic cytoskeletal destabilization as a direct result of mechanical breakage of microtubules, as well as catastrophic local calcium dysregulation resulting in microtubule depolymerization, impaired axonal transport, unmitigated accumulation of cargoes, local axonal swelling, and finally disconnection. The portion of the axon that is distal to the axotomy site remains initially morphologically intact. However, it undergoes sudden rapid fragmentation along its full distal length ~72 h after the original axotomy, a process termed Wallerian degeneration.

Remarkably, mice mutant for the Wallerian degeneration slow (Wld^S) protein exhibit ~tenfold (for 2–3 weeks) suppressed Wallerian degeneration. Yet,

pharmacological replication of the Wld^S mechanism has proven difficult. Further, no one has studied whether Wld^S protects from TAI. Lastly, owing to Wld^S presumed gain-of-function and its absence in wild-type animals, direct evidence in support of a putative endogenous axon death signaling pathway is lacking, which is critical to identify original treatment targets and the development of viable therapeutic approaches.

Novel insight into the pathophysiology of Wallerian degeneration was gained by the discovery that mutant *Drosophila* flies lacking *dSarm* (sterile α/Armadillo/Toll-Interleukin receptor homology domain protein) cell-autonomously recapitulated the Wld^S phenotype. The pro-degenerative function of the *dSarm* gene (and its mouse homolog *Sarm1*) is widespread in mammals as shown by *in vitro* protection of superior cervical ganglion, dorsal root ganglion, and cortical neuron axons, as well as remarkable in-vivo long-term survival (>2 weeks) of transected sciatic mouse *Sarm1* null axons. Although the molecular mechanism of function remains to be clarified, its discovery provides direct evidence that *Sarm1* is the first endogenous gene required for Wallerian degeneration, driving a highly conserved genetic axon death program.

The central goals of this thesis were to determine (1) whether post-traumatic axonal integrity is preserved in mice lacking *Sarm1,* and (2) whether loss of *Sarm1* is associated with improved functional outcome after TBI. I show that mice lacking the mouse Toll receptor adaptor *Sarm1* gene demonstrate multiple improved TBI-associated phenotypes after injury in a closed-head mild TBI model. $Sarm1^{-/-}$ mice developed fewer beta amyloid precursor protein (βAPP) aggregates in axons of the corpus callosum after TBI as compared to $Sarm1^{+/+}$ mice. Furthermore, mice lacking *Sarm1* had reduced plasma concentrations of the phosphorylated axonal neurofilament

subunit H, indicating that axonal integrity is maintained after TBI. Strikingly, whereas wild type mice exhibited a number of behavioral deficits after TBI, I observed a strong, early preservation of neurological function in *Sarm1*$^{-/-}$ animals. Finally, using *in vivo* proton magnetic resonance spectroscopy, I found tissue signatures consistent with substantially preserved neuronal energy metabolism in *Sarm1*$^{-/-}$ mice compared to controls immediately following TBI. My results indicate that the *Sarm1*-mediated prodegenerative pathway promotes pathogenesis in TBI and suggest that anti-*Sarm1* therapeutics are a viable approach for preserving neurological function after TBI.

Table of Contents

List of Tables

List of Figures

List of copyrighted Materials Produced by the Author

Portions of this dissertation appear in the following publications and are used with permission from the publisher (Oxford University Press. License numbers 3962070585391, 3962070769892, 3962070867078, and 4037250831064):

Henninger N, Bouley J, Sikoglu EM, An J, Moore CM, King JA, Bowser R, Freeman MR, Brown RH Jr. Attenuated traumatic axonal injury and improved functional outcome after traumatic brain injury in mice lacking *Sarm1*. *Brain*. 2016;139:1094-1105. doi: 10.1093/brain/aww001.

Bouley J, Henninger N. Lateral ventricle attenuates underlying traumatic axonal injury after closed head injury in the mouse. *J. Neurotrauma* 2017. doi: 10.1089/neu.2017.5005. (*epub*)

List of Third Party Copyrighted Material

Figure/Table Number	Publisher	License Number
Figure 1.2	Elsevier	4060981491116.
Figure 1.3	Elsevier	4061550264275.
Figure 4.1	Elsevier	4070370833215.
Table 1.1	Nature Publishing Group	4071400329162.

The following figures were reproduced from journals: No permission required.

Figure Number	Publisher
Figure 1.1	The American Physiological Society
Figure 4.2	eLife Sciences Publications, Ltd

List of Symbols, Abbreviations, or Nomenclature

^{1}H-MRS	proton magnetic resonance spectroscopy
ANOVA	Analysis of variance assessment
ARM	Armadillo/HEAT
ATP	adenosine triphosphate
βAPP	beta amyloid precursor protein
Ca^{2+}	calcium ion
CBF	cerebral blood flow
CCI	controlled cortical impact
CPP	cerebral perfusion pressure
Cre	causes recombination / cyclization recombinase
Cre-ER^{T}	Cre with tamoxifen inducible estrogen receptor ligand-binding domain
CRLB	Cramér-Rao lower bound
CSD	cortical spreading depolarization
CT	computed tomography
CTE	chronic traumatic encephalopathy
DAI	diffuse axonal injury
DAPI	4',6-diamidino-2-phenylindole
DNA	deoxyribonucleic acid
DTI	diffusion tensor imaging
ECL	electrochemiluminescence
EDTA	ethylenediaminetetracetic acid

Floxed	flanked by loxP
FOV	field of view
FPI	fluid-percussion injury
GCS	Glasgow coma scale
GFP	green fluorescent protein
HCO_3-	bicarbonate
iCa^{2+}	ionized calcium
ICP	intracranial pressure
K+	potassium ion
LDF	laser Doppler flowmetry
loxP	locus of X(cross)-over in P1 bacteriophage
MAP	mean arterial blood pressure
MAPK	mitogen-activated protein kinase
MRI	magnetic resonance imaging
Na^+	sodium ion
NAD+	nicotinamide adenine dinucleotide
NMNAT	nicotinamide mononucleotide adenyltransferase
NAMPT	nicotinamide phosphoribosyltransferase
NMDA	N-methyl-D-aspartate
NMN	nicotinamide mononucleotide
NSS	Neurological Severity Score
O_2	oxygen
PaO_2	partial pressure of oxygen in arterial blood

$PaCO_2$	partial pressure of carbon dioxide in arterial blood
PBS	phosphate buffered saline
PCV	packed cell volume
PFA	paraformaldehyde
pNFH	phosphorylated axonal neurofilament subunit H
PRESS	Point-REsolved Spectroscopy Sequence
RARE	Rapid Acquisition with Relaxation Enhancement
RM-ANOVA	repeated measures analysis of variance assessment
ROI	region of interest
rrCBF	relative regional cerebral blood flow
rsfMRI	resting state functional magnetic resonance imaging
SAM	sterile alpha motif
SaO_2	oxygen saturation
SEM	standard error of the mean
dSarm / Sarm1	sterile α/Armadillo/Toll-Interleukin receptor homology domain
tCh	total choline
tNAA	total n-acetylaspartate
TAI	traumatic axonal injury
TBI	traumatic brain injury
TE	echo time
TIR	Toll/interleukin-1 receptor homology
TLR	toll-like receptor
TR	repetition time

TUNEL	terminal deoxynucleotidyl transferase-dUTP nick end labeling
UMMS	University of Massachusetts Medical School
VAPOR	variable power and optimized relaxation delays
Wld^S	Wallerian degeneration slow

Preface

All work described in this thesis was done at the University of Massachusetts Medical School (UMMS) in the laboratory of Dr. Robert H. Brown, Jr.

Dr. Elif M. Sikoglu helped with the experimental setup and data analysis of mouse magnetic resonance spectroscopy.

James Bouley helped with animal surgery, behavioral testing, and animal husbandry.

Dr. Robert Bowser and Jiyan An, (Divisions of Neurology and Neurobiology, Barrow Neurological Institute, Phoenix, AZ) conducted the plasma phosphorylated neurofilament assays.

The UMMS Morphology Core Laboratory provided histotechnological assistance for βAPP immunostaining.

Dr. Lara Strittmatter (Electron Microscopy Core, UMMS) provided microscopy consultation and helped with tissue processing for Toluidine blue staining.

CHAPTER I:

INTRODUCTION

Epidemiology of traumatic brain injury

Traumatic brain injury (TBI) represents a major public health problem affecting more than 10 million people worldwide each year.[1] It is the leading cause of long-term disability among children and young adults in high-income countries and results in a high burden on patients' families and friends.[2] Annually, 150 to 200/1,000,000 people become disabled as a result of brain trauma.[3] According to projections from the World Health Organization a significant rise in TBI incidence is expected by 2020, which is related to a sharp increase in traffic accidents in low- and middle income countries.[4,5] Although TBI-related disability disproportionally affects young individuals due to their greater life expectancy, it is a disease of all ages with a trimodal incidence distribution across age groups.[6] The highest risk is among children aged 0-4 years (1,218 per 100,000) followed by age groups 15-19 years (896 per 100,000), and ≥75 years (932 per 100,000).[6] Across all ages there is male preponderance of TBI incidence with males approximately 1.4 times more likely to sustain a TBI than females.[6]

In the USA, each year approximately 1.7 million people present to emergency rooms after suffering a TBI.[6] Of these more than 300,000 patients require hospital admission, 52,000 of whom ultimately die as a consequence of their TBI and related injuries.[6] It has been estimated that an additional 1.1 million TBI patients seek medical attention in community health clinics and are seen by office based physicians.[7]

Accordingly, almost 3 million TBI patients require medical attention in the USA per year. Although the precise proportion of TBI survivors living with TBI-related disability is unknown, it has been estimated that about 5.3 million people live with long-term or life-long disability after hospitalization for TBI in the USA alone, corresponding to about 1 in 60 people.[8,9] Epidemiological data on TBI indicate an annual cumulative incidence of hospitalized and fatal TBI of approximately 41-600 per 100,000 population with substantial variation between different geographic localities and countries.[2,6,7,9-11] The estimated overall economic burden in the USA is a staggering US$ 60 – 406 billion, whereby the majority of the cost relates to work loss and loss of quality of life.[7,12]

Nevertheless, these estimates do not include the large number of patients who do not seek medical attention after mild TBI, such as after concussions related to recreational activities, household accidents, and after military deployment, which led to the coining of the term ‘silent epidemic’.[10] Approximately 70-90% of all TBIs are considered mild;[2] yet, despite the seemingly mild injury severity a significant subset of these patients suffer residual deficits including cognitive, behavioral, and emotional consequences that adversely affect a person’s ability to perform daily activities and to return to work.[13-17] For this reason mild TBI has been declared a major public health problem by the National Institutes of Health in 1999.[18] Given the high clinical relevance of mild TBI this thesis specifically sought to determine the molecular mechanisms of acute brain trauma using a mild TBI animal model.

Definition and classification of traumatic brain injury

TBI is a highly heterogeneous condition resulting from a variety of injury types and severities. Traditionally, TBI has been classified according to the injury mechanism (closed head, blast, penetrating, crash), clinical severity (e.g., level of consciousness as assessed by the Glasgow coma scale [GCS][19] or presence of additional non-brain injuries as assessed by the Injury Severity Score[20]), structural damage as determined by neuroimaging (e.g., Marshall computed tomography [CT] classification[21] or the Rotterdam CT Score[22]), and prognosis.[23,24]

Closed head injury constitutes the most common TBI mechanism with the leading causes relating to falls and traffic-related injuries.[6] Although penetrating TBI, such as after gunshot wounds and battle field injuries, represents only a small fraction of all TBI it is often devastating and associated with a high mortality rate of 44-100%.[25,26] In recent years, there has been a significant rise in the incidence of blast-related TBI related to changes in modern warfare that has seen an increased use of improvised explosive devices. Although overall mortality has decreased on the battle field through improved protective armor and battle field medical care, it is increasingly recognized that standard body armor does not provide the same protection from blast injuries as from ballistic injury.[27] Long underrecognized, given absent overt tissue damage on standard neuroimaging, it is now appreciated that blast injuries frequently cause unique microscopic brain damage that associates with lasting neurocognitive symptoms.[27]

Irrespective of the injury mechanism it is critical to accurately determine the clinical severity. Probably the most commonly used clinical TBI classification system is the GCS, which has evolved into a universal classification tool for the severity of TBI since its inception more than 4 decades ago.[5,19,28] The GCS assigns a sum score that ranges from 3 (worst) to 15 (best) of the best eye, motor, and verbal response scales.[19] Based on the sum score, TBI severity is graded as mild (14-15), moderate (9-13), and severe (3-8), whereby the GCS cut off for mild TBI is sometimes defined as GCS 13-15.[29] A major advantage of the GCS relates to the fact that it is widely recognized, allows for rapid and reliable patient assessment, has been proven and repeatedly validated for use in various clinical settings, and has additional use for outcome prediction.[30] Nevertheless, it is frequently limited for the assessment of the most severely affected patients given potential confounding of the mental status by medical sedation, paralysis, intoxication, and need for intubation (and thus inability of the patient to provide verbal responses), in the setting of facial injuries (inability to assess eyes) as well as due to its varied inter-rater variability particularly among inexperienced raters.[30] Furthermore, it overproportionally weighs the motor subscale while at the same time not capturing focal deficits:[30] a hemiplegic patient may score fully on the motor GCS as long as he has full use of the unaffected side. Although novel rating scales have been introduced for the assessment of the moderate-to-severe TBI none has gained similar universal acceptance as the GCS to date.[26,30,31] Lastly, available severity scores are heavily biased towards recognizing severe deficits. Although the overwhelming majority of all TBIs in both civilian and military populations are mild in nature, available clinical

severity scales lack the ability to differentiate mild injuries and accurately predict long-term sequelae following mild TBI.[6,32,33]

Assessment of structural brain injury by neuroimaging has the advantage that it is not influenced by clinical confounders of clinical severity rating tools. Given its widespread availability, rapid image acquisition, and absent contraindications, head CT remains the standard diagnostic modality to assess TBI-related hemorrhagic and non-hemorrhagic injuries.[34] The Marshall-CT classification is probably the most frequently used CT classification scheme for the assessment of structural TBI.[21] It considers the degree of brain swelling, mass lesions, and surgical evacuation to classify brain damage into 6 categories.[21] However, the CT-based classification is limited due to the broad differentiation between diffuse injuries and mass lesions and is particularly poor at identifying traumatic axonal injury (so-called “stealth” pathology), which particularly limits its use in mild TBI.[35,36] To overcome the limitations of CT for the assessment of subtle, but clinically important brain injury, various experimental brain magnetic resonance imaging (MRI) techniques have been developed that are highly promising for the detailed evaluation of axonal injury and to improve on outcome predicition such as diffusion tensor imaging (DTI) MRI.[37,38] However, though conventional MRI adds prognostic value with superior discrimination[39] compared to CT,[21,22] it is much less feasible in the early acute phases of trauma related to patient instability for transport and lying flat during the relatively long acquisition time.[39,40] Thus, until MRI, including advanced and highly sensitive techniques such as DTI, becomes a widespread standard modality for acute brain assessment in TBI, CT remains the mainstay of imaging evaluation during the critical acute phases of trauma.

In this dissertation, I probe brain integrity after mild TBI through a combination of behavioral, neuroimaging, cerebral blood flow, and histological assessments to account for the fact that outcome prognostication for this form of TBI remains challenging due to its heterogeneous presentation and pathophysiology that escapes detailed assessment by standard clinical tools that requires the integrative, simultaneous evaluation of multiple injury-related assessment domains.

Pathophysiology of brain trauma

Mechanical loading through sudden impact, acceleration, rotation, or explosive blast generate both localized and distributed forces throughout the brain. Often occurring in combination, these mechanical forces are associated with different injury types to the brain. Localized forces such as through a blunt hit against the head typically contribute to brain injury through deformation of the brain tissue during impact against the rigid skull and cause focal injuries such as brain contusion and hemorrhage near the impact site.[41-43] Focal injuries tend to increase with greater injury severity as they are the consequence of direct impact on the brain that results in tissue compression at the site of impact (*coup*) or the tissue opposite to the impact (*contre-coup*).[44-46]

Conversely, diffuse injuries dominate the neuropathological consequences after mild closed head TBI and explosive blast. The most common diffuse injury types are diffuse vascular and axonal injury that result from blast-induced increased pressure gradients; as well as rapid acceleration, deceleration, and rotation that are associated with diffuse brain tissue deformation and injury due to inertial effects whereby rotational brain acceleration more readily induces injury than isolated linear acceleration.[42,47-49]

As previously discussed, clinically available brain imaging with CT and MRI can readily identify focal brain pathology but has a low sensitivity for detecting diffuse brain injury, which may explain why the extent of detected brain pathology often does not well correlate with clinical outcomes, particularly after milder TBI.[50] Indeed, it is now well understood that diffuse brain injury is associated with widespread disruption of neuronal, axonal, and vascular integrity.[51-56] Injury to the neurovascular compartment

and the interaction between neurons and the vasculature (so called neurovascular unit) leads to disordered regulation of cerebral perfusion, metabolism, and brain function.

Traumatic vascular injury, brain hypoperfusion, and cerebral metabolic dysfunction

Like no other organ the brain relies on a steady state of blood supply for the delivery of oxygen and nutrients (glucose) to meet its high metabolic demands. The degree of brain perfusion is controlled *via* three main mechanisms. *Cerebral autoregulation* allows to maintain a constant cerebral blood flow (CBF) across a wide range of cerebral perfusion pressures. Furthermore, CBF can be adjusted through *cerebral vasoreactivity* in response to altered carbon dioxide levels. Lastly, *neurovascular coupling* is the increase in CBF in response to increased neuronal activity and metabolic demands. While the exact pathophysiology of traumatic cerebral hypoperfusion remains to be elucidated, disruption of each of these mechanisms has been described after TBI and associated with impaired brain function after both experimental and human TBI.[56-64]

Cerebral autoregulation

Pressure induced cerebral autoregulation is typically observed within a cerebral perfusion pressure range of 50 to 150 mmHg.[65,66] Within this range the cerebral vasculature maintains the CBF by dilation and constriction in response to an increased

and reduced systemic arterial blood pressure, respectively.[65,66] The constriction and dilatation occurs primarily in the cerebral arteries, arteriolar vessels, and to a lesser degree in the capillaries with the overall vascular response lagging about 10 seconds from the systemic blood pressure change.[67-69] However, these vessels have only a finite ability to vasoconstrict and vasodilate. Accordingly, CBF begins to decline once cerebral perfusion pressure falls below the lower limit of the autoregulatory range and *vice versa*. TBI of all severities has been shown to impair CBF autoregulation in response to both decreasing and increasing perfusion pressures across all age groups.[64,70-75] In its extreme, when autoregulatory mechanisms are abolished, the CBF linearly follows the cerebral perfusion pressure (CPP) and rapidly leads to cerebral ischemia with decreasing systemic blood pressure. Conversely, when the CPP increases cerebral hyperperfusion results and this leads to increased intracranial pressure. It needs to be emphasized that the autoregulatory perfusion pressure ranges discussed above are variable and also dependent on comorbid conditions. For example, both the lower and upper limits are shifted towards higher levels among individuals with chronic hypertension or in the setting of increased intracranial pressure (right shift of the curve).[76] Accordingly, critical cerebral hypoperfusion may already ensue at higher cerebral perfusion pressures particularly among the elderly who frequently have hypertension and when TBI is complicated by focal mass lesions. For this reason blood pressure monitoring and management needs to be individualized after TBI.[77] Although autoregulatory dysfunction is common after TBI, as many as 10-50% of patients may have preserved autoregulatory function particularly after mild TBI.[78] Conversely, although cerebral autoregulation gradually recovers and typically normalizes by day 14

after TBI,[57,66,77,79] it may remain perturbed long-term and has been related to lasting functional impairment.[80,81]

Cerebrovascular reactivity

Compared to the pressure-induced autoregulatory response, cerebrovascular reactivity to $PaCO_2$ is typically greater indicating that it has a more direct impact on cerebral vessels to dilate and constrict as compared to the CPP.[76,77] The physiological range of $PaCO_2$ is 35–45 mmHg and with each increase in $PaCO_2$ by 1 mmHg up to 5% increase in CBF has been found.[79] An acute decrease in $PaCO_2$ to approximately 25 mmHg (e.g., with hyperventilation) results in cerebral vasoconstriction and a decrease of CBF by 30-35%. Conversely, hypercapnia due to hypoventilation or CO_2-inhalation to a $PaCO_2$ of over 50 mmHg causes cerebrovascular dilatation and increase in CBF by about 75%.[76] However, the cerebrovascular response to $PaCO_2$ attenuates over several hours and baseline CBF levels are reached within about 6 hours despite constantly altered $PaCO_2$.[76] Because changes in the $PaCO_2$ can profoundly affect cerebral perfusion, tight monitoring and maintenance within the physiological range after TBI is required in patients to mitigate the risk for hypoperfusion-associated brain injury with hypocapnia ($PaCO_2$ <35 mmHg). Conversely, hypercapnia ($PaCO_2$ >45 mmHg) needs to be avoided to mitigate the risk for vasodilation-associated cerebral blood volume increases, which can raise the intracranial pressure (ICP) and cause secondary brain damage. Although cerebral autoregulation and cerebrovascular reactivity are both impaired after TBI, the extent of impairment may not correlate and depend on the

severity of brain trauma.[74,77,82] In particular, completely abolished cerebrovascular reactivity has been shown to carry a poor prognosis indicating that cerebrovascular reactivity may serve as a more robust predictor of outcome and aid therapeutic decision making to maintain CBF and perfusion.[74,77,83]

Neurovascular uncoupling

The phenomenon that links transient neuronal (but also glial) activity to a corresponding increase in CBF has been termed neurovascular coupling. It is now understood that the functional hyperemia accompanying neuronal activity is the result of a complex interplay between multiple vasoactive molecules (including ions, metabolic by-products, vasoactive neurotransmitters, and vasoactive factors) that are released in response to neurotransmitters from neurons and glia to act in concert on endothelial cells, pericytes, and smooth muscle cells to result in a highly coordinated adjustment of the CBF.[84] Correspondingly, perturbations of individual aspects of the complex molecular interplay underlying neurovascular coupling have the potential to adversely affect the finely tuned blood flow response to neuronal demand. Several studies have suggested that during trauma-related cerebral hypoperfusion metabolic needs of brain tissue are initially met, but that later neurovascular coupling is lost as evidenced by hyperemia beyond physiological values several hours after TBI.[62,85-89] The clinical importance of neurovascular uncoupling has been highlighted by observations that uncoupling by pharmacological means (i.e., in the absence of brain injury and other circulatory and neuronal changes) induces cognitive deficits in mice.[90] Discussed

underlying mechanisms include mitochondrial dysfunction, impaired local oxygen diffusion into cerebral tissues, vascular microthrombosis, endothelial cell damage, as well as capillary compression due to astrocytic endfeet swelling that leads to functional shunting of oxygenated blood through the capillary bed without efficient extraction of oxygen.[58,61,91]

Cortical spreading depolarizations

A unique cause for profound neurovascular uncoupling after TBI relates to the phenomenon of *cortical spreading depolarization* (CSD). CSDs represent a pathological event that has been consistently described in the cerebral grey matter of animals and patients with TBI and other brain injuries. CSDs were originally discovered and described as *spreading depression* by Aristides A. P. Leão during his thesis research on seizures.[92,93] The CSD phenomenon is highly conserved across species, has been observed in both invertebrates and vertebrates, and can occur in the cortex, striatum, thalamus, cerebellum, brain stem, spinal cord, and retina.[94] Although *spreading depression* can be induced in the healthy brain *via* electrical, chemical, and mechanical stimulation, it has been proposed that the occurrence of a *spreading depression* in the perturbed (e.g., ischemic) brain should be more aptly termed CSD because of differing pathophysiological details such as a prolonged time course, the possibility to occur in compromised brain tissue that is already electrically silent, and, probably most important, its contribution to brain injury.[95]

In the unperturbed brain CSDs are associated with normal neurovascular coupling to neuronal activation albeit with pronounced alterations of electrical, ionic, and metabolic disturbances that can be magnitudes larger than those seen with normal electrophysiological activity in the brain.[94-96] Interestingly, although the electrophysiological features of CSDs are conserved across species and nervous tissues, the associated vascular response differs quite substantially depending on the experimental condition, species, and the vascular bed.[94] Restoration of the ionic gradients after a CSD is in part energy dependent and requires a significant rise in O_2 and glucose consumption that is associated with substantial CBF changes that reflect multiple opposing vasomotor influences at different stages of the CSD wave.[94] The prototypical CBF response in the unperturbed brain consists of four components. Following initial hypoperfusion (component I) a massive peak hyperemia (component II) with 30–250% CBF increase is observed 15-20 s after CSD onset and peaks usually at 1-2 min.[94] Following the initial hyperemia peak a second smaller hyperemia peak (component III) with a 10-50% CBF increase is inconsistently observed 3-5 min later that can last 4-8 min.[94] Finally, prolonged oligemia (component IV) with a CBF reduction by 10-40% below baseline may persist for an hour or longer after a CSD.[94] Figure 1.1 depicts the characteristic CBF response to a CSD on the example of the mouse.

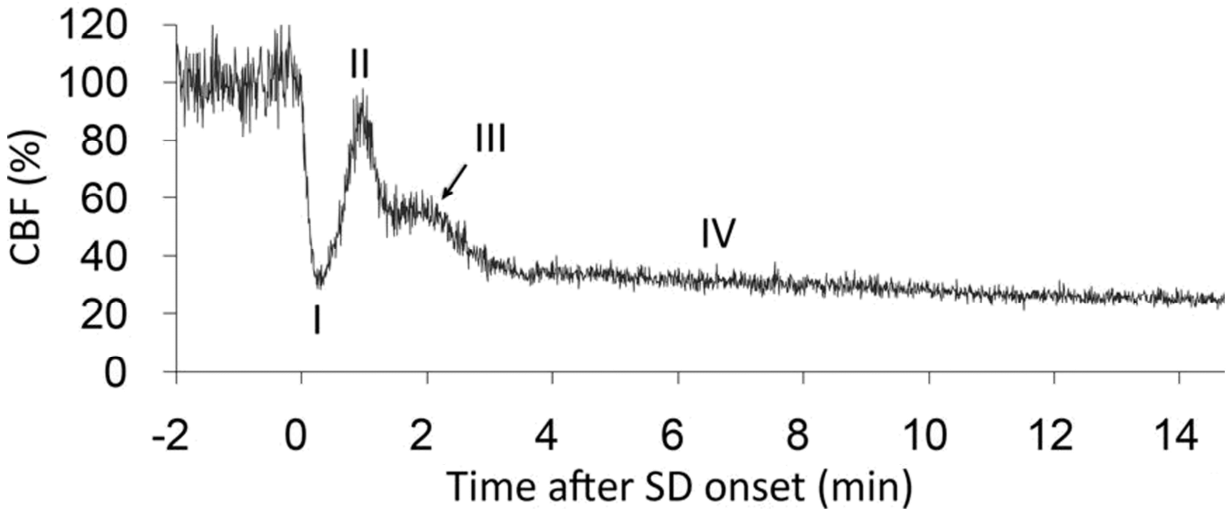

Figure 1.1 Prototypical CBF response after a cortical spreading depolarization (SD). Original laser speckle flowmetry tracing showing the multiphasic cerebral blood flow (CBF) response to a CSD in the cortex of an isoflurane-anesthetized mouse to demonstrate the timing and magnitude of the four prototypical vasomotor components (I–IV) shaping the CBF-response as described in text. From[94] (used with permission).

Because restoration of the massive ionic gradients after a CSD requires energy, CSDs may have deleterious consequences on tissue viability in the injured brain because they aggravate the already tenuous metabolic supply and demand mismatch in the affected tissue.[97-99] Indeed, among severe TBI up to 56% of patients have been shown to have CSDs that are frequently repetitive over hours to days and relate to a poor outcome.[100-103] However, although it is well established that CSDs occur in the setting of catastrophic TBI, their presence and possible contribution to outcome in mild TBI remains uncertain.[104,105]

In summary, TBI is associated with acute, complex, and heterogeneous CBF dysregulation that can lead to profound and long-lasting cerebral hypoperfusion and neurovascular uncoupling, which compounds the adverse effects on brain health and

overall functional outcome after TBI. For this reason it is critical to characterize the CBF dynamics after experimental TBI, which I incorporate in this thesis study.

Traumatic axonal injury represents a pathological hallmark of TBI

Historical perspective of traumatic axonal injury

The most common diffuse injury type, aside from the previously discussed diffuse vascular injury, is *diffuse axonal injury (DAI)*. Originally thought to represent a consequence of traumatic vascular injury-related cerebral hypoxia, ischemia, and brain herniation as well as other non-mechanical factors,[48] it is now recognized that DAI, though associated with vascular injury, occurs independently and as a direct consequence of TBI and constitutes a critical determinant of post-traumatic functional impairment.[48,106-110] Specifically, broad injury to axons within the cerebral white matter is observed following TBI of all severities.[107,111,112]

The term DAI was originally coined to describe the widespread and interspersed axonal injury pattern in clinical TBI. In an attempt to more clearly indicate the traumatic nature of TBI-related axonal injury and because axonal injury after TAI is not exactly diffuse, but rather preferentially involves specific locations within white matter tracts (in particular the corpus callosum, cerebral hemispheres, and brainstem) the term *traumatic axonal injury (TAI)* was subsequently introduced.[35] Because the distinction between DAI and TAI is largely based on historical reasons and TAI is the preferred terminology in reference to axonal injury after experimental TBI (the topic of this work), TAI will be the terminology used in this text.

Widespread white matter injury as a unique consequence of chronic TBI was first described by Rosenblath in 1899.[113] Subsequently, it was recognized that the subtle and widespread traumatic white matter injury represents a unique and important

consequence of chronic TBI.[114-116] From these early studies onward it became increasingly clear that axonal pathology was an early event after TBI that could be identified across a range of injury severities.[117-119] In the early 1980s the now accepted concept of TAI was introduced based on extensive neuropathological characterization of large series of human TBI as well as based on a landmark non-human primate TBI study that established the links between TBI-mechanism, TAI, and functional impairment.[48,54,108,120]

Microscopic findings of TAI

TAI has been assessed using various standard histological techniques including silver staining and hematoxylin & eosin staining techniques to detect axonal swellings or bulbs.[48,108,114-116] However, immunohistochemical methods using antibodies raised against proteins that are concentrated in injured axons, specifically beta amyloid precursor protein (βAPP), have the distinct advantage to identify even subtle TAI both clinically as well as in experimental studies with high sensitivity within minutes after TBI.[111,121-127] Although βAPP staining has some caveats including its non-specificity to TAI, loss of labeling after about 1 week, as well as the availability of various alternative immunohistochemical staining techniques, βAPP-staining remains the gold standard technique for the detection of TAI.[128-135] For this reason βAPP-immunohistology staining was chosen for this study to determine the extent of post-TBI TAI. With this approach it is possible to detect axonal swellings, which refer to a localized axonal distension (“axonal varicosity”) that commonly occurs in a periodic (“beaded”) arrangement along the length of an otherwise intact axon, whereas axonal bulb (“retraction ball”) refers to a

swollen end either proximal or distal to the site of disconnection.[35,136] Although axonal distension is probably the easiest and most characteristic pathological feature of TAI other pathologies including an undulating appearance have been described.[137] These morphological patterns likely indicate different stages of axon injury progression rather than distinct pathological entities.[133,137] Therefore, in this study the presence of any of these histopathological patterns is considered a sign of axonal injury that leads to axonal degeneration.

Mechanism of TAI

In contrast to many other neurological conditions associated with axonal degeneration, TAI has a comparably rapid onset within just a few hours of insult.[127,138] Although severe brain injury may rarely cause immediate disruption of axons (primary axotomy), it is now recognized that the most frequent form of TAI is mediated by a cascade of events that ultimately results in secondary axonal disconnection (secondary axotomy) within hours to days.[111,124,139]

The proposed key pathological mechanism underlying secondary axotomy relates to trauma induced cytoskeletal disruption. Axons are thought to be particularly vulnerable to mechanical forces due to their parallel arrangement within long white matter tracts and their ultrastructural linear organization of microtubules and neurofilaments.[111] Ultrastructural axon cytoskeletal assessment *in vitro* demonstrated periodic breaks of individual microtubules along axons within 2 minutes of axonal stretch injury that corresponded regionally with undulations.[137,140,141] Following this initial phase, axons resume their straight orientation while developing periodically organized

axon swellings over an hour that spatially correspond to the undulations; until they finally disconnect distal to these swellings (i.e., distal to the microtubular breakage site) due to the ensuing transport block for cargoes that causes an unmitigated local cargo accumulation and finally secondary axotomy by axonal membrane rupture.[137,140-142] Support for this hypothesis stems from the observation that application of the microtubule-stabilizing drug paclitaxel mitigates axonal degeneration after stretch injury.[140] This proposed sequence of events is summarized in Figure 1.2.

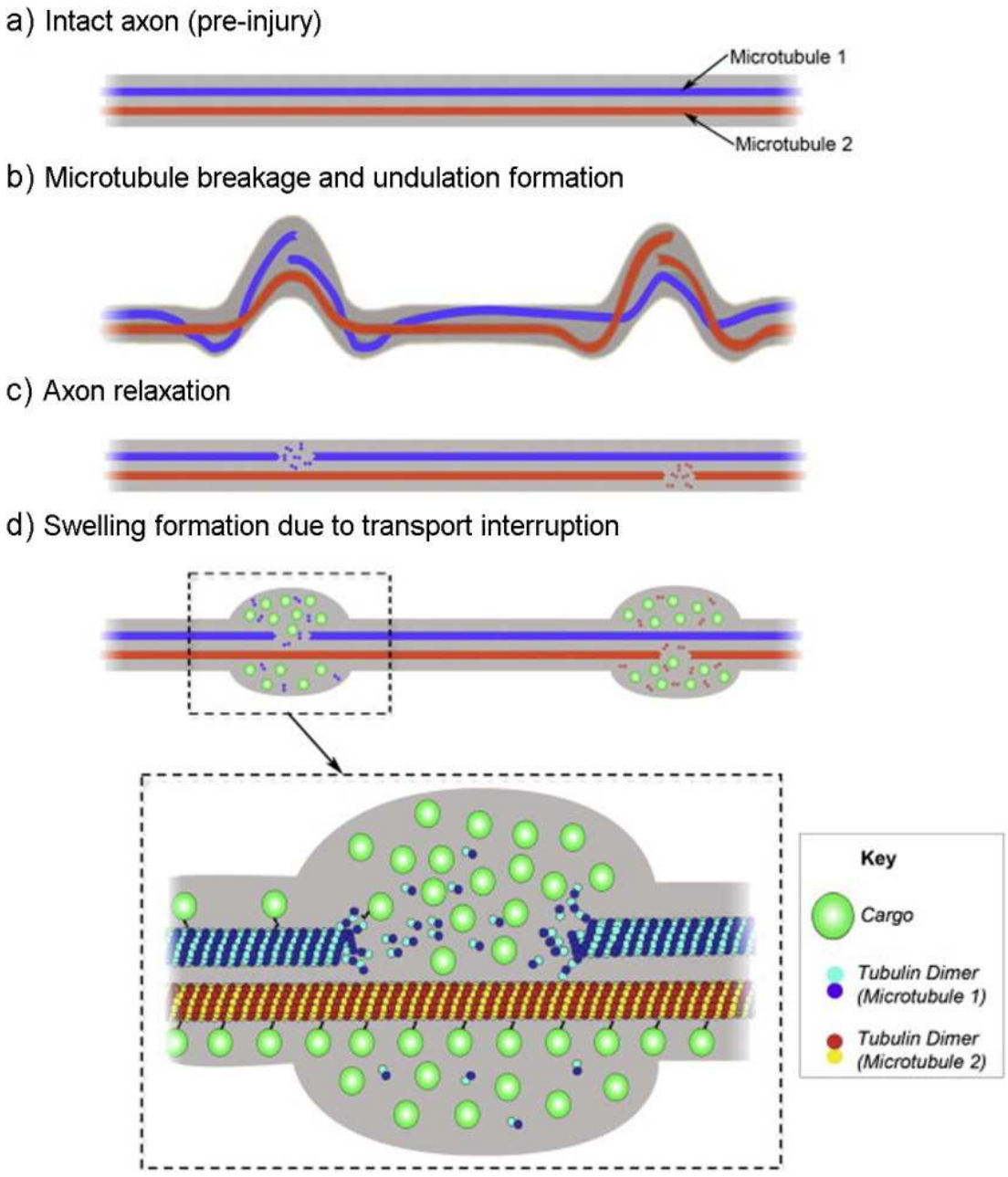

Figure 1.2 Proposed mechanism of varicosity formation after traumatic axonal injury. (a) Illustration displaying two illustrated microtubules within an intact axon (pre-injury). (b) Following injury, mechanical breaking occurs at different sites in microtubules resulting in their misalignment and deformation of the axon observed as two discrete undulations. (c) Shortly afterward, catastrophic depolymerization from the broken ends of the microtubules allows the undulations to collapse and the axon recovers its linear morphology. (d) Microtubule breakage leads to impaired axonal transport, subsequent accumulation of transported cargoes near the microtubule breaking point, likely accounting for the formation of swellings that give axons a varicose appearance following traumatic axonal injury. From[137] (used with permission).

In addition to microtubule disruption, alterations of neurofilaments, which represent a major component of the axonal cytoskeleton,[143] have also been described as an early event after TBI.[144] Specifically, reductions in the interfilament spacing due to altered phosphorylation or proteolysis of side arms (termed neurofilament compaction) has been demonstrated to precede microtubule fracturing.[145-147] Both neurofilament compaction and microtubule disruption represent early events after TBI indicating that cytoskeletal failure is a direct effect of mechanical trauma. While the role of microtubules in cytoskeletal disruption has been well characterized, the precise role of neurofilament protein pathology in TAI remains to be clarified. For example, it has been shown that microtubular breakage and neurofilament compaction do not exactly co-localize within traumatized axons indicating that they represent different aspects of TAI.[137,139-141,148,149] Importantly, serologic detection of microtubule and neurofilament breakdown products has been shown to correlate with the severity of TBI and it is increasingly explored as a non-invasive marker for trauma-related brain injury.[150-154] This study takes advantage of this correlation by using a plasma phosphorylated neurofilament heavy chain (pNFH) assay as a complementary method to serially determine the extent of TAI after mouse TBI.

Although cytoskeletal disruption in response to shearing and torsional mechanical forces is well documented, the precise mechanism by which TBI initiates this process, as well as subsequent secondary axon degeneration, is only incompletely understood. It is thought that local intra-axonal calcium dysregulation plays a central role in post TBI axonal degeneration. This hypothesis is supported by observations of altered calcium ATPase activity and calcium entry into axons after stretch injury.[155-158]

The post-traumatic increase in intra-axonal calcium appears to originate from intracellular stores as well as the trans-axolemmal sodium entry *via* mechanosensitive sodium channels that results in the reversal of the Na^{+}/Ca^{2+} exchanger and opening of voltage-gated calcium channels.[159,160] The primary mechanism by which Ca^{2+} is thought to lead to cytoskeletal breakdown is *via* Ca^{2+}-dependent activation of calpain. This serine-threonine protease is capable of cleaving critical components of the axonal cytoskeleton including neurofilaments and microtubule-associated components such as tubulin and spectrin.[135,161-167] In addition calpain appears responsible for ion channel degradation, which contributes to progressive increases of intra-axonal calcium concentrations.[159,168] Conversely, inhibition of calpain was found to mitigate TAI as well as improve post-traumatic outcome.[164,166,169] Figure 1.3 summarizes the major pathways that lead to cerebral compromise and functional impairment.

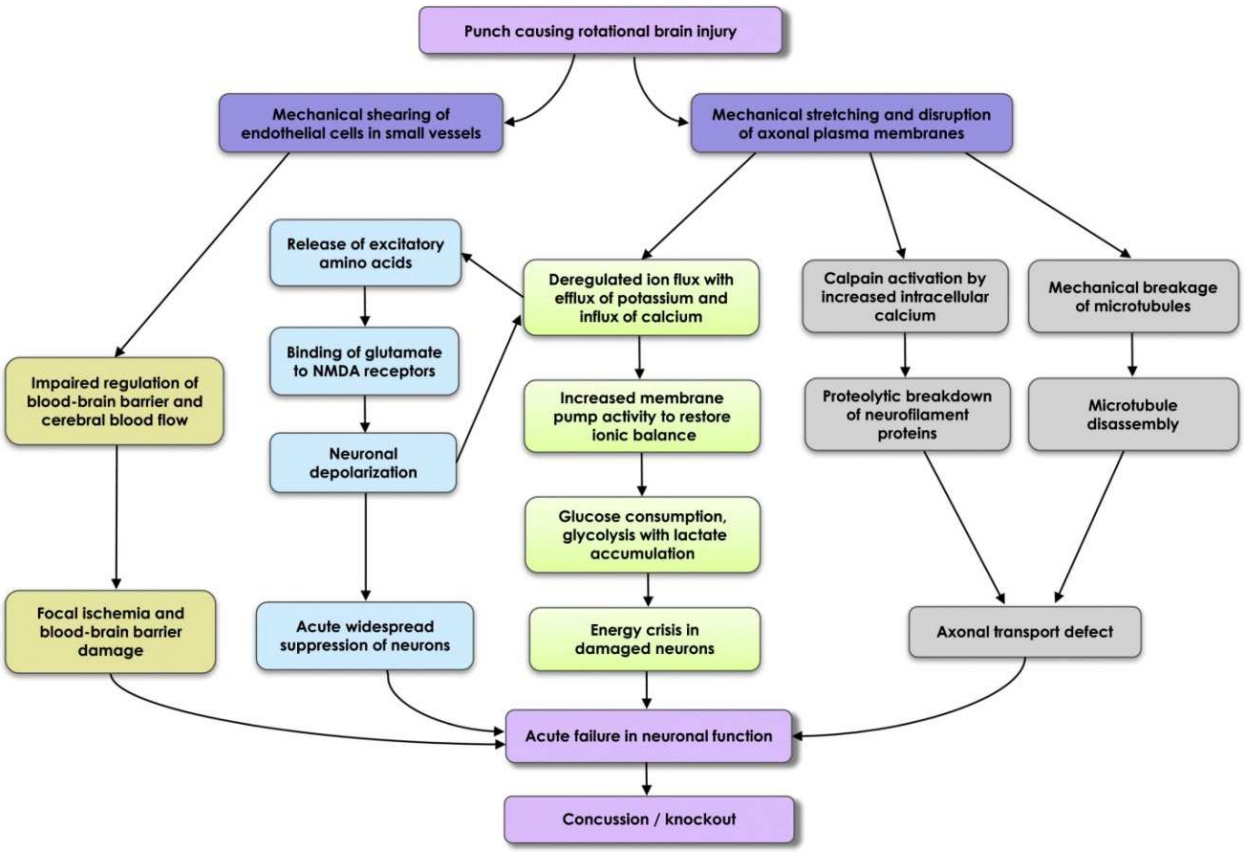

Figure 1.3 Summary flow chart of the major molecular pathophysiological pathways of mild TBI. NMDA indicates N-methyl-D-aspartate. Used with permission from.[46]

Sarm1-mediated Wallerian degeneration after axon injury

Intriguingly, the portion of the axon that is distal to the axotomy site remains initially morphologically intact. However, it undergoes sudden rapid fragmentation along its full distal length after a predictable lag-period of approximately 36-72 hours after the original axotomy.[106,111,170-174] This process has been termed Wallerian degeneration, honoring the British neurophysiologist Augustus Volney Waller who first described delayed distal axon degeneration in nerve transection experiments in 1850.[173] Originally, this process was thought to represent the passive wasting away of the distal axon portion because of its deprivation from a constant supply of nutrients and other molecules from the neuronal cell body. However, this view was fundamentally challenged by the serendipitous discovery of a mouse strain expressing the unique Wallerian degeneration slow (Wld^S) protein, in which the axon distal to the transection site remains morphologically and functionally intact tenfold (for 2–3 weeks) longer than normal.[170,175-177] This remarkable observation raised the possibility that injury-induced axonal degeneration must be controlled by a regulated endogenous and genetically encoded self-destruction pathway.

However, pharmacological replication of the Wld^S mechanism has proven difficult.[170] Further, although improved functional outcome after TBI has been described in Wld^S mice[178] no one has studied whether Wld^S protects from TAI.[179] Lastly, owing to Wld^S presumed gain-of-function and its absence in wild-type animals, direct evidence in support of a putative endogenous axon death signaling pathway has been lacking,[170] which is critical to identify original treatment targets and the development of viable therapeutic approaches.

Novel insight into the pathophysiology of Wallerian degeneration was gained by the discovery that mutant *Drosophila* lacking *dSarm* (sterile α / Armadillo/Toll-Interleukin receptor homology domain protein) cell-autonomously recapitulated the Wld^S phenotype.[180] Furthermore, artificial activation of SARM1 in intact axons induced degeneration[181] indicating that SARM1 is both essential and sufficient for axonal degeneration. The *dSarm* gene (and its mouse homolog *Sarm1*) encodes a protein with an Armadillo/HEAT (ARM) domain, two sterile alpha motifs (SAM), and a Toll/interleukin-1 receptor homology (TIR) domain. Its necessity for degeneration is conserved in mammals as shown by *in-vitro* protection of superior cervical ganglion, dorsal root ganglion, and cortical neuron axons as well as remarkable *in-vivo* long-term survival (>2 weeks) of transected sciatic mouse *Sarm1* null axons.[180] *Sarm1* is highly conserved across phyla.[182] *Sarm1* is enriched in the mouse brain and mutant mice lacking *Sarm1* display a broadly normal neural development, though a reduction in the complexity of neuronal dendritic arborization has been noted.[183-185] The discovery that axons lacking *Sarm1* are protected from injury-induced degeneration provided direct evidence that *Sarm1* is the first defined endogenous gene required for Wallerian degeneration, driving a highly conserved genetic axon death program.[180]

Although it has yet to be confirmed that the SARM1-mediated Wallerian degeneration pathway plays a critical role in trauma-induced axonal injury and degeneration, the data available indicate that the pro-degenerative SARM1 pathway is highly conserved and plays an integral role across different axon injury paradigms and neurological disorders that involve axon loss. Recent studies have shown that genetic depletion of *Sarm*1 prevents chemotherapy-induced peripheral axon degeneration[186] as

well as excitotoxicity-induced degeneration of retinal ganglion cells and their axons.[187] Accordingly, it appears possible that blocking *Sarm1* could attenuate TAI. Since TAI represents the pathological hallmark underlying TBI-induced functional impairment, it seems quite possible that mice lacking SARM1 not only exhibit reduced axonal degeneration but also improved functional outcomes, which forms the central hypothesis of my thesis.

The mouse as a model organism to study traumatic brain injury

Commonly used mouse models of human TBI

Given the heterogeneous nature and high complexity of TBI-related pathology and pathophysiology, no single animal model is capable of mimicking all aspects of human TBI. Accordingly, numerous models have been developed, each possessing distinct advantages and disadvantages.[188-190] Although animal species with larger, gyrencephalic brains may exhibit pathophysiology that more closely resembles that of humans, high cost and ethical considerations restrict their widespread use. In contrast, rodents are particularly advantageous for use in TBI owing to their modest cost, small size, availability of standardized functional outcome measurements, and—specifically with respect to the mouse—availability of many gene mutants and relative ease of genetic manipulation.[183,191]

A particular challenge is the modeling of TBI with TAI, because the rotational acceleration-deceleration forces required to induce axonal damage increase exponentially with decreasing brain sizes; for this reason no single model has been developed that reliably produces this type of injury in rodents without causing additional massive brain hemorrhage and high mortality.[190,192,193] Among the most commonly used mouse TBI models designed for the study of the complex molecular cascades accompanying TAI[188] are the fluid-percussion injury (FPI),[194] controlled cortical impact injury (CCI),[195-198] blast injury,[199-201] and weight-drop injury models.[191,202-208]

Although the FPI and CCI models have been extensively characterized, are highly reproducible, and show a close correlation between injury severity and outcome,

they have the main disadvantage that they require a skull trephination to allow for rapidly striking the exposed dura mater with either a fluid bolus (FPI) or an impactor (CCI).[191,194-198] Blast injury is typically induced by exposing the mouse to an overpressure gas shock wave of defined size, duration, and intensity delivered within a shock tube and has been shown to produce pathology that mimics war-fare related injuries as well as chronic, repetitive brain trauma.[199-201] However, none of these models represents the most common human TBI condition: mild TBI due to blunt, closed head trauma. Therefore, using a model that employs a mechanical impact to the closed skull promises easier translation of results from 'bench to bedside'. The weight-drop injury model fulfills this requirement by using a guided, free-falling weight onto the intact skull.[191] A further advantage relates to the brevity of the required surgical procedure as well as the ability to easily control injury severity through adjustment of the falling weight mass, fall height, and head displacement after impact to produce a reproducible focal brain injury that mimics a wide range of mild human closed head injury pathologies including TAI.[188,191,202-208] In addition, impairment of neurological function that correlates with injury severity has been repeatedly demonstrated.[191,202,205,206,209,210] Lastly, this model can be used to mimic repetitive TBI,[211,212] which provides a critical foundation for future studies investigating mechanisms of neuroaxonal degeneration in the context of repeated TBI, given its purported association with chronic neurodegenerative disorders.[213-216] To take advantage of these unique properties, a closed head mouse mild TBI model is utilized in all trauma studies described in this thesis.

Behavioral assessment after closed head TBI in the mouse

Arguably the most important outcome measure in neurological diseases is behavioral function. The Neurological Severity Score (NSS) is a standardized functional test battery that has been specifically designed to assess motor and other neurobehavioral (dys)function in the closed head mouse TBI model.[191,202,209,210] The NSS is easy to perform, sensitive to TBI-induced functional deficits, objective in interpretation and thus fairly robust against subjective investigator appraisal.[191] Equally important, it has been shown to correlate highly with the severity of TBI-induced brain damage as assessed by histology and brain MRI rendering it suitable for the comparison of functional outcomes with the herein used study methods.[191] The NSS assigns 1 point each for the presence of paresis, failure of the mouse to walk straight, failure to exit a circle within 3 minutes, failure to exhibit a startle response to a loud clap, absent physiological seeking behavior, inability to cross beams of different width (3, 2, and 1 cm, respectively), as well as ability to balance on a 7 mm square and 5 mm round stick, respectively (Table 1.1).[202,210] Accordingly, a score of zero indicates normal function and a score of 10 a maximal deficit. A score of 3-4 at 1-4 hours after TBI is considered consistent with a mild injury and a score of >6 considered a severe injury. Depending on the injury severity, but also the tested mouse strain, animals spontaneously recover until they reach their pre-TBI functional status within approximately 1-7 days.[191,207,210] Finally, given the number of tests and variability between animals and strains, mice may exhibit pre-TBI baseline functional deficits.[191] These potential confounders are considered in this study by serially evaluating animals and including a pre-TBI test session.

Task	Description	Score (success/failure)
Exit circle	Ability and initiative to exit a circle of 30 cm diameter within 3 min	0/1
Paresis	Paresis of upper and/or lower limb of the contralateral side	0/1
Straight walk	Alertness, initiative and motor ability to walk straight	0/1
Startle response	Innate reflex; the mouse will bounce in response to a loud noise clap	0/1
Seeking behavior	Physiological behavior as a sign of 'interest' in the environment	0/1
3 cm beam	Ability to cross a 30-cm long beam of 3 cm width	0/1
2 cm beam	Same task, increased difficulty on a 2-cm wide beam	0/1
1 cm beam	Same task, increased difficulty on a 1-cm wide beam	0/1
7 mm beam	Ability to balance on a beam of 7 mm width for at least 10 s	0/1
5 mm beam	Ability to balance on a round stick of 5 mm diameter for at least 10 s	0/1
Maximal score		**10**

Table 1.1 Neurological severity score. Used with permission from.[191]

Significance of the work in this thesis

In summary, traumatic axonal injury and subsequent Wallerian degeneration of the axon represent key pathological events that relate to functional deficits after TBI of all severities. Although it is now well established that axon degeneration is an active process, the molecular mechanisms driving this process are incompletely understood. Discovery of SARM1 as a prodegenerative molecule driving this process has propelled the field forward as it provided first evidence for an endogenous axon “suicide” pathway.

The central goal of this dissertation is to determine whether the *Sarm1* pathway is critical for trauma-induced axonal degeneration. Specifically, I hypothesize that *Sarm1* deficiency preserves axonal structure and results in improved functional outcome after TBI. To closely mimic the most common form of human TBI I employ a mild closed head brain trauma model.

I first characterize the CBF response to TBI given the reported association between traumatic vascular and axonal injury. I provide evidence that mild TBI causes profound cerebral hypoperfusion that is consistent with CSD and that relates to worse brain tissue integrity and functional outcome. However, I show that *Sarm1* wild type and knockout mice show a similar CBF-response to TBI assuaging concerns that loss of *Sarm1* affects traumatic vascular injury, which could have confounded the main investigation. I demonstrate that *Sarm1* knockout mice have significantly attenuated TAI, improved brain metabolism, and functional outcome providing novel insight into the pathophysiology of TBI by showing for the first time that TAI after TBI is mediated by a

SARM1-associated “programmed axonal death” pathway representing a unique and novel target for TAI therapy.

CHAPTER II:

ACUTE CEREBRAL BLOOD FLOW DYNAMICS AFTER MOUSE TRAUMATIC BRAIN INJURY

Data in this chapter has been presented at the annual National Neurotrauma Society meeting 2016 as:

Bouley J, Henninger N. Association between hyperacute, transient, cerebral blood flow changes and outcome after mild closed head injury in the mouse.

Author contributions: J.B. conducted animal surgery, behavioral testing, histological preparations, and genotyping. N.H. designed the study, conducted animal surgery, laser Doppler measurements, histology analyses, statistical analyses, wrote the abstract, and presented the data.

Summary

Traumatic vascular injury and cerebral hypoperfusion accompany TBI and have been associated with a worse outcome. However, the acute CBF dynamics after mild closed head TBI have not been well characterized and it remains unclear whether observed CBF alterations related to a worse outcome. This study shows that mild TBI induces a siginficant decrease in the CBF immediately following the traumatic impact, which is followed by a progressive decline in CBF to reach a nadir (median 56±5% of baseline values) at 20 min. Subsequently, the CBF recovers to approximately 80% of baseline by 90 min after TBI. When stratified according to the median CBF at 20 min, mice with a CBF below the median showed significantly greater histological tissue injury and worse functional outcome as compared to mice with a CBF remaining above the median. I show that the CBF responses were unrelated to cardiovascular depression as indicated by a stable mean arterial blood pressure throughout the observation period. Careful examination of the temporal and spatial CBF responses to TBI revealed cortical blood flow dynamics that were prototypical for those seen in the wake of CSDs. These results indicate that mild TBI in the used mouse model triggers CSDs in a subset of animals, which is associated with profound, transient depression of CBF, as well as worse histological and functional integrity after TBI. These observations may inform experimental study design and provide novel avenues for outcome prediction and therapeutic intervention.

Introduction

Profound and lasting decreases in CBF have been consistently observed after moderate-to-severe TBI. However, relatively little is known about the association between mild TBI and very early CBF dynamics and how they relate to the degree of brain injury and functional outcome. Specifically, there is a paucity of data regarding the relation of early CBF-changes on outcome. The importance of TBI induced CBF alterations is highlighted by the fact that post traumatic hypoperfusion has been associated with adverse functional outcomes because intact neuronal metabolism relies on a constant, and carefully adjusted, blood supply, which, when disrupted, impairs neuronal function and structural integrity.[56-64]

To gain novel insight into the pathophysiological CBF dynamics after TBI this study sought to determine (i) the temporal and spatial CBF responses to TBI in the immediate post-injury period, as well as their relation to (ii) the mean arterial blood pressure and (iii) the degree of histological and functional outcome in an established mouse TBI model.

The results gained from these experiments will lay the foundation for the studies designed to examine the central thesis goal: to determine whether blocking the axon prodegenerative *Sarm1* pathway attenuates TAI after TBI. This is important because it is unknown whether *Sarm1* wild type and knockout mice have a differential vascular response to trauma, which could confound data interpretation.

Material and Methods

Ethical approval

All procedures were approved by the University of Massachusetts Medical School Institutional Animal Care and Use Committee (Protocol #A-2405-15).

Mice

Spontaneously breathing male C57BL6/J mice (Jackson Laboratories) age 8-12 weeks were subjected to closed head injury (n=38 [n=32 over the ipsilesional and n=6 over the contralesional hemisphere]) or sham injury (n=6) to assess CBF-changes after TBI. A femoral artery catheter was placed in an additional 6 TBI mice to continuously assess the mean arterial blood pressure during the first 60 min after TBI and in 5 mice cortical light transmission was used to determine spatial CBF dynamics after TBI. Mice who had a femoral catheter placed (n=6) were euthanized immediately after the end of the CBF measurements and did not undergo histological assessment.

Anesthesia, analgesia, and TBI induction

Animals were anesthetized with isoflurane (5% for induction, 2% for surgery, 1.5% for maintenance) in room air. Anesthesia was discontinued immediately prior to TBI and sham injury. Body temperature was monitored continuously with a rectal probe and maintained at 37.0 ± 0.5 ℃. To alleviate pain, animals received 0.05 mg/kg

subcutaneous buprenorphine (Patterson Veterinary, Devens, MA, USA) 30 min before the end of anesthesia and every 6 h afterwards for 24 h. Additionally, each animal received 5 mg/kg subcutaneous carprofen (Patterson Veterinary, Devens, MA, USA) at the end of the anesthesia.

Closed head TBI was produced using a weight drop device as previously described in detail and as adapted for use in mice[191,217] with the following modified specifications: Briefly, the skull was exposed, anesthesia discontinued, and the animal positioned on a 6.4 mm thick Ethylene Propylene Diene Monomer (EDPM) rubber surface (60 durometer hardness) with the head placed under the weight drop device. A weight (50 g) was freely dropped 15 cm to strike a cylindrical polyacetal transducer rod (Delrin©, tip-diameter 2 mm, 17.4 g) that was placed with its tip directly on the mouse's skull (-2.4±0.3 mm posterior and 2.6±0.3 mm lateral from Bregma) under the tip at an angle of 90° (Figure 2.1 A-C). Holding the transducer rod with one hand immediately following the initial impact prevented rebound impact. Following TBI, skulls were examined for potential fracture and the wound closed with interrupted sutures. Sham animals were anesthetized, surgically prepared and placed under the impact device, but were not subjected to injury.

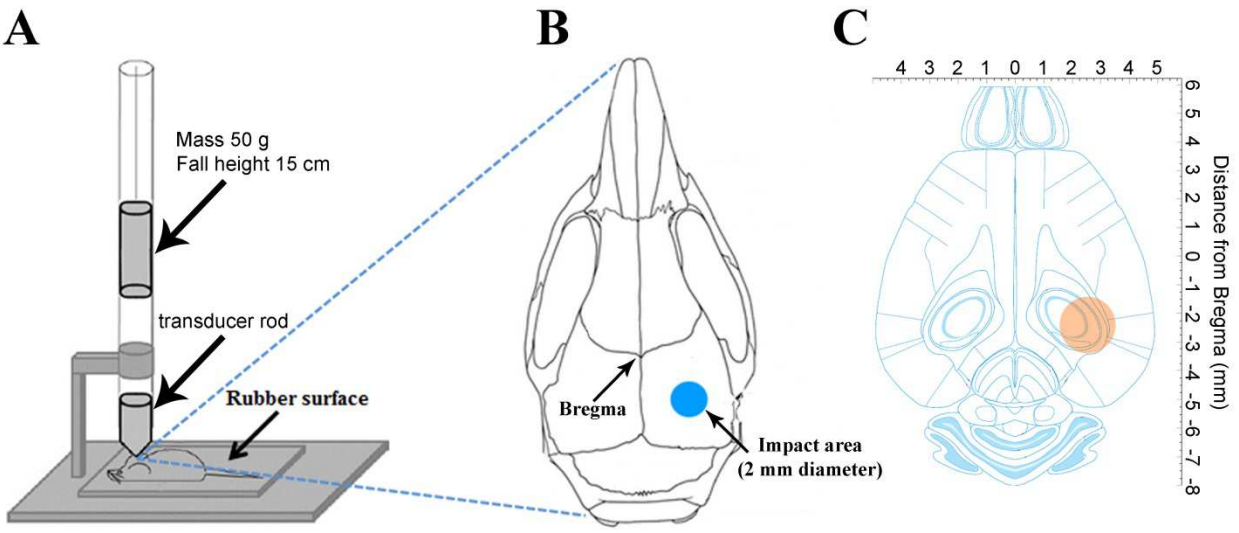

Figure 2.1 Traumatic brain injury setup. (A) Schematic of the impact device (adapted from[208]). (B) Approximate impact center over the intact mouse skull. (C) Impact area (orange) relative to the mouse brain (adapted from [218]). Figure modified from.[219]

CBF measurement

CBF was measured in animals using a PR407-1 straight needle LDF-probe (Perimed, Järfälla, Stockholm, Sweden) connected to a standard laser Doppler monitor (PF5010 LDPM Unit and PF5001 main unit, Perimed, Järfälla, Stockholm, Sweden). The probe was placed over the traumatized hemisphere (approximately 3 mm posterior, 6 mm lateral, and 1 mm ventral to the Bregma) on the intact lateral aspect of the skull to assess CBF (Figure 2.2 A) [220]. A stable baseline was established and recorded for 15 min, TBI was induced, anesthesia resumed following return of regular spontaneous breathing, and relative regional CBF (rrCBF) was continuously assessed for 90 min. For analysis, values were averaged across 1 min epochs at the designated time points (at baseline as well as 1, 5, 10, 15, and 20 min as well as every 10 min afterwards).

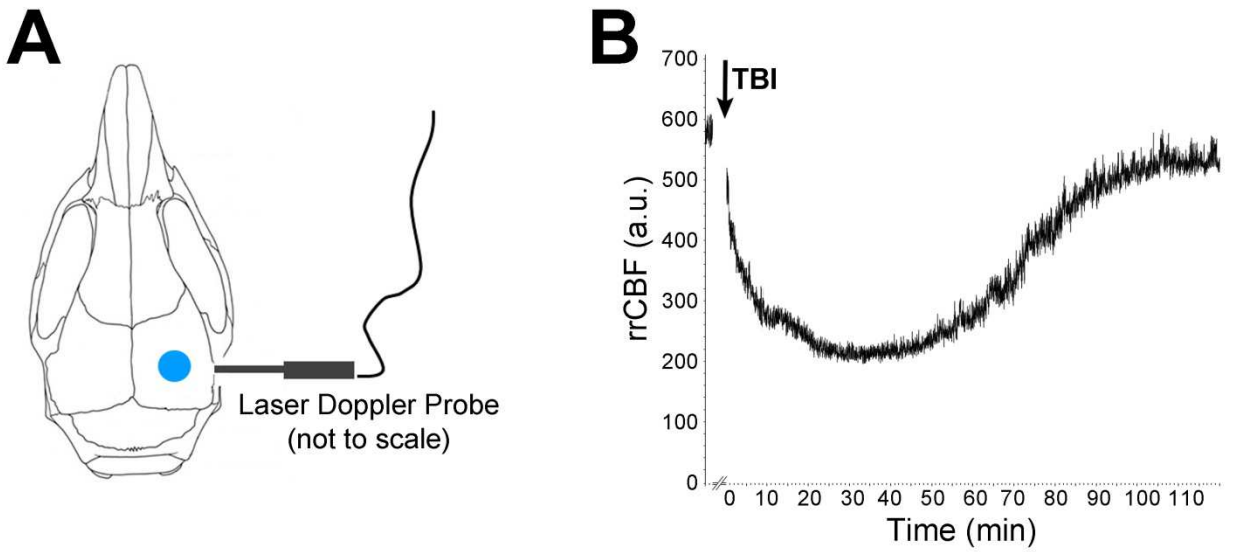

Figure 2.2 Laser Doppler setup. (A) Approximate location of the laser Doppler probe relative to the impact site (blue). (B) Representative relative regional cerebral blood flow (rrCBF) time curve over the right, traumatized hemisphere as assessed by laser Doppler (arbitrary units). Figure modified from.[219]

Cortical light transmission

After midline incision and scalp reflection, the intact skull overlying both hemispheres was covered with a thin layer of mineral oil to prevent drying and enhance transparency. Images were continuously obtained every 2 s from pre-TBI to 30 min post-TBI using a 3.1 megapixel microscope digital camera (Model #300MU-CK, AmScope, Irvine, CA, USA). Raw images (10x; 2048x1536 resolution) were converted off-line to inverted grey-scale (arbitrary units) and by subtracting each image from the subsequent image to highlight temporal changes using Matlab (version R2016a, MathWorks, Natick, MA, USA).

Neurologic evaluation

Presence of seizure activity was evaluated clinically (facial twitching as well as tail, forelimb, and hindlimb tonic-clonic or tonic movements). All seizures occurred while animals were still unconscious. Therefore, no attempt was undertaken to grade seizure severity according to previously developed grading scales as these are partially based on loss of posture in previously conscious animals.[221]

Sternal recumbency was measured as the time (s) from TBI/sham injury to righting from a supine to prone position after discontinuation of anesthesia.

The NSS was assessed prior to TBI as well as at 2 h, 24 h, and 48 h, 7 d, 14 d, 21 d, and 28 d postoperatively as previously described in detail.[191] To account for the fact that with repeat testing animals no longer crossed the beams consistently due to

inactivity, we modified the readout as follows: If a mouse did not cross the 1, 2, or 3 cm beams within the allotted time of 3 min, it was gently nudged once. If the mouse then successfully crossed the beam it was assigned a score of zero. Only if they still did not cross were they assigned a score of one. In addition, mice were tested on all beams irrespective of whether they crossed the next wider beam (e.g., if a mouse did not cross the 3 cm beam but then crossed the 2 and 1 cm beams it was assigned a total of 1 point for these three subtests).

Histological assessment

For histology, animals received an overdose of pentobarbital (150 mg/kg Fatal-Plus, Vortech Pharmaceuticals). Then animals were perfused under isoflurane anesthesia through the ascending aorta with 50 mL saline and then with ice cold phosphate-buffered 4% paraformaldehyde (PFA) for 10 min. Brains were removed from the cranium, postfixed overnight in the same fixative, and then stored in 0.5% PFA at 4℃ until further processing. Prior to paraffin embedding, brains were pre-sectioned using a brain matrix. Histological paraffin sections, 10-µm thick, were obtained from a slice below the impact site and evaluated with immunohistochemistry. All histological analyses were performed by an investigator blinded to the animal groups (N.H.). Immunohistochemistry was performed against βAPP (1:200, CT695, polyclonal rabbit, Zymed, San Francisco, CA, USA) as previously described.[217] Briefly, for antigen retrieval, sections were washed for 5 min with phosphate buffered saline (PBS) and three times for 5 min with 1% PBS + Triton. Endogenous peroxidase was blocked with 0.5% H_2O_2 in PBS and methanol (1:1) for 30 min and sections heated for 20 min in a

600 W-microwave. After incubation in normal swine serum (10%) for 30 min followed by the primary antibody overnight at 4℃, immunoreactivity was visualized by the avidin–biotin complex method (Vectastain, Vector Laboratory Inc.) with consecutive enhanced diaminobenzidine staining. Omitting the primary antisera in a subset of control slides resulted in no immunostaining.

To evaluate axonal injury, the number of βAPP immunopositive axon profiles were quantified within the corpus callosum. To this end all axons that included axonal deposits, swelling, and bulbs were systematically counted in non-overlapping fields of view (FOV) at a magnification of 63x. Counts were conducted in 2 adjacent sections (100 µm apart) from beneath the impact center to obtain the mean number of βAPP immunopositive axonal profiles across the width of the entire corpus callosum. βAPP has been shown to localize almost exclusively to the proximal (but not distal) end of the injured axon and identifies axons that proceed towards complete disconnection and degeneration.[194,222] This property of the βAPP stain has the advantage that it minimizes the risk for multiple counting of the same injured axon and thus overestimation of the degree of axonal injury.

To assess cell death, the *In Situ* Cell Death Detection Kit (Sigma-Aldrich, Billerica, MA, USA) was used following the manufacturer's instructions. Samples were imaged at 10x magnification to quantify the number of terminal deoxynucleotidyl transferase-dUTP nick end labeling (TUNEL) / 4',6-diamidino-2-phenylindole (DAPI) co-stained cells in each section and averaged for both sections to provide the final count. Cell counts were counted separately for the corpus callosum, caudate putamen, and the cerebral cortex.

Statistics

Unless otherwise stated, continuous variables are reported as mean ± SEM and categorical variables are reported as proportions. Normality of data was examined using Shapiro-Wilk test. Between-group comparisons for continuous variables were made with unpaired t-Test, Mann-Whitney U-test, Kruskal Wallis with post-hoc Dunn's method, two-way repeated measures analysis of variance (ANOVA), and two-way ANOVA as appropriate. Categorical variables were compared using the χ^2-test or Fisher exact test as appropriate. Two-sided significance tests were used throughout and a two-sided $P<0.05$ was considered statistically significant. All statistical analyses were performed using SigmaPlot 12.5 (Systat Software, Inc., Germany) or IBM® SPSS® Statistics 22 (IBM®-Armonk, NY).

Results

Cerebral blood flow response to trauma

Figure 2.3 summarizes the temporal evolution of the rrCBF changes observed in sham and TBI animals during the first 90 min after trauma. In sham operated animals rrCBF remained stable over the 90 min observation period. In contrast, there was an immediate, progressive reduction of the rrCBF in the ipsilateral, traumatized hemisphere reaching a nadir of 56±5% of baseline values by 20 min post TBI. Thereafter rrCBF gradually recovered to 81±3% of pre-TBI values by 90 min. Over the contralesional, non-traumatized hemisphere rrCBF also immediately declined after TBI to 75±6% of baseline values by 1 min post TBI, but rapidly recovered to 90±3% of baseline values by 5 min and remained stable afterwards over the remaining observation period.

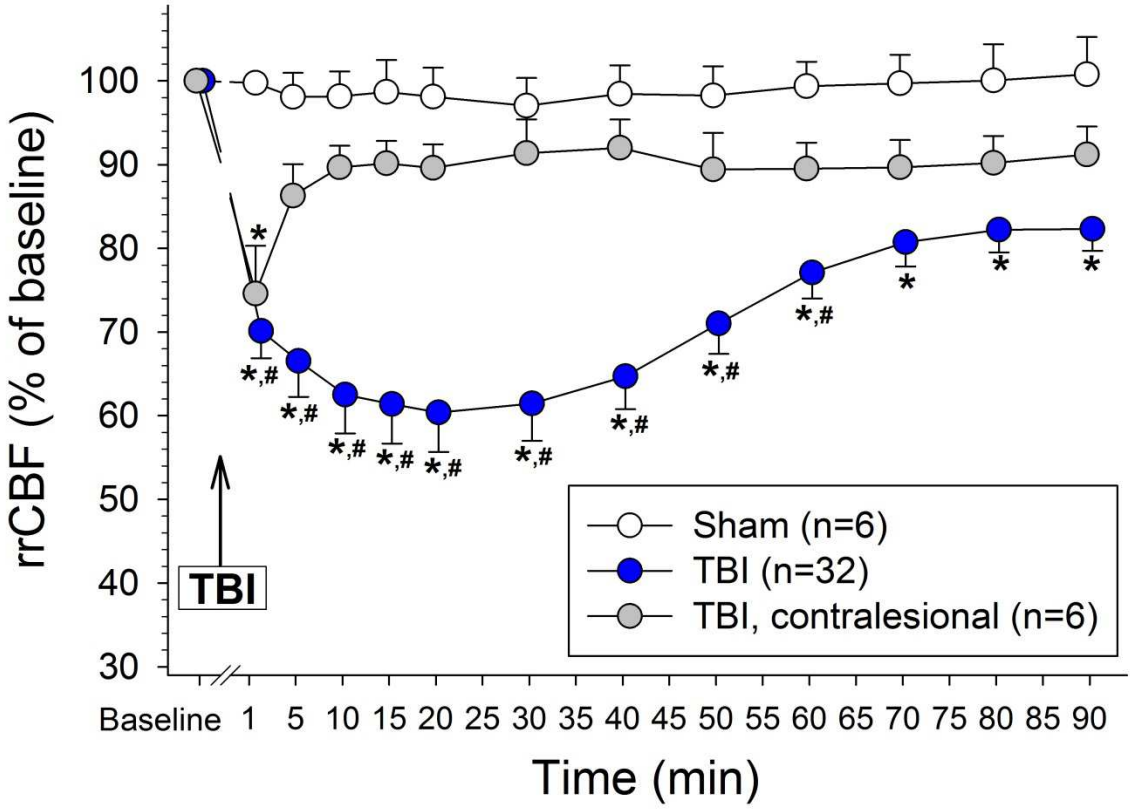

Figure 2.3 CBF responses after TBI. Temporal evolution of the relative regional CBF (rrCBF) in the ipsilesional (blue circles) and contralesional (grey circles) hemisphere after traumatic brain injury (TBI) or sham (open circles) surgery. TBI mice had a significant decrease in the rrCBF immediately following impact with a progressive decline to a nadir (median 56±5%) at 20 min and subsequent recovery to 81±3% by 90 min. rrCBF was relatively less affected in the non-traumatized hemisphere. There were significant group ($P<0.001$) and time ($P<0.001$) effects as well as presence of a significant group x time ($P<0.001$) interaction (*$P<0.05$ for within-group comparisons versus baseline; #$P<0.05$ for between-group comparisons versus sham; two-way RM ANOVA with post-hoc Holm-Šídák test).

Reduced CBF is associated with histological markers of brain injury

Sham animals (n=6) had virtually no TUNEL positive cells. Overall, in TBI mice (n=24) there was a trend towards a greater number of apoptotic cells in the traumatized compared to the non-traumatized hemisphere (P=0.1470). This trend was similar for all investigated regions and only reached significance for the corpus callosum (P=0.0335) but not the caudate putamen (P=0.5538) and cerebral cortex (P=0.2251; Figure 2.4).

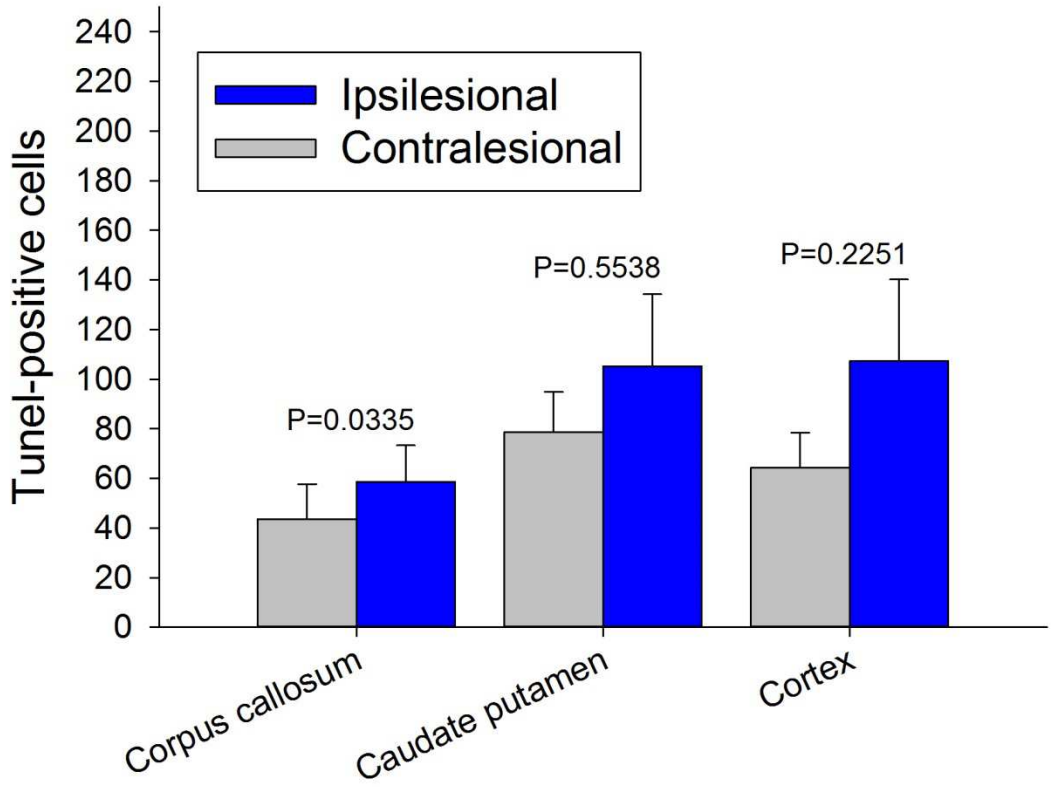

Figure 2.4 Comparison of apoptotic cell death in the ipsi- versus contralesional hemisphere. Quantification of apoptotic cell profiles within the traumatized versus contralesional, non-traumatized (grey) hemisphere at 48 h after TBI (n=24). There were significantly more apoptotic cells in the ipsilesional versus contralesional corpus callosum but not the caudate putamen or cerebral cortex. Sham animals (n=6) had virtually no TUNEL positive cells and data are omitted from the figure for clarity (Mann-Whitney U-test). Cell counts are averages from 2 adjacent sections (100 µm apart) from beneath the impact center.

Strikingly, there was substantial variability in the degree of the ipsilesional CBF reduction during the first 60 min with the CBF ranging from 24.5% to 104.9% of baseline values at 20 min between mice. To determine whether the degree of CBF-reduction relates to the extent of histological brain injury and functional outcome, TBI mice with available ipsilesional CBF measurements were assigned to “low” versus “high” CBF groups based on the median CBF measured over the traumatized hemisphere at the 20 min nadir (56±5% of baseline). Using this stratification scheme, substantial differences in the temporal rrCBF evolution between low and high CBF mice were noted from 1 to 60 min after TBI (Figure 2.5). However, by 70 min rrCBF was similar between subgroups.

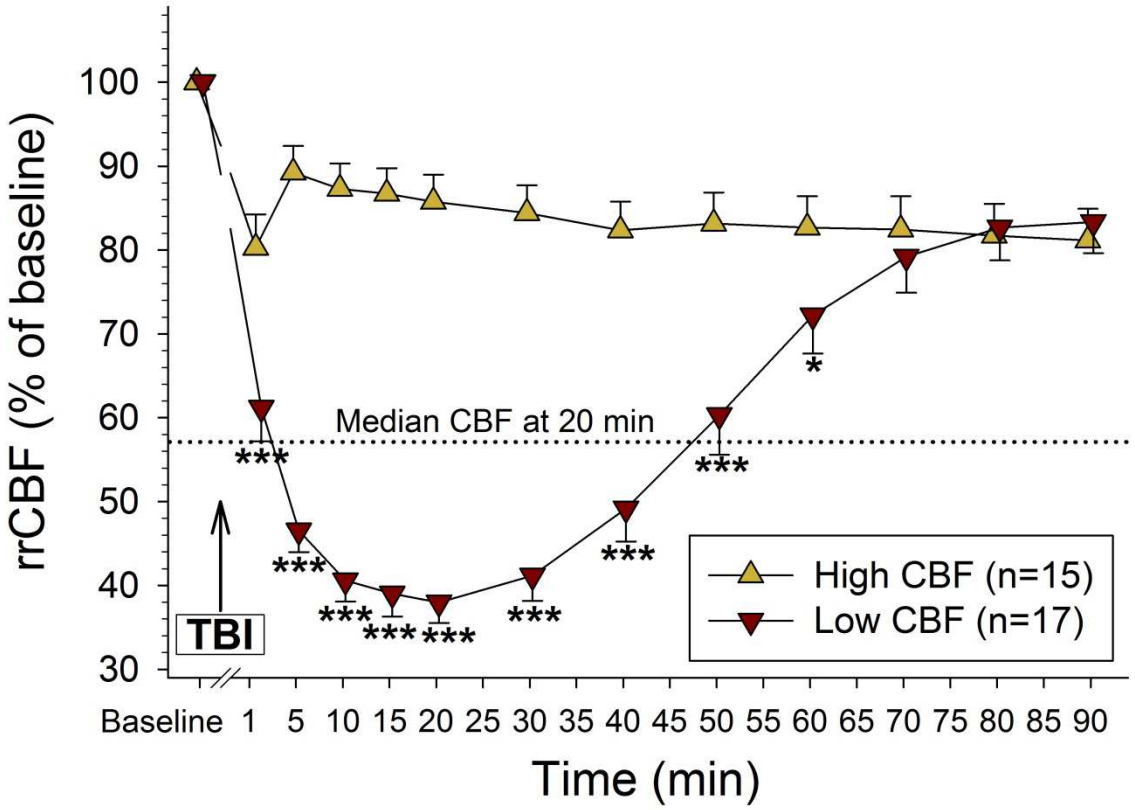

Figure 2.5. Stratification of TBI-related CBF responses to low versus high. Temporal evolution of the relative regional cerebral blood flow (rrCBF) after TBI in mice stratified according to their CBF above (high CBF, yellow triangles) or below (low CBF, red triangles) the 20 min CBF nadir. Despite significant early between-group differences in the hyperacute rrCBF, values in both groups were similar by 70 min post TBI (***P<0.001; *P<0.05 for between-group differences). There were significant group and time effects, as well as presence of a significant group x time interaction (P<0.001, each). In both groups post-TBI values remained significantly below baseline throughout the entire observation period (P<0.05 for each time point). All statistical comparisons were made by RM-ANOVA with post-hoc Holm-Šidák test. Due to movement related artifacts CBF was not recorded at the time of impact.

Histological comparison indicated significantly greater numbers of TUNEL and βAPP positive cell profiles in the traumatized hemisphere in low versus high CBF mice ($P<0.05$ each; Figure 2.6 A-B).

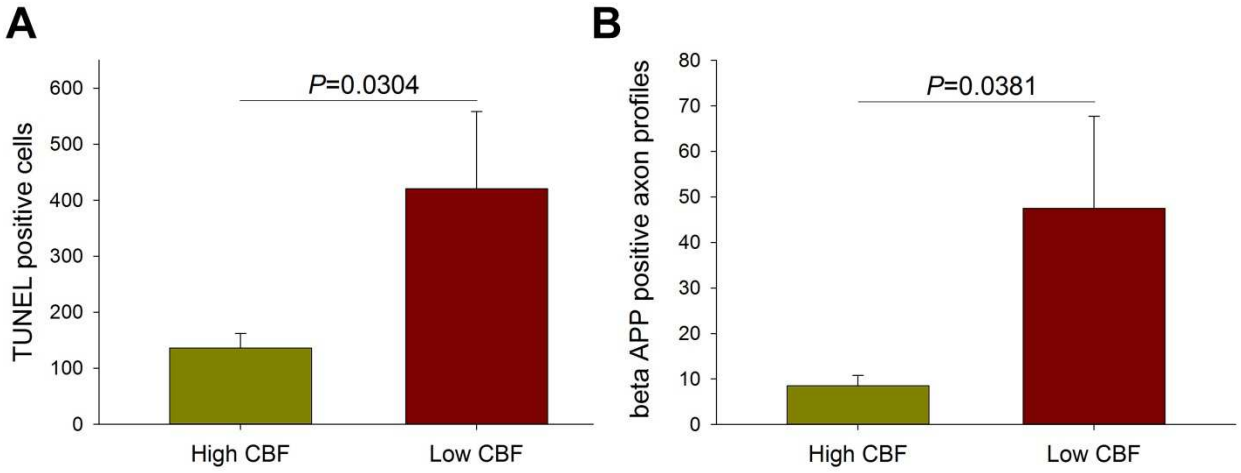

Figure 2.6. Low CBF mice have greater tissue injury. Histological comparison of low (red bars; n=12) with high (yellow bars; n=12) CBF mice 48 h after TBI. High CBF mice had significantly fewer (A) TUNEL and (B) βAPP positive profiles in the injured hemisphere than high CBF mice indicating that lower CBF relates to a greater degree of apoptotic cell death and traumatic axonal injury (Mann-Whitney U test).

Lower CBF relates to worse neurological function

There was no significant difference in the proportion of impact seizures immediately after trauma in low (52.9%; n=9 of 17) versus high (40%; n=6 of 15) CBF mice (P=0.502; Fisher exact test).

Furthermore, there was no difference in the time to regain sternal recumbency after discontinuation of anesthesia at the end of the observation period in low (339±68 s; n=12) versus high (460±75 s; n=12) CBF mice (P=0.964; t-Test).

Neurological function was serially assessed by the NSS. I found that compared to pre-TBI, mice with a lower CBF remained significantly impaired by 48 h post-TBI, whereas mice with a high CBF showed no significant functional deficits by 24 h (Figure 2.7 A). The differences between the two CBF-groups were mainly attributable to worse performance on 7 mm beam balancing, 10 mm beam balancing, startle response, and circle exiting in low CBF mice (Figure 2.7 B-D).

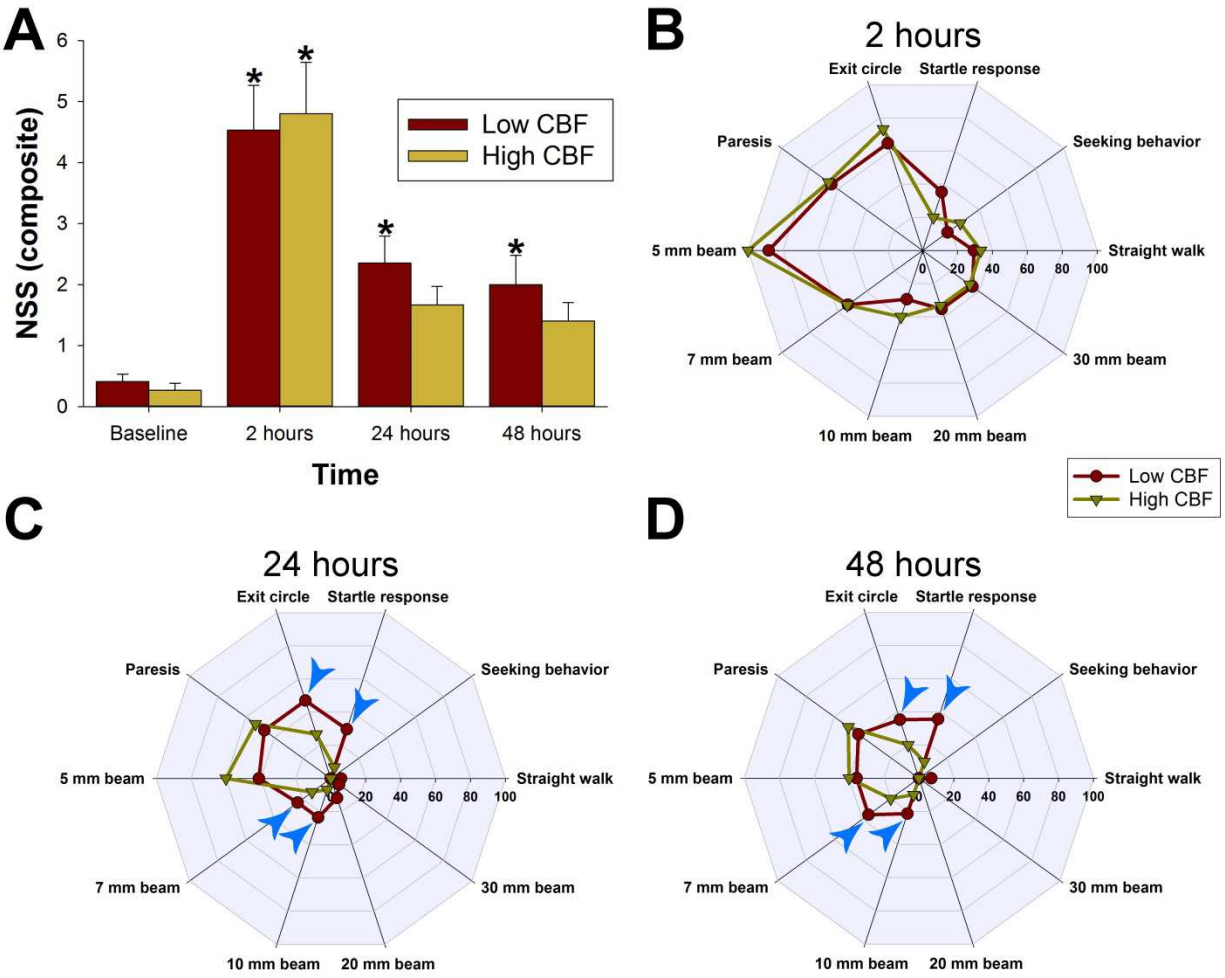

Figure 2.7 Acute CBF responses impact functional outcome. Neurological severity score (NSS) before and after TBI stratified by low versus high CBF. (A) By 24 h after TBI, there was no significant difference in the NSS to pre-TBI values in high CBF mice. Conversely, in low CBF mice a significant difference remained by 48 hours (*P<0.05 versus baseline; two-way RM ANOVA). (B-D) Differences in the NSS between low and high CBF groups at 24 h and 48 h were driven by the subscores derived from the 7 mm beam balancing, 10 mm beam balancing, startle response, and circle exiting (blue arrowheads; two-way RM ANOVA: P<0.05 for between group differences; group x time interaction P=0.0464).

Acute CBF dynamics are consistent with the phenomenon of traumatic CSD

Given the transient and heterogeneous nature of the observed profound cerebral hypoperfusion after TBI, this followup study sought to determine whether the CBF dynamics were related to global cardiovascular depression and systemic hypotension as well as to assess whether the temporal and spatial blood flow dynamics in the cerebral cortex indicate cortical spreading depolarization. By concurrently assessing the mean arterial blood pressure and rrCBF it was noted that there was no significant change in the MAP throughout the observation period (Figure 2.8). In contrast, characteristic rrCBF changes were observed after TBI that closely match the CBF dynamics seen in CSDs indicating the profound CBF alterations occurring in this mouse head injury model are driven by CSDs (Figure 2.8).

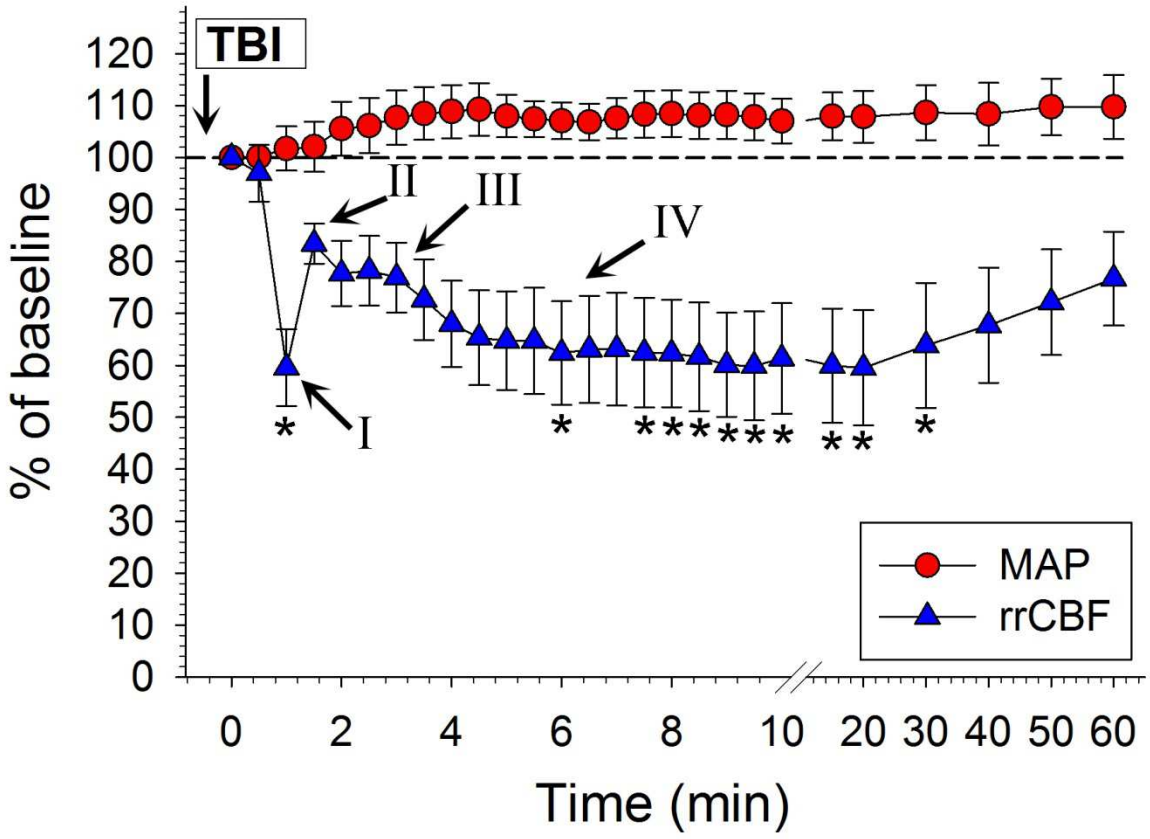

Figure 2.8 Absent association between systemic blood pressure and acute cerebral blood flow. Temporal evolution of the mean arterial blood pressure (MAP) and relative regional cerebral blood flow (rrCBF) during the first 60 min after TBI in 6 mice. There was no significant change in the MAP (red circles) during the study period (one-way RM ANOVA, P=0.08). Conversely, rrCBF (blue triangles) significantly declined by 1 min, partially recovered, and then demonstrated a secondary decline with significantly depressed rrCBF from approximately 6 -30 min after TBI after rrCBF again recovered (*P<0.05 versus baseline; one-way RM ANOVA on Ranks with post hoc Dunnett test). The observed rrCBF dynamics match the prototypical four components (I-IV) observed in the wake of a cortical spreading depolarization elicited in the same mouse strain and under the same anesthetic (compare also with Figure 1.1).[94] Note, rrCBF flow curves were averaged by denoting the time just prior to the initial CBF decline after TBI as “zero” minutes.

To gain further insight into the CBF dynamics after trauma, non-invasive cortical light transmission was used to map the temporospatial evolution of CBF changes, which cannot be achieved with standard LDF due to its low spatial resolution. These experiments revealed the occurrence of a spreading concentric wave of cortical hypoperfusion that coincided with the CBF dynamics as assessed by LDF (Figure 2.9). Conversely, mice without a spreading wave of cortical hypoperfusion after TBI had no significant perturbation of CBF as assessed by LDF.

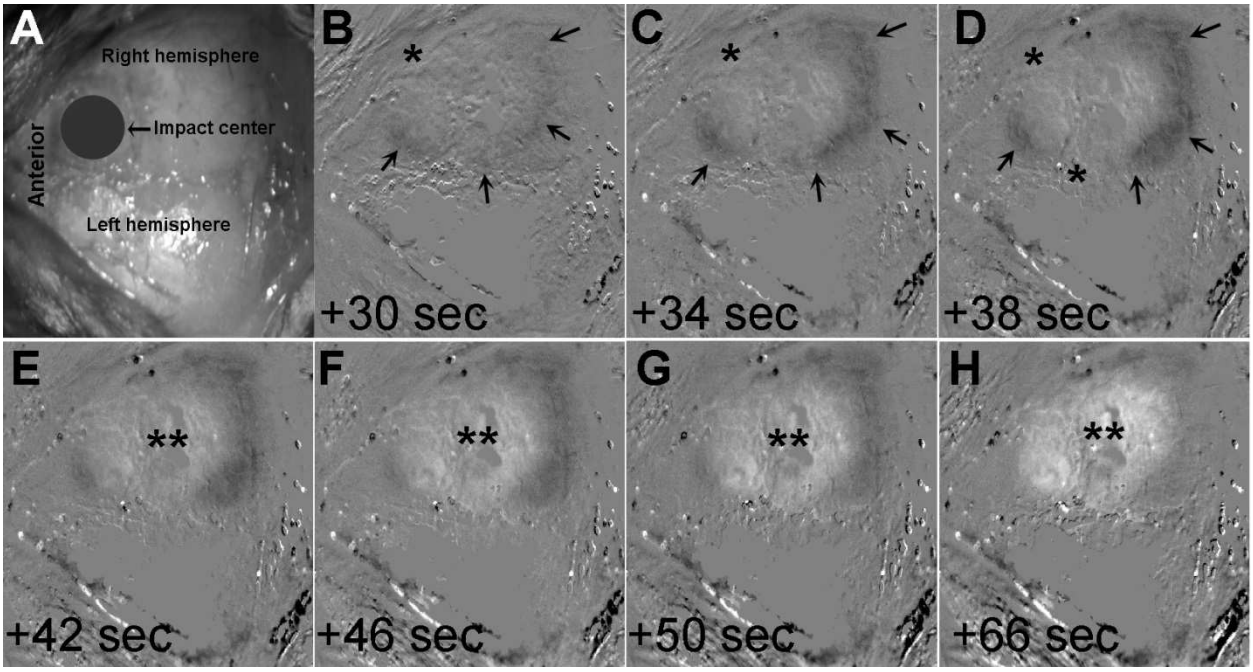

Figure 2.9 Spatiotemporal evolution of post-traumatic cortical hypoperfusion. (A) Representative view of the intact mouse skull after TBI. (B-H) Corresponding time-lapse subtraction images of transilluminated cortical light transmission (intensities inverted) show a spreading concentric wave of an initial increase in light transmittance (i.e., reduction in cortical CBF; arrows) followed by a central decrease in light transmittance (**) consistent with cortical spreading depolarization related CBF dynamics. *indicates the edge of skull at which point the spreading wave moves ventrally out of the field of view. Of note, in this mouse the impact center was located ~3 mm cephalad to the usually used impact location.

Discussion

Although the complex molecular and cellular mechanisms responsible for post-traumatic functional deficits are incompletely understood, there is substantial data indicating that trauma-induced cerebral hypoperfusion underlyies a significant proportion of TBI-related disability.[56-64] Yet, the mechanisms driving traumatic cerebral hypoperfusion, particularly after mild TBI, remain relatively understudied.[223] Several different mechanisms may contribute to CBF depression and associated functional impairment, including impaired cerebral autoregulation, cerebrovascular reactivity, and neurovascular uncoupling.[57,62,66,74,77,79-81,83,85-89]

In this study, I demonstrate profound, transient cerebral hypoperfusion after mild closed head injury as assessed by non-invasive LDF. Consistent with prior studies, I show that worse cerebral hypoperfusion is associated with greater tissue injury and worse functional outcome. Importantly, no significant change in the systemic blood pressure was observed after injury. Furthermore, lasting cerebral hypoperfusion was exclusively noted in the ipsilesional (traumatized) hemisphere, but not in the contralesional (non-traumatized) hemisphere. This rules out significant cardio-respiratory depression as a cause for the CBF alterations as it would have been expected to result in a concomitant blood pressure decline, as well as to affect the entire brain rather than one hemisphere.

Although not specifically assessed, these results further argue against a significant contribution of cerebral dysautoregulation to the observed histological damage and functional impairment. In the setting of impaired autoregulation the CBF

follows the systemic blood pressure and, falling below a critical threshold, leads to cerebral ischemia and brain injury. However, because the blood pressure remained stable within the physiological range, cerebral hypoperfusion as a result of impaired autoregulation (even if present) would not be expected to ensue.

A likely explanation for the noted CBF-responses is the occurrence of CSDs. The herein described temporal and spatial CBF dynamics are highly consistent with the published prototypical CBF responses to CSD.[94] Although CSDs were originally defined based on associated electrophysiological phenomena, assessment of the characteristic spatial and temporal CBF dynamics in response to a CSD are increasingly utilized as accepted surrogate markers for CSDs and to assess related pathophysiology.[97,224-226] In this respect, the presented data may serve as a valid marker for CSD in the used mouse model. Nevertheless, future studies seeking to provide comprehensive insight into the association between traumatic CSDs may benefit from additional assessment of neuronal electrical activity, which represents the foundation of cerebral function.

The minimal volume of brain tissue that needs to be simultaneously depolarized in the rodent brain to elicit a CSD has been estimated to be ~1mm^3 *in vivo*.[227] In the herein used TBI model the impacted cortical brain surface is approximately 3 mm^2. Using the most conservative estimates that only the cortex beneath the impact zone is impacted (which is unlikely due to impact-related skull deformation and strain related energy propagation to cortical tissues beyond the actual impact zone[228,229]) and a cortical thickness of 1 mm,[218,230] a cortical volume of approximately 2 mm^3 is directly impacted in the used model—well above the critical threshold of 1mm^3. Nevertheless, it is interesting to note that only a subset of traumatized mice exhibited CSD-like CBF

changes (~53%; compare Figure 2.5). However, inter- and intra-individual variability in CSD occurrence, propagation, and duration is a well-recognized phenomenon in both animal and human studies.[95,96,226,231-233] The reasons for this are not well understood, but may include differences in the cortical vascular anatomy as well as possible cytoarchitectural differences.[226] In addition, preceding depolarization, anesthetic depth, differences in physiological parameters, baseline CBF, studied species and strain, as well as the cortical location have been shown to modulate CSDs.[94,224,226] Yet, a confounding effect of these factors appear less likely given absent cardiovascular depression, occurrence of only a single CSD, non-invasive surgical approach (assuaging concerns regarding inadvertent CSD-triggering during animal surgery), and identical experimental conditions between studied animals.

The importance of understanding the association between CSDs and TBI is highlighted by the fact that CSDs have been shown to aggravate tissue injury in the setting of acute brain injury including after TBI.[97-103,234] During a CSD, neurons are unable to elicit action potentials because the sustained depolarization remains above the threshold for inactivation of the membrane channels that generate action potentials.[235] In addition to massive ion shifts during a CSD there is an additional massive release of amino acid neurotransmitters including glutamate and aspartate.[95] It has been proposed that CSDs represent a rudimentary form of cell-to-cell signaling; yet, a physiological role is unlikely because they do not originate spontaneously in the healthy brain.[96,236] The release of depolarizing glutamate *via* N-methyl-D-aspartate (NMDA) receptors in conjunction with K^+-release into the extracellular space overloads the extracellular K^+-clearing mechanisms and thus generates depolarization in

neighboring regions that gives rise to a self-propagating depolarization wave front.[94,237,238] Consistent with this hypothesis, tissue susceptibility to CSDs is increased in the setting of chemical or genetic astroglial dysfunction as astroglia have a high K^+-buffering capacity.[239-241] In addition, it is possible that CSDs propagate directly *via* gap-junctional neuron-to-neuron transcellular channels.[96] CSDs typically expand at a speed of 2-5 mm/min over the cerebral cortex and are characterized by near-complete and sustained depolarization of neurons as well as astrocytes causing suppression of synaptic activity (hence the original term *spreading depression*).[95,96,99,101,102,242-245] Because of the substantial metabolic demands to restore homeostasis after a CSD it is not surprising that in the injured brain CSDs are associated with deleterious consequences on tissue viability by aggravating the already tenuous metabolic supply and demand mismatch in the injured brain tissue.[97-99]

In summary, my data closes an important knowledge gap by showing that CSD-related CBF changes are common after mouse TBI. This is an important finding because it (i) provides a pathophysiological rationale for the observed CBF responses, (ii) helps explain possible inter-animal variability with respect to their histological and functional outcome, (iii) and may inform experimental study design. The CSD-related CBF alterations have the potential to confound results despite their transient nature and may be easily missed unless CBF is continuously assessed after TBI. This observation may provide the impetus for human studies to determine whether CSDs occur after mild (concussive) head injury, which could provide novel avenues for outcome prediction and therapeutic intervention.

CHAPTER III:

ATTENUATED TRAUMATIC AXONAL INJURY AND IMPROVED FUNCTIONAL OUTCOME AFTER TRAUMATIC BRAIN INJURY IN MICE LACKING *SARM1*

The following work has been published in the *Brain* article of the same name published as:

Henninger N, Bouley J, Sikoglu EM, An J, Moore CM, King JA, Bowser R, Freeman MR, Brown RH Jr. Attenuated traumatic axonal injury and improved functional outcome after traumatic brain injury in mice lacking *Sarm1*. *Brain*. 2016;139:1094-1105. doi: 10.1093/brain/aww001.

Author contributions: N.H. conducted animal surgery, laser Doppler measurements, ^{1}H-MRS imaging, histology analyses, statistical analyses, and wrote the paper. J.B. conducted animal surgery, behavioral testing, histological preparations, and genotyping. E.M.S. and C.M.M. performed ^{1}H-MRS analysis and were involved in the study design. J.A. and R.B. conducted plasma pNFH quantification. N.H., J.A.K., M.R.F., and R.H.B. were involved in the study design. M.R.F. and R.H.B. contributed equally to this study. All authors discussed the results and commented on the manuscript.

Summary

Axonal degeneration is a critical, early event in many acute and chronic neurological disorders. It has been consistently observed after TBI, but whether axon degeneration is a driver of TBI remains unclear, molecular pathways underlying the pathology of TBI have not been defined, and there is no efficacious treatment for TBI. This study shows that mice lacking the mouse Toll receptor adaptor *Sarm1* gene, a key mediator of Wallerian degeneration, demonstrate multiple improved TBI-associated phenotypes after injury in a closed-head mild TBI model. *Sarm1*$^{-/-}$ mice developed fewer βAPP aggregates in axons of the corpus callosum after TBI as compared to *Sarm1*$^{+/+}$ mice. Furthermore, mice lacking *Sarm1* had reduced plasma concentrations of the phophorylated axonal neurofilament subunit H, indicating that axonal integrity is maintained after TBI. Strikingly, whereas wild type mice exibited a number of behavioral deficits after TBI a strong, early preservation of neurological function in *Sarm1*$^{-/-}$ animals was observed. Finally, using *in vivo* proton magnetic resonance spectroscopy, tissue signatures were found consistent with substantially preserved neuronal energy metabolism in *Sarm1*$^{-/-}$ mice compared to controls immediately following TBI. These results indicate that the *Sarm1*-mediated prodegenerative pathway promotes pathogenesis in TBI and suggest that anti-*Sarm1* therapeutics are a viable approach for preserving neurological function after TBI.

Introduction

It has long been recognized that wide-spread axonal degeneration accompanies TBI of all severities and it is thought to represent a key pathological feature underlying the observed functional deficits in affected patients.[35,106,107,111] However, whether axon degeneration is in fact a driver of pathology and functional loss in TBI has not been directly tested, the molecular pathophysiology promoting axon loss in TBI remains undefined, and there is no efficacious treatment for TBI.[111]

A number of studies suggest that axon degeneration after TBI is similar to that of Wallerian degeneration,[173,174,246,247] which is the catastrophic fragmentation of the distal portion of an axon severed from its cell body.[173,179] Recently, novel insight into Wallerian degeneration and axonal death has been gained by identifying endogenous genes that actively promote axon death. It has previously been shown that Wallerian degeneration of transsected nerves can be suppressed weeks in homozygous mutant mice lacking the *Sarm1* gene.[180] This exciting observation provided a direct target for potential therapeutic intervention during axon degeneration. It also raised the intriguing possibility that *Sarm1*-mediated axon death pathways play a critical role in many neurological conditions associated with axonal degeneration including TBI.[179]

To test this hypothesis, I use a mouse model of mild closed head injury to determine whether loss of *Sarm1* mitigates the histological and behavioral pathophysiology of TBI by promoting axonal integrity. Such a model is highly relevant clinically given epidemiological studies showing that 80% of TBIs are due to blunt, closed head trauma.[6] If true this would indicate (i) that traumatic axonal injury is driven

by molecular pathways similar to those promoting Wallerian degeneration, (ii) that axon degeneration through these pathways is associated with the functional deficits observed after TBI, and (iii) that *Sarm1*-based therapies could represent a viable and novel opportunity for TBI treatment.

Material and Methods

Experimental design

This preclinical study was designed to determine whether *Sarm1* knockout in mice protects from axonal injury and improves outcome after TBI. βAPP immunohistology was performed to determine the spatiotemporal distribution of axonal pathology after TBI. Assays of plasma pNFH concentration were assessed by electrochemiluminescence assay (ECL) to determine axon cytoskeletal breakdown products in peripheral blood as a complementary marker of axonal injury. Neurobehavioral deficits were determined from acute to subacute time points utilizing the NSS, which has been validated to determine neurological sequelae in closed head mouse TBI.[191] Cerebral neurochemical profiling was conducted using proton magnetic resonance spectroscopy (^{1}H-MRS). In addition, parameters shown to influence post-TBI outcome including blood gases and CBF were assessed.[58] For each experiment, G*Power[248,249] was used to calculate sample sizes to achieve a power (1-β) of 0.8 to detect a significant between-group difference at a two-sided significance level of 0.05. All experiments were conducted in a randomized manner and masked to the mouse genotype and experimental group.

Ethical approval

All procedures were approved by the University of Massachusetts Medical School Institutional Animal Care and Use Committee (Protocol #A-2405-12).

Mice

Sarm1$^{+/-}$ males and females on the C57BL6/J (Jackson Laboratories) were bred to obtain age-matched, male *Sarm1*$^{+/+}$ and *Sarm1*$^{-/-}$ littermate mice.[183] All animals were socially housed on 12-h light : 12-h dark lighting with food and water *ad libitum*. In light of prior data indicating lack of protection from Wallerian degeneration in *Sarm1*$^{+/-}$ mice,[180] this study focused examinations on *Sarm1*$^{-/-}$ mice.

Spontaneously breathing mice (n=120) weighing 25.8±2.5 g (age 8-12 weeks) were subjected to closed head injury (n=88) or sham injury (n=32) to assess neurological deficits (all animals), βAPP staining (n=86; of note βAPP staining was repeated at the 48 h time point in a subset of TBI mice [n=7, each] resulting in n=13 for this time point), and plasma pNFH concentrations (n=98). In addition, 32 mice were used for laser Doppler blood flow analyses to avoid confounding of behavioral and neurochemical profiles given the need for prolonged anesthesia. Further, 14 mice were used to determine brain neurochemical profiles *in vivo* using ^{1}H-MRS and 5 mice for axon fiber quantification using Toluidine blue staining and light microscopy.

We excluded 5 *Sarm1*$^{+/+}$ mice (1 had a depressed skull fracture, 1 had traumatic diastasis of cranial sutures; 1 with subdural hematoma; 1 perioperative death; 1 animal moved at impact) and 9 *Sarm1*$^{-/-}$ mice (1 with pre-TBI skull deformation; 5 had traumatic diastasis of cranial sutures; 2 perioperative deaths; 1 animal moved at impact). An additional 4 mice were excluded from the ^{1}H-MRS experiments (see below for details). Figure 3.1 summarizes the time line of key experiments.

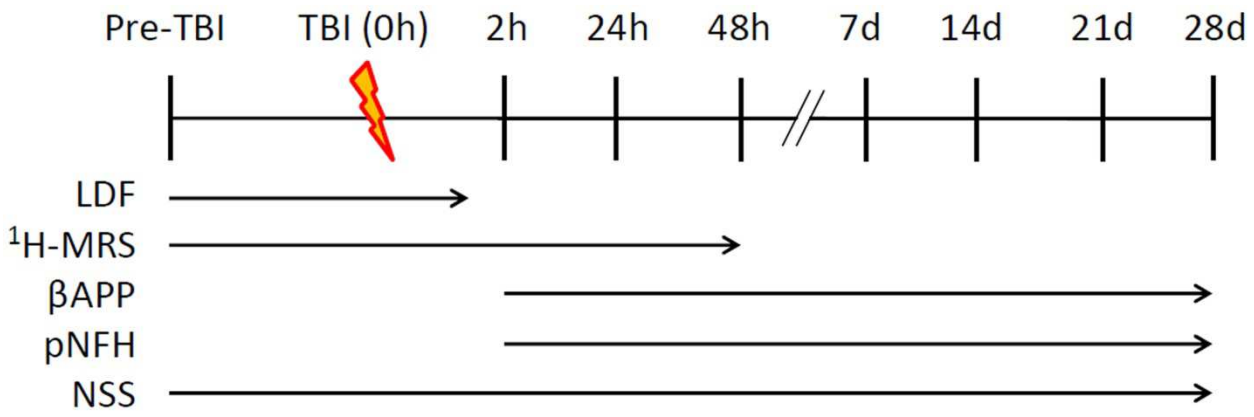

Figure 3.1 Experimental timeline. (LDF=laser Doppler flowmetry; 1H-MRS=proton magnetic resonance spectroscopy; βAPP=beta amyloid precursor protein; pNFH=plasma phosphorylated neurofilament heavy chain; NSS=neurological severity score).

Closed head TBI, cerebral blood flow measurements, neurologic evaluation, and βAPP immunohistochemistry

For details regarding the closed head TBI model, CBF measurements with LDF, details of the immunohistological methods to detect βAPP positive axon profiles, clinical seizure assessment, quantification of the time to regain sternal recumbency, and assessment of the NSS see Chapter II. In this experiment the NSS was assessed prior to TBI as well as at 2 h, 24 h, 48 h, 7 d, 14 d, 21 d, and 28 d postoperatively as previously described in detail.[191]

Anesthesia, analgesia, and TBI induction

Animals were anesthetized with isoflurane (5% for induction, 2% for surgery, 1.5% for maintenance) in room air. Anesthesia was discontinued immediately prior to TBI and sham injury. Body temperature was monitored continuously with a rectal probe and maintained at 37.0 ± 0.5 ℃. To alleviate pain, animals received 0.05 mg/kg subcutaneous buprenorphine (Patterson Veterinary, Devens, MA, USA) 30 min before the end of anesthesia and every 6 h afterwards for 24 h. Additionally, each animal received 5 mg/kg subcutaneous carprofen (Patterson Veterinary, Devens, MA, USA) at the end of the anesthesia.

In a subset of animals (n=12), whole blood (100 µL) was obtained after trauma surgery from the tail artery to measure blood gases (pH, PaO_2, $PaCO_2$, base excess, HCO_3, SaO_2), electrolytes (Na^+, K^+, ionized Ca^{2+}), glucose, hematocrit, and hemoglobin concentration (CG8+ Cartridge; VetScan iStat1; Abaxis, Union City, CA).

Toluidine blue staining, axon fiber quantification, and βAPP immunohistochemistry

Three *Sarm1*$^{+/+}$ and 2 *Sarm1*$^{-/-}$ mice were transcardially perfused with 4% formaldehyde in 0.9% saline. Brains were removed and post-fixed in 2.5% glutaraldehyde in 0.1 M cacodylate buffer, pH 7.2, and left overnight at 4^{o}C. The samples were then rinsed four times (10 min each time) in 0.1 M cacodylate buffer and then post-fixed with 1% Osmium Tetroxide for 1h at room temperature. Samples were

then washed three times with distilled water for 20 minutes each at room temperature and then dehydrated through a graded ethanol series of 20% increments, before two changes in 100% ethanol. Samples were then infiltrated first with two changes of 100% Propylene Oxide and then with a 50%/50% propylene oxide / SPI-Pon 812 resin mixture. The following day three changes of fresh 100% SPI-Pon 812 resin were done before the samples were polymerized at 68^{o}C in flat embedding molds. Finally, 1 µm-thick sections were obtained from 1 mm blocks cut in the mid-saggital plane and from -1.5 mm to -3.5 mm from Bregma, placed on glass slides, and stained with Toluidine Blue.

Analysis of the axon density in the Toluidine blue stained images (magnification 63x; resolution 72 dpi; 8 bit grey scale) was performed using CellProfiler (http://www.cellprofiler.org).[250] Image series were acquired using an oil immersion objective with identical camera settings at constant conditions and were processed using the NIS-Elements analysis software (Version 4.2, Nikon).

In a derivation cohort, all axons within 1 randomly sampled 25x25 µm region of interest (ROI) from each *Sarm1*$^{+/+}$ mouse were manually counted using Photoshop. For derivation, CellProfiler was used to automatically quantify axon profiles by adjusting the settings until the results matched the manual counts both quantitatively as well as qualitatively. Key module settings were as follows: Object size 3 to 20 pixel. Thresholding: adaptive as per Otsu method with two-class thresholding and minimizing of the weighted variance as well as automatic smoothing. Threshold correction factors were 0.0 for the lower and 1.0 for the upper bound. Clumped objects were distinguished based on shape and intensity with automatic smoothing for declumping and calculation

of minimally allowed distance between local maxima. For validation, CellProfiler and manual counts were compared in three separate randomly selected ROIs, indicating 98.9% accuracy of the automatically counted axon profiles. Following this procedure, 5 ROIs for each animal were randomly chosen from 3 adjacent toluidine blue stained sections to quantify axon profiles for a total of 15 ROIs per animal.

Plasma phosphorylated neurofilament heavy chain

Under deep isoflurane anesthesia whole blood (500-800 µL) was collected from the right ventricle into Eppendorf tubes containing 6 µL ethylenediaminetetracetic acid (EDTA). Samples were immediately centrifuged at 3000-g for 15 minutes at 4℃ and the layer containing plasma immediately removed and stored in low bind Eppendorf tubes at −80℃. Plasma pNFH levels were measured using an ECL and a Meso Scale Discovery (MSD, Gaithersburg, MD) SECTOR 2400 Imager. Briefly, MSD 96-well plates were coated overnight with mouse anti-human pNFH antibody (EnCor Biotechnology Inc., Gainesville, FL, USA). Plasma was diluted 1:1 with 0.5M urea and 40 µL added per well for 90 min incubation at room temperature. After washes, 40 µL of sulfo-tagged polyclonal anti-pNFH antibody (EnCor Biotechnology) was added to each well and incubated for 60 min. After final washes, 150 µL 2X Read Buffer (MSD) was added to each well and ECL measured in the SECTOR 2400 Imager. Samples were run in triplicate and each experiment repeated at least twice.

MRI

MRI experiments were performed on a 4.7 T/40 cm horizontal magnet (Oxford, UK) equipped with 450 mT/m magnetic field gradients and interfaced with a Biospec Bruker console (Bruker, Germany). A ^{1}H radiofrequency coil configuration with 23 mm inner diameter was used. Throughout the imaging experiment, mice were anesthetized with isoflurane (1.5%) delivered through a nose cone and custom-fitted with a head restrainer containing a built-in saddle coil. The body temperature of the animal was monitored and maintained at 37 ℃ with a feedback c ontrolled heating pad. For each imaging session, anatomical images were acquired using a multi-slice fast spin-echo sequence (RARE) (repetition time [TR]: 2000 ms, echo time [TE]: 12 ms, RARE factor: 8, matrix size: 256 × 256, FOV: 1.8 cm × 1.8 cm, slice number: 18, slice thickness: 0.7 mm). The ^{1}H-MRS data acquisition was performed using single voxel Point-REsolved Spectroscopy Sequence (PRESS) (TR: 2500 ms, TE: 20 ms, $N_{average}$: 512) with variable power and optimized relaxation delays (VAPOR) sequence for water suppression, following shimming using the FASTMAP sequence. The voxel (3 mm × 3 mm × 3 mm) was placed in the right hemisphere and centered beneath the impact zone of each animal using high-resolution anatomical images. PRESS was run with exactly the same voxel placement and parameters except for water suppression was off and the $N_{average}$ was set to 16. Imaging was conducted immediately prior to TBI as well as at 2 h and 48 h after TBI. The overall imaging time including animal setup and sequence optimization was approximately 1.5 h.

^{1}H-MRS data analysis

The proton spectra were fit using LCModel (Version 6.3-0l), which analyzes *in vivo* proton spectrum as a linear combination of model *in vitro* spectra from individual metabolite solutions (including l-alanine [Ala], aspartate [Asp], creatine [Cr], phosphocreatine [PCr], GABA [γ-Aminobutyric acid], glucose [Glc], glutamine [Gln], glutamate [Glu], glycerophosphocholine [GPC], phosphocholine [PCh], glutathione [GSH], inositol [Ino], l-lactate [Lac], n-acetylaspartate [NAA], n-acetylaspartylglutamate [NAAG], scyllo-inositol [Scyllo], taurine [Tau], total choline [tCh], total n-acetylaspartate [tNAA], total creatine [tCr], glutamate and glutamine [Glx], lipids and macromolecules).[251,252] LCModel utilizes a built-in (simulated) radial basis set for the PRESS sequence we are using and produces absolute fits, metabolite quantifications (in institutional units), and percent standard deviation of the estimated concentration of each metabolite (Cramér-Rao lower bound [CRLB]) as a measure of the reliability of the fit. The spectral inclusion criteria (CRLB) were less than 15% for all metabolites. Values are institutional units and expressed as mean±S.D.

One *Sarm1*$^{-/-}$ mouse died during the first MRI scan and data from an additional 3 mice (2 *Sarm1*$^{+/+}$ and 1 *Sarm1*$^{-/-}$ mouse) were excluded because their metabolite concentrations were more than 2 standard deviations from the mean for their groups.

Statistical analysis

Unless otherwise stated, continuous variables are reported as mean ± S.E.M. and categorical variables are reported as proportions. Normality of data was examined using Shapiro-Wilk test. Between-group comparisons for continuous variables were made with unpaired t-Test, Mann-Whitney U-test, Kruskal Wallis with post-hoc Dunn's method, two-way repeated measures ANOVA, and two-way ANOVA as appropriate. Categorical variables were compared using the χ^2-test or Fisher exact test as appropriate. Two-sided significance tests were used throughout and a two-sided $P<0.05$ was considered statistically significant. All statistical analyses were performed using IBM® SPSS® Statistics 22 (IBM®-Armonk, NY).

Results

To determine whether Sarm1 knockout attenuates axon pathology after TBI, a closed head mouse trauma model was used. The primary outcome of this study was the degree of axonal injury as measured by βAPP immunohistology after TBI. Secondary outcomes were neurobehavioral deficits measured throughout the 4-week observation period using the NSS,[191] pNFH concentration as assessed by ECL assay, and cerebral neurochemical profiling using ^{1}H-MRS. In addition, physiological parameters shown to influence post-TBI outcome including blood gases and CBF were assessed.[58]

Sarm1$^{-/-}$ is associated with long-term suppression of traumatic axonal injury

First, the temporal evolution of axonal pathology was determined by quantifying the number of βAPP positive aggregates (a marker for axonal injury) in axon profiles within the corpus callosum from 2 hours to 4 weeks after TBI. A remarkable reduction of axonal βAPP staining in *Sarm1*$^{-/-}$animals was observed when compared to *Sarm1*$^{+/+}$ mice at 2 h and 48 h after TBI (Figure 3.2 A). Importantly, no increase in βAPP aggregation in axons of *Sarm1*$^{-/-}$ mice was observed between 48 hours and the first 28 days after TBI. This indicates that *Sarm1* loss does not merely delay axonal degeneration, but is associated with long lasting axonal preservation. Next the spatial distribution of axonal βAPP staining was examined within the corpus callosum at the time of maximal axonal injury (48 h). While the distribution of βAPP aggregates across the width of the corpus callosum was similar between groups (i.e., maximal injury was observed beneath the impact zone), a substantial reduction in axonal βAPP staining in

Sarm1$^{-/-}$ versus *Sarm1*$^{+/+}$ mice was noted (Figure 3.2 B and D). Importantly, when the number of axons within the uninjured corpus callosum of sham operated *Sarm1*$^{+/+}$ and *Sarm1*$^{-/-}$ mice was quantified no significant difference was observed between groups in the number of axons (Figure 3.2 E and F). Therefore, the reduction in βAPP-positive axon profiles in *Sarm1*$^{-/-}$ mice was not biased by differences in baseline axon density within the corpus callosum in germ-line knockout mice. Together these data demonstrate that loss of *Sarm1* is associated with suppressed axon pathology after TBI and long-lasting effects on axonal preservation.

Sarm1$^{-/-}$ is associated with reduced plasma concentrations of the axon injury marker pNFH

TBI-related axon injury results in the release of pNFH into the plasma. In a rat model of cortical impact, levels of pNFH increased and peaked in the plasma within 48 h after injury.[152] Time dependent increased levels of plasma pNFH have also been correlated to the extent of axonal injury and patient outcomes from mild TBI.[253,254] Therefore plasma pNFH concentrations were quantified in this study as an additional marker of axonal injury after TBI in *Sarm1*$^{-/-}$ animals and controls using an ECL. In this study the plasma pNFH concentration peaked in wild type mice within 48 h post injury, similar to prior reports.[152] However, *Sarm1*$^{-/-}$ mice exhibited no statistically significant increase in pNFH in the plasma post-injury (Figure 3.2 C). As with the studies of βAPP, this suppression of pNFH release was sustained, lasting for 28 days after TBI.

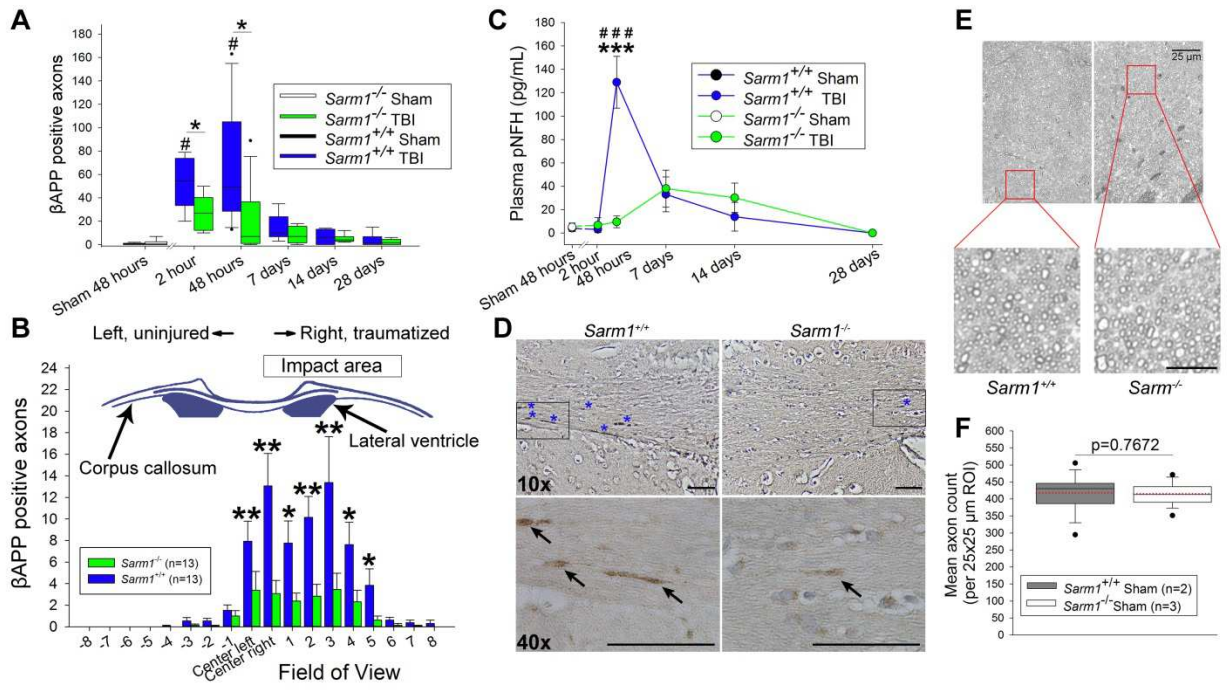

Figure 3.2 Suppressed axon pathology after TBI in mice lacking *Sarm1*. (A) Temporal evolution of traumatic axonal injury as assessed by βAPP-staining in the corpus callosum (n=6 for all time points except 48 h TBI with n=13, each; two-way ANOVA) Overall, there were significant group (P=0.013) and time (P<0.001) effects as well as presence of a significant group x time (P=0.011) interaction (#P<0.01 versus *Sarm1*$^{+/+}$ Sham; *P<0.05, **P<0.01, ***P<0.001 for between-group differences). (B) Spatial distribution of βAPP-stained axons within the corpus callosum 48 h after TBI (two-way RM ANOVA). Overall, there were significant differences in the counts of βAPP-stained axons between groups (P=0.008), the left-to-right distribution across the corpus callosum (P<0.001), as well as significant group x distribution (P<0.001) interaction (*P<0.05, **P<0.01 for between-group differences). (C) *Sarm1*$^{+/+}$ mice had significantly earlier and higher peak phosphorylated neurofilament heavy chain (pNFH) concentrations as compared to *Sarm1*$^{-/-}$ mice (two-way ANOVA; n=8-9 per group, n=6 for 28 d *Sarm1*$^{-/-}$). There were significant group (P=0.016) and time (P<0.001) effects as well as presence of a significant group x time (P<0.001) interaction (***P<0.001 for between group difference at 48 h; $^{###}$P<0.001 for *Sarm1*$^{+/+}$ Sham versus *Sarm1*$^{+/+}$ TBI at 48 h). (D) Representative βAPP-stained sections from the corpus callosum showing βAPP-positive axons in the field of view corresponding to "center right" in panel B at low power (asterisks) and higher power (black arrows) magnification. Bars represent 100 μm. (E) Representative toluidine blue stained transection of the corpus callosum of uninjured *Sarm1*$^{+/+}$ and *Sarm1*$^{-/-}$ mice (bar at high power magnification represents 10 μm). (F) Quantification of callosal axons in the mid-sagittal plane indicated no significant difference in the number of axons between *Sarm1*$^{+/+}$ and *Sarm1*$^{-/-}$ mice (Mann-Whitney U test). For clarity in the figure only significant results are indicated in panels A-C.

Improved functional phenotype in *Sarm1*$^{-/-}$ mice after TBI

Given the significant axonal preservation observed in *Sarm1*$^{-/-}$ mice, this study explored the possibility that blockade of *Sarm1* signaling might also suppress neurological defects associated with TBI. Therefore it was investigated whether loss of *Sarm1* was associated with improved functional outcome after TBI by subjecting animals to the NSS: a battery of behavioral tests specifically developed to assess motor and neurobehavioral outcome in mice subjected to closed head TBI.[191] The NSS is a composite of ratings measuring a combination of overall inquisitiveness, postural stability, and motor function. The NSS is highly correlated with the severity of brain damage; a score of 10 points represents maximal neurological impairment and 0 is normal.[191] Remarkably, when compared to controls, *Sarm1*$^{-/-}$ mice had significantly attenuated neurological deficits as early as 2 h after TBI (Figure 3.3 A). When the temporal evolution of functional deficits was examined, *Sarm1*$^{+/+}$ mice were found to recover approximately 1 week after TBI whereas *Sarm1*$^{-/-}$ animals displayed reduced functional performance only 24 h post-TBI (Figure 3.3 A). Analysis of the individual NSS components revealed that *Sarm1*$^{-/-}$ was associated with improved outcomes across key functional domains tested by the NSS, including more frequent circle exiting at 48 h ($P=0.026$, not shown) and improved straight walk at 2 h ($P=0.044$, not shown), but not startle response and seeking behavior ($P>0.05$ for each time point). More importantly, *Sarm1*$^{-/-}$ mice had less focal paresis (Figure 3.3 B) and improved postural instability as shown by improved balance beam testing across all beam sizes at 2 h post-TBI ($P<0.05$ each; Figure 3.3 C-D summarizes the results for the 5, 7, and 10 mm beams). This is notable since postural instability is a commonly observed sequela of closed head TBI,

highlighting the potential clinical relevance of the observations with *Sarm1*$^{-/-}$ animals in this study.[255] Notably, the recovery time from anesthesia (defined as the time to spontaneously right from a supine to prone position after discontinuation of anesthesia) was similar between *Sarm1*$^{+/+}$ and *Sarm1*$^{-/-}$ groups subjected to TBI versus sham injury (Figure 3.3 F). This observation indicates that anesthetic effects are unlikely to have contributed to the observed between-group differences in the NSS. Finally, there was no significant difference in the incidence of impact seizures between TBI groups ($P>0.05$) and no sham injured animals exhibited seizure activity (Figure 3.3 G).

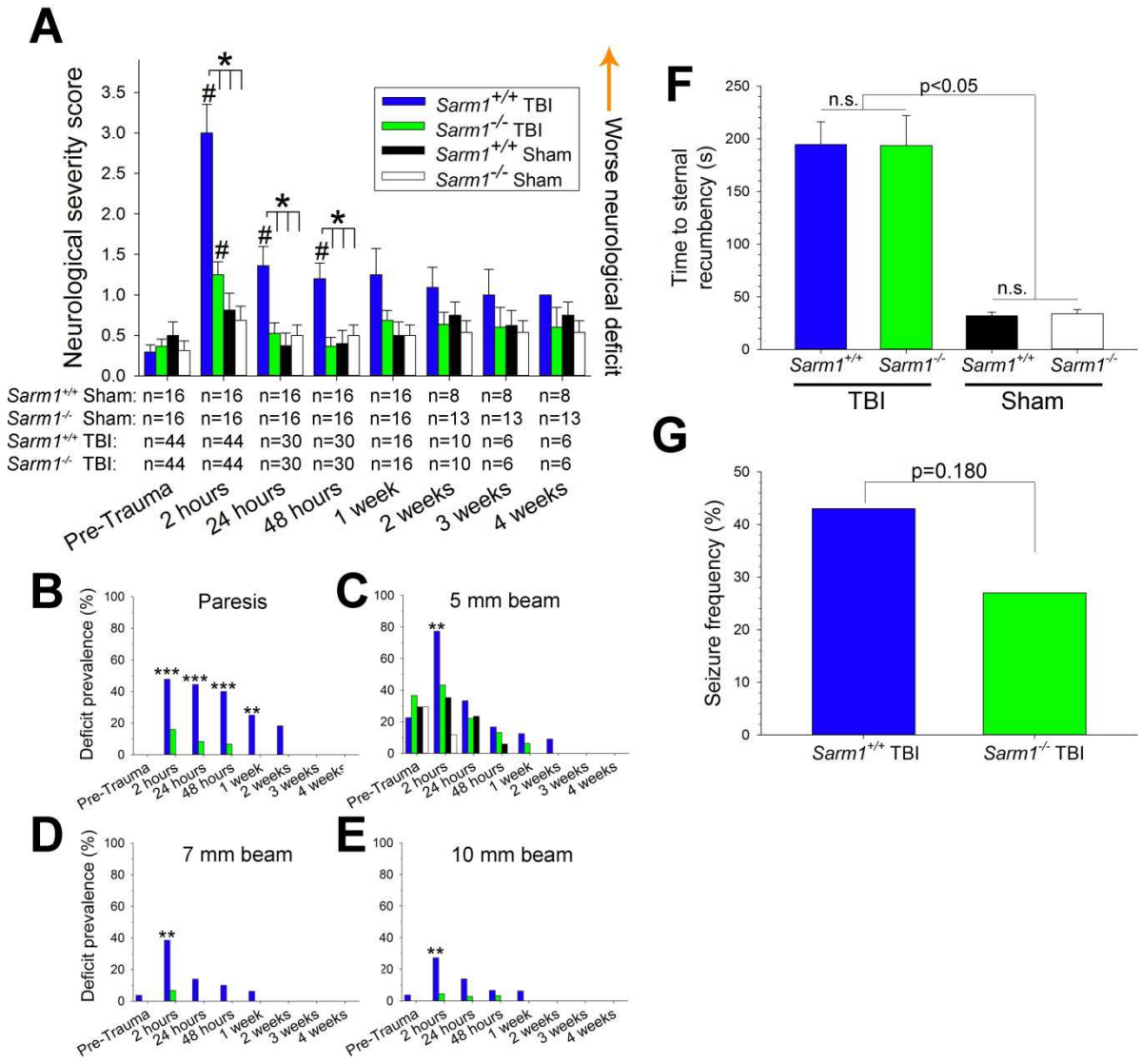

Figure 3.3 Attenuated TBI-induced behavioral deficits in *Sarm1*$^{-/-}$ mice. (A) Composite neurological severity score (NSS; $^{\#}$P<0.05 versus pre-Trauma; *P<0.05 versus *Sarm1*$^{+/+}$ TBI; two-way ANOVA). Overall, there were significant group and time effects as well as presence of a significant group x time interaction (P<0.001, each). (B-E) Temporal evolution of the deficit prevalence in select individual functional components assessed by the NSS (***P<0.001, **P<0.01, *P<0.05 for *Sarm1*$^{+/+}$ TBI versus *Sarm1*$^{-/-}$ TBI mice; χ^2-test with post-hoc Bonferroni correction; for n per group and time point refer to panel A). (F) Similar time to regain sternal recumbency after discontinuation of anesthesia in *Sarm1*$^{+/+}$ and *Sarm1*$^{-/-}$ mice subjected to TBI and sham injury, respectively (ANOVA on ranks with post-hoc Dunn's; n=44 for TBI groups and n=16 for sham injury groups). (G) There was no difference in the incidence of impact seizures between *Sarm1*$^{+/+}$ and *Sarm1*$^{-/-}$ TBI mice (χ^2-test; n=44 for TBI groups and n=16 for sham injury groups). All statistical comparisons were made between all 4 experimental groups including for assessment of seizure frequency. For clarity in the figure only significant results are indicated in panels A-E.

Attenuated neurometabolic dysfunction after TBI in *Sarm1*$^{-/-}$ mice

TBI induces dramatic changes in the brain metabolic state. ^{1}H-MRS provides a sensitive technique to quantify subtle alterations in neurochemical profiles after TBI that relate to functional outcome in patients.[256] To determine whether TBI differentially affects the cerebral neurochemical profile in wild type versus *Sarm1*$^{-/-}$ mice, *in vivo* ^{1}H-MRS was conducted in a subset of mice prior to injury, 2 h, and 48 h post-TBI. This analysis of cerebral metabolites acquired from a single voxel within the right traumatized hemisphere (spectral fits with a Cramér-Rao lower bound [CRLB] of <15%) revealed that two metabolic parameters (total choline [tCh], and total n-acetylaspartate [tNAA]) were transiently reduced at 2 h post-trauma in *Sarm1*$^{+/+}$ mice (Table 3.1; Figure 3.4 A and B). These metabolites play important roles in myelination and membrane metabolism[257] and have been previously shown to transiently decrease after TBI in rodents.[258,259] For example, NAA, which is the most abundant of these metabolites,[256,258] is a marker of neuroaxonal integrity and viability; its reduction after TBI probably reflects impairment of neuronal metabolism.[52,256-260] Strikingly, the cerebral metabolic depression observed in Sarm$^{+/+}$ mice after TBI was abolished in the absence of *Sarm1*.

Metabolite	Time	*Sarm1*$^{+/+}$ (n=5)	*Sarm1*$^{-/-}$ (n=5)	Between group P-value†
Creatine	Pre	161.7 ± 20.9	161.0 ± 23.6	n.s.
	2 h	157.9 ± 22.4	159.3 ± 18.0	n.s.
	48 h	156.3 ± 27.0	155.6 ± 28.5	n.s.
Glu	Pre	282 ± 8.5	282.7 ± 6.1	n.s.
	2 h	266.8 ± 12.5	289.8 ± 16.3	n.s.
	48 h	278.4 ± 34.0	288.6 ± 29.4	n.s.
Gln	Pre	113.7 ± 9.9	114.0 ± 7.0	n.s.
	2 h	138.4 ± 46.9	117.1 ± 9.9	n.s.
	48 h	132.3 ± 21.0	123.6 ± 2.1	n.s.
Inositol	Pre	122.1 ± 10.9	122.4 ± 7.1	n.s.
	2 h	119.9 ± 10.0	119.3 ± 19.5	n.s.
	48 h	128.4 ± 13.9	121.0 ± 16.3	n.s.
NAA	Pre	162.5 ± 6.8	174.2 ± 11.2	n.s.
	2 h	164.1 ± 6.0	173.9 ± 13.8	n.s.
	48 h	161.1 ± 27.3	174.0 ± 24.7	n.s.
Taurine	Pre	201.8 ± 12.8	204.1 ± 9.5	n.s.
	2 h	216.2 ± 11.8	219.8 ± 10.7	n.s.
	48 h	217.7 ± 21.9	227.9 ± 33.0	n.s.
tCr (Cr+PCr)	Pre	187.0 ± 8.7	197.4 ± 2.7	n.s.
	2 h	177.4 ± 6.0	195.4 ± 10.0	n.s.
	48 h	191.9 ± 15.2	191.6 ± 16.1	n.s.
tCho (GPC+PCho)	Pre	64.1 ± 2.0	63.7 ± 5.2	0.901
	2 h	51.3 ± 3.2	60.2 ± 5.3	0.004
	48 h	65.3 ± 6.2	62.9 ± 2.5	0.369
Glx (Glu+Gln)	Pre	393.1 ± 12.8	395.0 ± 7.8	n.s.
	2 h	373.6 ± 20.3	397.7 ± 24.6	n.s.
	48 h	405.0 ± 12.7	398.1 ± 7.8	n.s.
tNAA (NAA+NAAG)	Pre	195.6 ± 15.4	208.6 ± 4.8	0.137
	2 h	188.1 ± 10.5	209.8 ± 5.9	0.021
	48 h	202.2 ± 6.2	209.5 ± 16.7	0.391

Table 3.1 *In vivo* neurochemical profile alterations in *Sarm1*$^{-/-}$ and *Sarm1*$^{+/+}$ control mice as assessed by ^{1}H-MRS. Values are institutional units and expressed as mean±S.D. †P-value comparison of *Sarm1*$^{+/+}$ with *Sarm1*$^{-/-}$ mice (two-way RM ANOVA with post-hoc Holm-Šídák test). n.s, indicates not significant; Cr=creatine; Gln=glutamine; Glu=glutamate; Glx=glutamate and glutamine; GPC=glycerophosphocholine; NAA=n-acetyl aspartate; NAAG=n-acetyl aspartatyl glutamate; PCho=phosphocholine; PCr=phosphocreatine; tCho=total choline (GPC+PCho); tCr=total creatine (Cr+PCr); tNAA=total n-acetyl aspartate (NAA+NAAG).

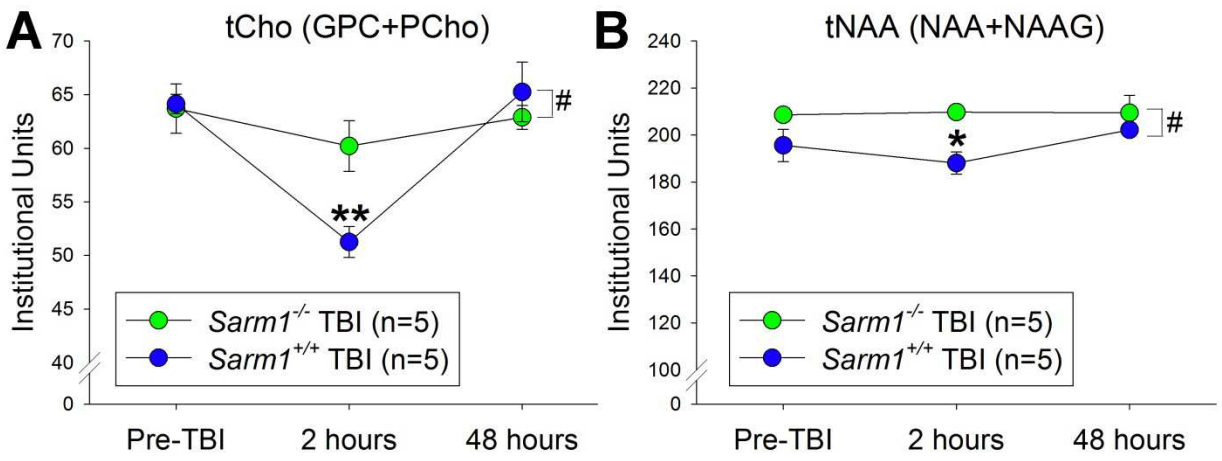

Figure 3.4 Loss of *Sarm1* is associated with suppressed TBI-induced alterations in brain neurochemical profiles. ^{1}H-MRS showed a transient reduction in (A) tCho (total choline = glycerophosphocholine [GPC] + phosphocholine [PCho]) and (B) tNAA (total n-acetyl aspartate = n-acetyl aspartate [NAA] + n-acetyl aspartatyl glutamate [NAAG]) within the right hemisphere of *Sarm1*$^{+/+}$ but not *Sarm1*$^{-/-}$ mice ($^{\#}$P<0.05 for overall group difference; *P<0.05, **P<0.01 versus *Sarm1*$^{-/-}$ at 2 h; two way RM ANOVA with post-hoc Holm-Šídák test).

Impact of *Sarm1*$^{-/-}$ on CBF and blood gases after TBI

Importantly, the effect of *Sarm1* loss on ^{1}H-MRS profile changes was not associated with changes in CBF as there was no significant difference in the degree of post-TBI cerebral perfusion between *Sarm1*$^{-/-}$ *and* *Sarm1*$^{+/+}$ mice (Figure 3.5). Furthermore, there was no difference in the number of animals that had versus did not have a CBF reduction below the median 20-min post-TBI CBF (P=0.653, χ^2-test), suggesting a similar incidence of post-traumatic CSD.

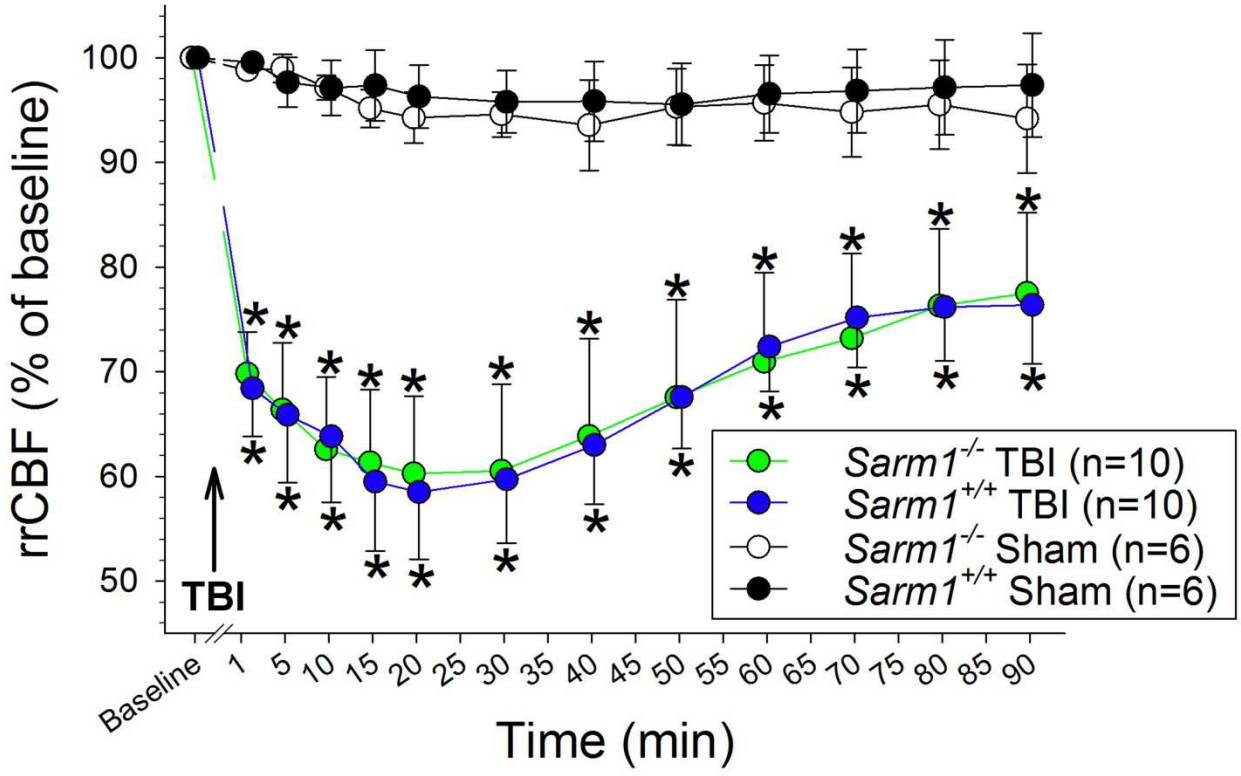

Figure 3.5 Similar CBF response to TBI in *Sarm1* wild type and knockout mice. After TBI, relative regional cerebral blood flow (rrCBF) decrease to a similar degree in *Sarm1*$^{+/+}$ and *Sarm1*$^{-/-}$ mice. Values reached a nadir of ~60% of baseline at 20 min following trauma. Subsequently, rrCBF recovered partially to ~75% of baseline values at 90 min following impact. Sham injured animals displayed a stable rrCBF through the sampling period. Values are slightly shifted on the x-axis for better visibility (*P<0.05 versus baseline; RM ANOVA on ranks with post-hoc Dunnett's test). For clarity in the figure only significant results are indicated throughout.

Lastly, blood gases, electrolytes, glucose, hematocrit, and hemoglobin concentration assessed in a subset of animals at the end of anesthesia indicated values within the normal physiological range without significant differences between wild type and *Sarm1*$^{-/-}$ mice (Table 3.2). Therefore the observed differences in neuronal metabolism as assessed by ^{1}H-MRS were unlikely to be a result of differences in post-traumatic cerebral CBF responses, hypoperfusion, or hypoxia.[77]

	Sarm1$^{+/+}$ TBI (n=6)	*Sarm1*$^{-/-}$ TBI (n=6)	P-value
pH	7.45 ± 0.07	7.45 ± 0.04	0.971
$PaCO_2$ (mmHg)	29.6 ± 4.5	27.0 ± 2.6	0.248
PaO_2 (mmHg)	81.2 ± 6.5	86.2 ± 6.0	0.197
Base excess (mmol/L)	-3.9 ± 2.1	-4.7 ± 2.1	0.530
HCO_3- (mmol/L)	19.8 ± 1.8	18.5 ± 0.8	0.116
SaO_2 (%)	96.5 ± 1.0	97.2 ± 0.8	0.235
Na^+ (mmol/L)	144 ± 2	142 ± 1	0.190
K^+ (mmol/L)	4.8 ± 0.3	4.9 ± 0.2	0.675
iCa^{2+} (mmol/L)	1.26 ± 0.04	1.23 ± 0.06	0.429
Glucose (mg/dL)	290 ± 51	286 ± 63	0.902
Hematocrit (%PCV)	41.7 ± 3.9	41.3 ± 0.8	0.843
Hemoglobin (g/dL)	14.2 ± 1.3	14.1 ± 0.3	0.838

Table 3.2 Physiologic parameters at the end of anesthesia. Post-TBI blood gases, electrolytes, glucose, hematocrit, and hemoglobin concentration values were within the normal physiological range without significant between-group differences between *Sarm1*$^{+/+}$ and *Sarm1*$^{-/-}$ mice subjected to TBI (P>0.05 each; t-Test). Data are mean ± S.D. PCV indicates packed cell volume.

Discussion

Wallerian degeneration represents an active process that involves an autonomous self-destruction pathway leading to rapid fragmentation of the distal portion of a separated axon after a predictable latent phase of 2-3 days.[179] Critically, though complete axon transection is irreversible, *in vitro* studies have shown that axonal degeneration in a non-transection model can be prevented by WLD^S before a commitment point is reached.[179,261] This suggests that therapies targeting Wallerian degeneration pathways may preserve axons in neurological conditions where axon degeneration and transection are not immediate.

This approach is of particular interest to treat TBI-related axon injury, in which the majority of damaged axons undergo secondary disconnection (secondary axotomy) with a delay of hours to days after the initial trauma.[111] However, while WLD^S is axon protective in a wide range of neurological conditions, it has not been shown to prevent axonal degeneration after TBI.[179] Given that no pharmacological treatment is yet available for patients with debilitating functional impairment due to traumatic axonal injury caused by TBI, identifying the potential contribution of a putative active axonal death program in traumatic axonal degeneration is important as it holds great promise for the identification of original treatment targets and the development of viable therapeutic approaches.

This study shows that loss of *Sarm1*, the first endogenous gene whose loss potently suppresses Wallerian degeneration,[180] remarkably attenuates surrogate markers of traumatic axonal degeneration and functional deficits after TBI. At 48 h, the

median count of injured βAPP-positive axons was reduced by 85% in *Sarm1*$^{-/-}$ mice. Similarly, at 48 h the plasma pNFH-concentration, which is released into the bloodstream after axonal injury, was blunted by >90% in *Sarm1*$^{-/-}$ mice. Importantly, though the peak pNFH-concentration was delayed in *Sarm1*$^{-/-}$ mice, values did not exceed those from wild type animals indicating that *Sarm1* loss prevents axonal degradation rather than merely delaying it. Most important, *Sarm1*$^{-/-}$ mice exhibited substantially preserved neurological function after TBI providing the rationale to develop anti-*Sarm1* therapies as a means to protect from TBI-related sequelae in humans.

Precisely how *Sarm1* activates axonal degeneration is not known. SARM1 negatively regulates Toll-like receptor–activated transcriptional programs,[262] but the exact mechanisms by which it exerts its pro-degenerative function are not yet well understood. TIR domain-multimerization, mediated by its SAM domain, appears to be required for SARM1's pro-degenerative function, while the N-terminal ARM domain is auto-inhibitory.[179,263,264] Purportedly, the key initial step in the activation of SARM1 relates to injury-induced axoplasmatic Ca^{2+} elevation, possibly *via* Ca^{2+}-calmodulin kinase.[265,266] The concept that SARM1 acts downstream of Ca^{2+} is interesting because traumatic axonal degeneration is initiated by increases in axoplasmatic Ca^{2+}[155,160,267] with subsequent activation of Ca^{2+}-dependent proteases of the calpain family that drive cytoskeletal proteolysis and ultimately axonal degeneration.[179,268-270] As an innate immunity signaling molecule, SARM1 may be activated through molecules that participate in post-traumatic inflammatory cell damage signaling. Conversely, *Sarm1* knockdown has been shown to increase the expression levels of the inflammatory cytokines interleukin-6 and interferon-β in the mouse brain,[184] which have been linked to

outcome after rodent TBI.[271-273] This may suggest that SARM1 at least in part mediates axon degeneration through modulating the cerebral inflammatory response after TBI. Lastly, loss of SARM1 has been demonstrated to protect neurons from ischemic injury.[183] This is of relevance for TBI, which is commonly associated with post-traumatic cerebral hypoperfusion that can contribute to brain injury as shown in this study as well as by others.[77,274] Indeed, we observed significant hypoperfusion following head impact in both *Sarm1*$^{+/+}$ and *Sarm1*$^{-/-}$ mice. Yet, associated cerebral metabolic dysfunction as assessed by ^{1}H-MRS was significantly attenuated in *Sarm1*$^{-/-}$ mice. This observation is consistent with prior *in vitro* studies reporting rescued glycolysis in cultured *Sarm1*$^{-/-}$ neurites[275] potentially related to maintained levels of its key substrate nicotinamide adenine dinucleotide (NAD^{+}).[264,275,276] This also provides a possible explanation for the observed early functional protection of *Sarm1*$^{-/-}$ mice in our model.

Together, these examples indicate that SARM1 may confer axon protection through modulating several mutually not exclusive pathophysiological cascades and further study is required to identify the precise role of SARM1-signalling in TBI to develop efficacious therapeutic approaches to axon protection. From a therapeutic standpoint, it will also be key to establish the time window for intervention. For example, in light of experience with other acute brain injuries (such as ischemic stroke) there may only be a tight therapeutic window of several hours after TBI[111] before the axon injury cascade has progressed to the point that Wallerian like degeneration cannot be rescued. Further, it has been shown that blocking Wallerian degeneration (such as through WLD^{S}) may hinder axonal regeneration.[277,278] Accordingly, it will be important to

determine whether loss of *Sarm1* impairs axonal regeneration and thereby negatively impact functional recovery.

Though the results presented in this thesis are highly suggestive, they do not establish direct evidence that observed improvement in functional outcome in *Sarm1*$^{-/-}$ mice was exclusively the result of axonal protection. Thus, further studies may benefit from including functional assays to directly determine the contribution of axonal functional integrity to sensorimotor and cognitive deficit severity. A further limitation relates to the fact that consistent with the mild model severity the number of βAPP stained axons in our model was relatively low. Given the low ratio of injured-to-uninjured axons no attempt at quantifying the degree of axon loss over the study period was made. Thus, further study is required to confirm whether noted attenuation of βAPP staining in *Sarm1*$^{-/-}$ mice truly translates to long-term survival of cerebral axon after TBI.

In summary, my findings support the notion that Wallerian degeneration may be an underlying pathological feature of TBI and its behavioral consequences. My study highlights the translational potential of anti-*Sarm1* directed therapies as a valuable and novel avenue to clinical treatment of TBI and other impact-based injuries in the nervous system, and potentially also in a wide range of human neurological diseases associated with axonal injury and degeneration.

CHAPTER IV:

COMPREHENSIVE DISCUSSION

Rationale for Studies

TBI constitutes a major public health problem as a leading cause of adult death and disability worldwide.[3] Despite the devastating impact and prevalence of TBI, molecular pathways that drive pathology after TBI remain to be clarified.

Axonal injury and degeneration represents a pathological hallmark of TBI of all severities and constitutes a critical determinant of post-traumatic functional impairment.[106,107] It is now well established that the vast majority of injured axons do not, as originally thought, rupture as a direct consequence of the trauma forces but rather degenerate as a result of complex biochemical cascades that lead to the catastrophic destruction of the axon cytoskeletal components and axotomy over a period of hours to days.[111,124,139] Moreover, following axotomy the distal axon portion undergoes sudden rapid fragmentation along its full length ~72 h after the original axotomy, a process termed Wallerian degeneration.[106,111,170-174] Intriguingly, this is an active process driven by an endogenous “axonal death” pathway that can be suppressed for days to weeks in homozygous mutant mice lacking the *Sarm1* gene, providing evidence of a programmed axonal death pathway.[180]

The central goal of this thesis was to use an animal model of TBI that closely mimics the human condition and could be used to determine whether blockage of the *Sarm1* pathway attenuates axonal injury and degeneration as well as neurological

sequelae after TBI. If true, this would provide novel insight into the molecular mechanisms underlying TAI by showing for the first time that (i) TAI after TBI is governed by a Wallerian degeneration-like process and (ii) that this process is mediated by a SARM1-associated “programmed axonal death” pathway representing a unique and novel target for TBI therapy.

Review of Results

In this dissertation, I provide experimental evidence that the acute adverse effects of head trauma on neuro-axonal morphology, brain metabolism, neural function, and on whole animal behavior are related to the pro-degenerative axon death signaling cascade mediated by SARM1.

In Chapter II, I characterize the acute CBF responses to TBI. I demonstrate post-traumatic profound CBF reductions in the traumatized hemisphere and show that despite the transient nature of these CBF alterations, animals with lower CBF values have greater histological brain damage and worse functional deficits. I identify that the specific temporospatial CBF dynamics are consistent with the occurrence of CSDs. My observations are important because they establish that cortical hypoperfusion and CSD are common in the acute phase after mild TBI and relate to a worse outcome.

In Chapter III, I present data that animals lacking SARM1 are similar to wild-type mice with respect to their baseline neurological function, number of axons within the corpus callosum, incidence of impact seizures, time to awakening from anesthesia after TBI, physiological parameters, and post-traumatic CBF responses. However, *Sarm1* knockout mice had significantly fewer βAPP positive axons in the corpus callosum, reduced plasma pNFH concentrations, ^{1}H-MRS-defined tissue signatures of preserved neuronal energy metabolism, and exhibited a strong, early preservation of neurological function. This provides evidence that the *Sarm1*-mediated prodegenerative pathway promotes pathogenesis in TBI.

Impact of the Results

The work presented in this thesis has focused on (i) characterizing the acute post-traumatic CBF dynamics and their relationship to histological and functional outcome; and (ii) the mechanisms of trauma-induced axon degeneration through the study of the axon prodegenerative gene *Sarm1*. These data have been discussed in the previous chapters, but what is their potential impact for treating TBI?

Acute post-traumatic cerebral hypoperfusion and metabolic dysfunction

Moderate-to-severe TBI is associated with profound CBF impairment and metabolic derangements that predict a poor outcome.[64,70-75] Although mounting evidence indicates lasting perturbation of CBF regulation, as well as metabolic dysfunction after mild TBI,[52,57,66,77-81,256-260] there are no detailed analyses of the acute (within one hour) CBF responses after human mild TBI.[58,279-283] This lack of human data is largely owing to practical and technical limitations because non-invasive assessment requires timely transfer of the patient to a facility with advanced neuroimaging capabilities.[279-282] Experimental studies do not suffer from this limitation because trauma onset is under the investigator's control. Yet, surprisingly few experimental studies have determined the CBF within the first hour after mild TBI and none of these has provided a detailed characterization of the hyperacute temporospatial CBF dynamics and their specific relation to cerebral metabolic dysfunction and overall outcome.[57,60,284-287] The information gained from this thesis work may therefore be of significant value to the field.

First, this study included ^{1}H-MRS investigations, which in prior studies demonstrated that certain brain metabolites are altered in the acute phase of TBI and may aid in diagnosing concussion related injuries.[52,257-259,288-291] In particular, similar to this study, transient NAA reductions are consistently identified after TBI, indicating impaired neuroaxonal metabolism, integrity, and viability.[52,256-260] Data for choline, the second most frequently altered metabolite after TBI, have been less consistent. While some investigators found post-traumatic increases in choline,[291] this and other studies reported decreased levels indicating post-traumatic changes in membrane integrity and metabolism.[257-259,292] Overall, the results in this study are consistent with the majority of publications and thus add to the notion that ^{1}H-MRS can be used to detect subtle neurochemical alterations after rodent mild TBI, which correlate with the degree of functional impairment. Nevertheless, caveats in the interpretation of these results relate to the fact that ^{1}H-MRS is based on relatively large tissue volume sampling (27 mm^3). Further, image acquisition is relatively long. Accordingly, ^{1}H-MRS is not well suited to track hyperacute changes with high spatial and temporal resolution in rodents and should be considered hypothesis generating only. Nevertheless, ^{1}H-MRS may be of great value for investigating human TBI to predict cognitive sequelae and provide novel insight into the underlying pathophysiology when combined with other imaging modalities.[293]

Second, by using non-invasive LDF, I provide indirect evidence for CSDs based on the prototypical CBF responses observed in TBI mice. It has long been suspected that CSDs may occur after mild TBI;[104] yet, evidence for this hypothesis had been lacking. Importantly, CSDs have been associated with a poor outcome after severe TBI;

however, given the catastrophic TBI types in which CSDs have been studied it is not possible to determine with certainty whether CSDs are the cause for the observed poor outcomes or whether they represent a mere epiphenomenon.[100-105] The herein described model enables the study of the contribution of CSDs to outcome after brain trauma in the absence of confounding pathologies such as ischemia, edema, hemorrhage, and other contusion-related injuries.

Third, in addition to improving the understanding of the underlying pathophysiological processes accompanying mild TBI, these data may also inform future study designs seeking to investigate novel neuroprotective treatments. The data presented herein indicates that CSD and related CBF phenomena are not a uniform response to trauma with only a subset of animals exhibiting profound CBF decreases. Although CBF was similar across mice as early as one hour after TBI, the earlier CBF responses were correlated with the degree of histological and functional outcome. This is of particular interest for neuroprotection studies. To date all preclinically tested therapies failed to translate from the lab in TBI.[294,295] The reasons for this are manifold and have been discussed extensively elsewhere.[294] However, even in highly rigorous studies conducted by an expert consortium, inter-lab variability has been cited as a likely contributing factor: “a certain amount of ‘‘wobble’’ in the models was observed given the desire to produce behavioral deficits.”[295] Among other molecules, this consortium sought to determine potential neuroprotective properties of cyclosporine A.[296] Intriguingly, none of their experimental protocols included CBF measurements. Considering that cyclosporine A has been shown to mitigate CSD-related CBF decreases,[297] it is thus tempting to speculate that unmeasured phenomena with variable

prevalence such as the herein described TBI associated CBF reductions could have contributed to model variability and bias. From a clinical investigational standpoint, it may be possible to refine existing concussion assessment tools to predict recovery after a mild TBI by emphasizing symptoms indicative of a CSD.[298-300] It may be envisioned to use such information to inform concussion trials and select patients for acute pre-hospital treatment aimed at mitigating CSD related sequelae.[94,301,302]

Assessment of axonal injury after mild TBI

Mild TBI accounts for the vast majority of traumatic brain injuries in the United States. However, despite its designation, consequences of these “mild” brain injuries are often not benign. For this reason, mild TBI has been referred to as the silent epidemic because problems such as impaired memory are often not visible. A major challenge in outcome prediction after TBI relates to its heterogeneous presentation. Most concussions are uncomplicated and resolve within days to weeks. However, it has been estimated that up to 15% of affected patients remain symptomatic more than 1 year after TBI.[303,304] Frequent complaints in the first weeks to months after TBI include easy distractibility, slow information processing, as well as impairment of executive function and memory.[305] Although persistent cognitive deficits have been reported beyond the first months after mild TBI, there is insufficient evidence whether a single mild TBI is associated with long-term cognitive impairment.[305] Interestingly, greater deficit persistence has been linked to pre-injury neuropsychiatric disorders and subacute symptoms do not consistently differ from those in trauma control groups.[306,307]

Therefore, there is a great interest in developing confirmatory tests that allow for predicting persistent cognitive deficits attributable to the original TBI.[308]

As discussed in the previous chapter, ^{1}H-MRS and CBF measurements may help diagnose post-traumatic derangements of cerebral metabolism and blood flow. However, these phenomena do not necessarily correlate with TAI and acute imaging is challenging to implement clinically.[279-282,293] Because TAI represents a key determinant of post-TBI outcome,[48,54,309,310] non-invasive tests aimed at specifically quantifying the degree of TAI are of particular promise. It has been suggested that neurofilaments may serve as sensitive markers for injury severity and recovery in both animals and humans.[150-152,154,253,254,311-313] This thesis work included such an assay and found that mild TBI resulted in significant pNFH elevations in wild-type mice that temporally correlated with the degree of TAI as assessed by gold standard immunohistological techniques. More important, pNFH increases were blunted in *Sarm1* knockout mice reflecting the attenuated TAI in the absence of SARM1. This indicates that neurofilament based assays may not only be used as a marker for TBI / TAI severity but may also serve as a sensitive means to determine the efficacy of therapeutic approaches to mitigating TAI. A major advantage over conventional histological techniques is the ability to non-invasively and serially monitor the progression of TAI in rodents, and by extrapolation, in human therapeutic TBI trials.

Sarm1‘s possible role in traumatic axonal degeneration

In this study I show that loss of the *Sarm1* gene relates to attenuated neuro-axonal injury, brain metabolic and behavioral dysfunction after TBI. In particular, by using sensitive immunohistological (βAPP) and serological (pNFH) assays I demonstrate that *Sarm1* knockout mice have significantly attenuated TAI. These findings are consistent with the notion that Wallerian degeneration represents a key pathological feature driving axonal degeneration and behavioral impairment after TBI.

The mechanisms by which *Sarm1* promotes Wallerian degeneration remain incompletely understood. SARM1 is an intracellular protein that co-localizes with the outer mitochondrial membrane, microtubules, and is present at synapse.[183,185,314] Although it contains a C-terminal TIR domain (Figure 4.1) indicating a role in toll-like receptor (TLR) signaling, loss of *Sarm1* does not impair TLR signaling.[181,183,315] SARM1 promotes neuronal death in response to hypoxia and neurotropic viral infection.[183,316] SARM1 has three major domains that seem critical for its regulation and activity. Its N-terminal domain, which is comprised of multiple ARMs, possesses auto-inhibitory function because its ablation renders SARM1 constitutively active to promote axon degeneration.[263,266,317] Its tandem SAM domains are likely critical for SARM1 dimerization / multimerization[318] to bring its TIR domains into proximity for downstream signaling because forced dimerization of the TIR domains triggers rapid axon degeneration (Figure 4.1).[181,263,266,317]

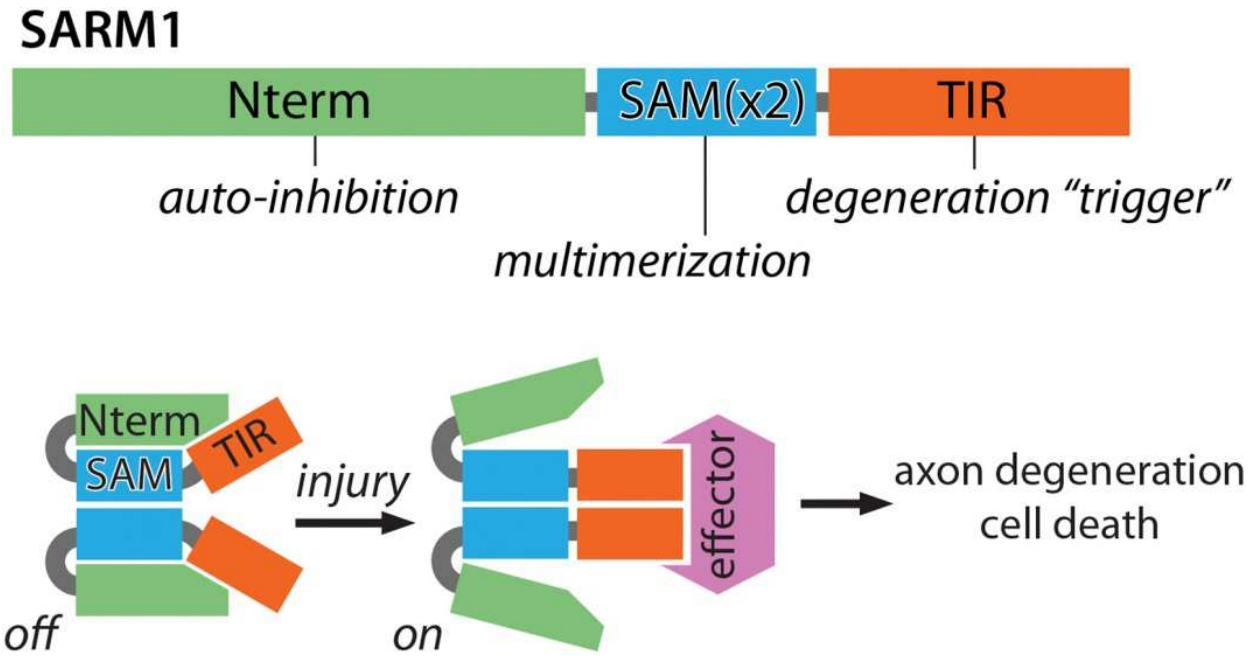

Figure 4.1 Model of SARM1 Auto-inhibition and Activation upon Injury. Top: SARM1 is made up of three regions: (1) an auto-inhibitory N terminus (Nterm) comprised of multiple ARMs, (2) tandem SAM domains that mediate SARM1-SARM1 binding (SAMx2), and (3) a TIR domain that triggers axon degeneration upon multimerization. Bottom: SARM1 multimers are inactive (auto-inhibited) in uninjured axons. Injury leads to SARM1 activation, perhaps through release of inhibition, exposing TIR domain multimers that transmit a pro-destructive signal to unknown effector molecule(s). Used with permission from.[181]

As previously discussed, SARM1 appears to act downstream of Ca^{2+},[265,266] which represents an interesting concept given the central role of intra axonal Ca^{2+} to activate proteases that subsequently cleave the cytoskeleton and trigger axonal degeneration.[155,160,179,267-270] Recent work has indicated that SARM1-signaling relates to a local energy deficit in injured axons. Specifically, whereas NAD+ levels declined after axotomy in wild-type axons, NAD+ loss was substantially suppressed in *Sarm1* null axons.[264,319] Conversely, TIR dimerization resulted in rapid NAD+ depletion within minutes, presumably *via* cleavage into nicotinamide, that was followed by loss of ATP and finally axon destruction.[264] TIR domains are not known to have any intrinsic catalytic activity for which reason it was thought that a, yet to be discovered, co-factor executed NAD+ cleavage.[320] However, recent data provided unexpected insight into how SARM1 may result in NAD+ depletion by showing that the SARM1-TIR domain itself might have intrinsic NADase activity.[321]

It has been proposed that NAD+ depletion is the essential function of SARM1[264] because (i) SARM1-independent NAD+ breakdown in *Sarm1* null cells triggers axon degeneration and (ii) SARM1-induced axon destruction can be blocked by NAD+ supplementation as well as increased NAD+ synthesis *via* expression of the NAD+ biosynthetic enzymes nicotinamide phosphoribosyltransferase (NAMPT) and nicotinamide mononucleotide adenyltransferase (NMNAT).[264] However, how SARM1 cleaves NAD+ is presently unknown.

Importantly, NMNAT, and specifically its axonal isoform NMNAT2 (NMNAT1 is located in the nucleus and NMNAT3 in the mitochondria), is an endogenous axon survival factor that synthesizes NAD+ from nicotinamide mononucleotide (NMN) and

ATP (adenosine triphosphate).[261,322] In fact, it has been shown that WLD^S prevents the early depletion of NAD+ in injured axons indicating that loss of NMNAT function is a crucial event in the Wallerian degeneration pathway.[106] It has been hypothesized that loss of NMNAT2 may be key for the activation of SARM1. This is based on observations that axonal defects and embryonal lethality in NMNAT2 knockout mice are rescued by NMNAT2/SARM1 double knockout.[323] In addition, that SARM1 function follows a similar temporal profile as NMNAT2-loss after axotomy.[264] Lastly, NMNAT expression blocks axon degeneration, not by increasing NAD+ synthesis, but rather by blocking SARM1-dependent NAD+ depletion.[324] Under this hypothesis, loss of the NAD+ synthesizing NMNAT2, which has a short half-life and requires constant transport to the axon, would result in SARM1-activation and NAD+ cleavage and thus in catastrophic axonal NAD+ loss due to both reduced production and increased destruction of NAD+.[181]

But how does SARM1 activation cause axon loss? It has been shown that SARM1-dimerization activates mitogen-activated protein kinase (MAPK) signaling, which is required for ATP-depletion after axon injury and represents an essential component of axon degeneration.[317,325] However, a recent study found that MAPK signaling is not necessary for NAD+-depletion and axon degeneration induced by activated SARM1. This suggests that the MAPK pathway is a critical early event that leads to SARM1 activation, but once SARM1 is active the MAPK pathway is no longer essential to promote NAD+ and axon loss.[326] The authors proposed that MAPK signaling may control the levels of the axon survival factor NMNAT2 and thus the axon's susceptibility to degenerate (Figure 4.2).[326]

Nevertheless, whether this proposed pathway applies to TBI remains to be clarified. The mouse model used in this thesis work appears well suited to further dissect the specific molecular mechanisms driving traumatic axon degeneration and investigate how manipulating specific pathways may translate to functional and behavioral outcome after TBI.

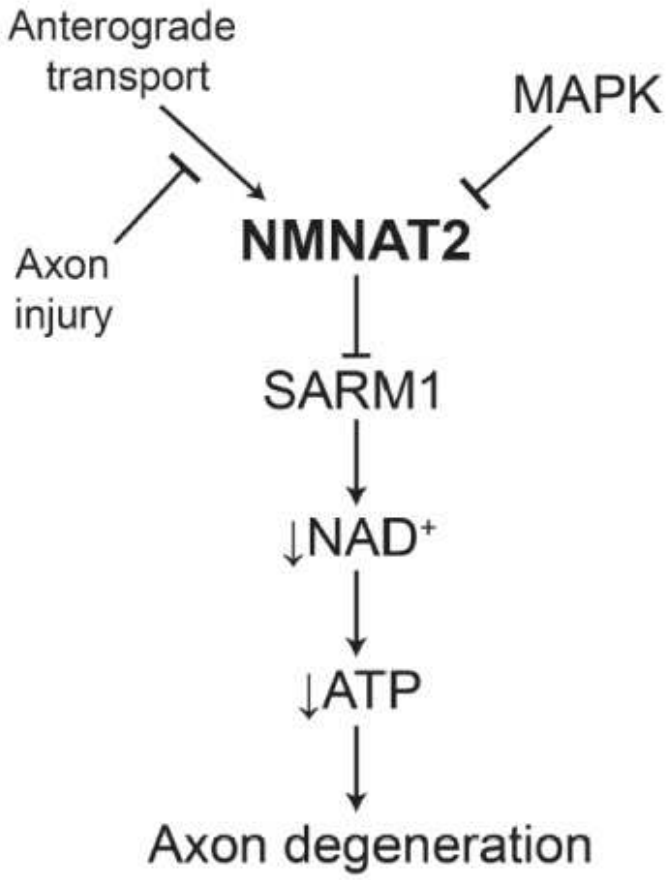

Figure 4.2 Simplified linear model of the axonal degeneration program. Mitogen-activated protein kinase (MAPK) signaling controls the levels of NMNAT2, which blocks SARM1-activation. Upon axon injury, delivery of the labile survival factor, nicotinamide mononucleotide adenyltransferase 2 (NMNAT2) *via* anterograde transport is blocked, levels fall below a critical threshold, thus activating SARM1. Activated SARM1 depletes nicotinamide adenine dinucleotide (NAD+), leading to loss of adenosine triphosphate (ATP) inducing a metabolic crisis and axon fragmentation (for details see text). Modified from.[326]

Future Directions

The results presented in this dissertation provide several major avenues for future studies to further dissect underlying pathophysiology and test treatment strategies of mild TBI and TAI.

Exploration of alternative mechanism of *Sarm1* mediated axon degeneration

TBI has a complex pathophysiology, requiring the interaction of multiple cell types.[189] Germline *Sarm1* knockout mice are viable and do not exhibit obvious pathology, and brains of *Sarm1* knockout mice appear morphologically intact.[183] However, SARM1 appears to be important for embryonic and early postnatal development[183,185] and *in vitro* and *in vivo Sarm1* knockdown results in reduced dendritic arborization.[185] Hence, observed protection from TAI in germline *Sarm1* knockout mice may stem from selection of intrinsically more resistant neurons rather than due to inhibition of a specific axon death pathway.

Furthermore, post-traumatic glial pathology has been shown to contribute to axonal death.[327] SARM1 has been linked to microglial activation[328] and it is possible that knockout mice have less axon pathology due to attenuated microglial response, which would provide a fascinating link between innate immunity and axonal damage sensing. Likewise, oligodendroglial apoptosis may lead to axonal demyelination with subsequent axon death; thus it is important to determine whether *Sarm1* knockout increases oligodendroglial survival.

Creating mouse models that provide the opportunity to investigate cell-autonomous effects of *Sarm1* gene disruption in the adult brain would be a significant advance in the field. Though expression of green fluorescent protein (GFP)-tagged *Sarm1* has been exclusively observed in neurons,[183] low expression beneath the visible threshold for GFP-tagged *Sarm1* in non-neuronal cell types is possible and does not reliably exclude the possibility that non-neuronal sources of SARM1 may activate axon death. Creating mouse lines that allow for spatially and temporally controlled (conditional) *Sarm1* disruption will allow to test whether cell-type specific *Sarm1* deletion differentially affects axon degeneration after TBI. Such conditional gene knockout can be achieved by leveraging the Cre-loxP technology. Cre-loxP is a conditional gene-targeting system based on the use of the site-specific recombinase Cre that catalyzes recombination between two loxP DNA recognition sites. An essential exon within *Sarm1* (gene of interest) is flanked with two loxP sites (floxed) by homologous recombination in embryonic stem cells (loxP sites are not native to the mouse genome). Subsequently, transgenic mice expressing Cre are crossed with the strain carrying the floxed target gene.

Spatial control (tissue specificity) is achieved by using mice in which Cre is driven by a promotor that is specific to the tissue of interest. Once transcribed, Cre excises the intervening DNA including the exon from the chromosome creating a null allele in all cells where Cre is active. *Temporal* control of target gene expression is attained by using tamoxifen inducible Cre-systems. This approach can limit unwanted Cre activity and potential associated side effects such as ectopic recombination due to transient Cre expression during development or toxic effects due to prolonged high levels of Cre

activity. To accomplish temporal Cre-expression a fusion protein of Cre and a mutant estrogen receptor ligand-binding domain (Cre-ER^T) are employed. In the absence of the specific ligand, the ER^T domain is bound by heat shock proteins that presumably block recombinase activity. *In vivo* induction of recombinase activity is achieved by administration of tamoxifen or its active metabolite 4-hydroxy-tamoxifen, which releases the heat shock protein from the ER^T domain resulting in translocation of Cre to the nucleus where it can excise the floxed target gene. Importantly, ER^T binds tamoxifen with greater affinity than endogenous estrogens, which allows Cre-ER^T to remain cytoplasmic in animals untreated with tamoxifen (newer, more specific, generations of this system have been developed and are denoted by ER^{T1} and ER^{T2}, respectively). Several CreER^T mouse strains have been developed and are commercially available to target neurons, microglia, astroglia, or oligodendroglia for homogenous cell-type specific Cre recombination after tamoxifen (but not vehicle) injection.[329-332]

To determine, whether SARM1 cell autonomously drives TAI in the brain *in vivo*, Cre-ER^T activity can be induced *via* intraperitoneal injection of tamoxifen (200 mg/kg) once a day for 5 consecutive days in mice ~2 months of age prior to TBI.[332] Cre-mediated excision of the floxed exons within the *Sarm1* gene results in the transcription of aberrant RNA. This results in nonsense-mediated decay of the *Sarm1* RNA due to frameshift and the unmasking of a premature stop codon, and thus, absent SARM1 protein production.[333] To validate the recombination properties of the Cre lines and tamoxifen treatment regimens it will be important to ascertain Cre expression on a cellular level, such as by immunohistochemistry using a monoclonal anti-Cre recombinase antibody[334] or by crossing mice to a global double-fluorescent Cre reporter

line.[335] Direct detection of SARM1 on a cellular level can be achieved by using *Sarm1* antibodies.[185,336] Furthermore, complementary RT-PCR and Western blot can be employed to determine *Sarm1*- and SARM1-expression in the brain, respectively.[183,187] Finally, βAPP-staining after TBI can be used to determine the cell types in which *Sarm1* disruption leads to axon protection following TBI in the inducible *Sarm1* knockout mouse lines as well as Cre-control lines[337] that have received tamoxifen or vehicle, respectively.

Based on *in vitro* observations that *Sarm1* promotes axonal degeneration in the absence of other cell types,[180,264,321] I expect that only mice with neuron-specific *Sarm1* disruption would be protected from TBI and show attenuated TAI. This would support the hypothesis that SARM1 neuron-autonomously mediates axonal death in the brain after TBI. Nevertheless, if other mouse lines also show axon protection, this would provide exciting new insight into the contribution of other cell types to SARM1-mediated axon degeneration following TBI. Conversely, it is possible that no mouse line shows protection following localized *Sarm1* disruption. This would hint that germline *Sarm1* knockout contributes to brain protection through a different, yet to be discovered, mechanism. Alternatively, it could be that *Sarm1* disruption in multiple cell types simultaneously is needed for protection, which could be determined by combination of different Cre lines. Ubiquitously expressed tamoxifen-inducible Cre lines[338] could be used to determine whether multiple cell types are involved versus presence of a developmental confound.[339] This would represent a critical experiment, because future therapeutic approaches to target *Sarm1* in adulthood may not provide significant post-traumatic axonal protection if protection requires SARM1 absence during development.

Possible disadvantages of the Cre-ER^T approach relate to the possibility that tamoxifen injection results in high mortality rates, which however, could be mitigated by oral administration of tamoxifen. Tamoxifen induced recombination efficiency may also decline with advancing age,[340] requiring injection at an earlier age of 4-6 weeks.[337] Further, tamoxifen-induced recombination may be mosaic (with a hypomorphic phenotype) and recombination sensitivity of the Cre reporter may not correlate with that of the floxed target gene. Therefore, immunohistochemistry will be required to provide an anatomical resolution of SARM1 expression.[184,185]

Assessment of brain functional connectivity

TAI-associated disconnection of cerebral functional domains is considered to underlie observed persistent neurological deficits after TBI.[48,54,309,310,341] Axon protection is a promising target for the treatment of brain trauma to improve functional brain connectivity and outcome. In this dissertation I show that loss of SARM1 confers profound axonal protection from TBI by using histological and serological markers of axon integrity. In addition, I demonstrate that *Sarm1* knockout mice have significantly fewer functional deficits than wild type littermates. However, direct evidence that preserved axon integrity translates to improved functional connectivity remains to be established.

To probe axon function and brain functional connectivity several techniques could be employed to determine whether *Sarm1* knockout preserves functional connectivity after TBI. For example, transcallosal evoked responses allow to directly probe axon function.[342-344] After craniotomy, stimulation electrodes are inserted into the cortex to a

depth of approximately 600-800 µm. For non-invasive recording from the contralateral cortex, a silver ball-tip electrode is placed on the intact skull at corresponding contralateral coordinates. To record transcallosal evoked responses, current pulses are applied. Once a stable response is observed, intensity response curves are recorded and several consecutive sweeps, obtained at maximal response, will be averaged. Using this technique, several prior investigations demonstrated reductions in compound action potential amplitudes evoked in the corpus callosum after rodent TBI both *in vitro* and *in vivo*, with the degree of amplitude reduction correlating with injury severity.[342-344] Accordingly, I would expect that *Sarm1* knockout results in greater preservation of peak amplitudes after TBI when compared to wild type mice, and that the degree of amplitude reduction correlates with the severity of axonal degeneration.[342-344] Absence of such a difference could indicate that white matter tracts other than the corpus callosum are involved in the behavioral deficits observed in this study. This would inform the design of future studies investigating functional white matter tract integrity in this model. Alternatively, this may indicate the exiting possibility that SARM1 is implicated in post-traumatic neuronal dysfunction through action in other neuronal structures such as the dendrites or synapse. Potential pitfalls of this technique include the confounding of the electrophysiological recordings by differences in anesthetic depth and brain temperature. Therefore, head temperature will need to be maintained within the physiologic range and the anesthetic regimen kept constant between animals. Lastly, because the overall TBI severity is mild in the used model, assessment of the compound action potential may not be sensitive enough to depict minor differences between genetic strains. However, in this case a more severe model could be tested for

proof-of-principle (see also next chapter). A more important potential limitation relates to the need for a craniotomy. Because the used mouse model is based on a closed-head TBI paradigm it would not be possible to establish baseline recordings or conduct serial long-term monitoring. Nevertheless, this issue could be mitigated by using appropriate control groups (sham injury and comparison with wild type mice) as well as testing subgroups at different time points similar to the experimental design used for the histological and pNFH analyses in this study.

An alternative, non-invasive technique to assess brain connectivity is resting state functional magnetic resonance imaging (rsfMRI). This MRI-based technique studies the temporal dependency between spatially remote neurophysiological events that occur when brain regions communicate during rest. Importantly, regions with a higher level of functional connectivity also show a higher level of structural connectivity through white matter tracts and decreases in white matter integrity can directly affect functional connectivity including after mild TBI.[345,346] Based on the same general principle as rsfMRI, functional connectivity optical intrinsic signal imaging represents a novel way to assess brain function.[347] It converts changes in reflected light intensity from the brain surface to changes in local hemoglobin concentration to determine intrinsic functional connectivity and has been successfully applied to determine disruption of brain functional connectivity in mouse models of Alzheimer's disease and acute ischemic stroke.[347-349] Similar to the invasive transcallosal evoked responses, both rsfMRI and functional connectivity optical imaging are susceptible to confounding by anesthesia and changes in animal physiology. Accordingly, careful attention to anesthetic depth, body temperature, and cardiorespiratory function is needed.

Repetitive TBI and chronic traumatic encephalopathy

First evidence for an adverse compounding effect of multiple traumas stems from observations in boxers exhibiting cognitive, behavioral, and motor abnormalities almost a century ago.[350-352] Originally coined “punch drunk” syndrome the term dementia pugilistica was subsequently introduced.[352,353] Over the last decades, a concept emerged that multiple (mild) brain traumas can lead to a unique clinical and pathological picture termed chronic traumatic encephalopathy (CTE).[354] Clinically, CTE is characterized by delayed neurodegeneration, cognitive decline, and behavioral abnormalities long after the recovery from the acute effects of the original TBI.[354] On a pathological level the disease is associated with the accumulation of the microtubule associated protein tau in the form of neurofibrillary inclusions (neurofibrillary tangles, neuropil threads, and glial tangles) suggesting that repetitive TAI-related breakdown of the cytoskeleton and dissolution of microtubules and neurofilaments may serve as a toxic gain of function trigger that leads to continued accumulation of tau and to promote neurodegeneration.[351,354,355] Given its high clinical relevance, SARM1’s role in repetitive TBI will need to be elucidated. I have been able to adapt the mouse model used in this dissertation to produce repetitive TBI. The preliminary data gained from these exploratory analyses indicates that *Sarm1* knockout mice have significantly improved survival and a better functional outcome (for additional details see Appendix).

APPENDIX

Modeling repetitive TBI in the mouse

Material and Methods

Ethical approval

All procedures were approved by the University of Massachusetts Medical School Institutional Animal Care and Use Committee (Protocol #A-2405-15).

Mice, TBI paradigm, anesthesia, and analgesia

Spontaneously breathing male C57BL6/J mice (Jackson Laboratories) age 8-12 weeks (n=48) were subjected to 5 mild closed head injuries spaced 24 h apart using the same weight-drop paradigm as described in chapter II. To alleviate pain, animals received 0.05 mg/kg subcutaneous buprenorphine (Patterson Veterinary, Devens, MA, USA) 30 min before the end of anesthesia and every 6 h afterwards until 24 h after the last TBI. Additionally, each animal received 5 mg/kg subcutaneous carprofen (Patterson Veterinary, Devens, MA, USA) after each TBI.

Neurological evaluation

For neurological evaluation the NSS was assessed prior to the first TBI as well as at 2 h, 24 h (immediately prior to the second TBI), 26 h, 48 h (prior to the third TBI), 50 h, 72 h (prior to the fourth TBI), 74 h, 96 h (prior to the fifth TBI), 98 h, as well as 7 d, 14 d, 21 d, and 28 d after the initial TBI as described in chapter II. The time to sternal recumbency and presence of seizure activity was recorded after each TBI as detailed in chapter II.

Statistical analysis

Unless otherwise stated, continuous variables are reported as mean±SEM. Between-group comparisons for continuous variables were made with Mann-Whitney U-test, two-way repeated measures ANOVA, and two-way ANOVA as appropriate. Survival was assessed with the Log-Rank test. Categorical variables were compared using the Fisher exact test. A two-sided $P<0.05$ was considered statistically significant. All statistical analyses were performed using SigmaPlot 12.5 (Systat Software, Inc., Germany) and IBM® SPSS® Statistics 22 (IBM®-Armonk, NY).

Results

Sarm1 knockout is associated with improved survival after repetitive TBI

Compared to controls, *Sarm1* knockout mice had remarkably improved survival by 28 days after repetitive (5x) TBI (52% versus 17.4%; *P*=0.031; Figure A.1).

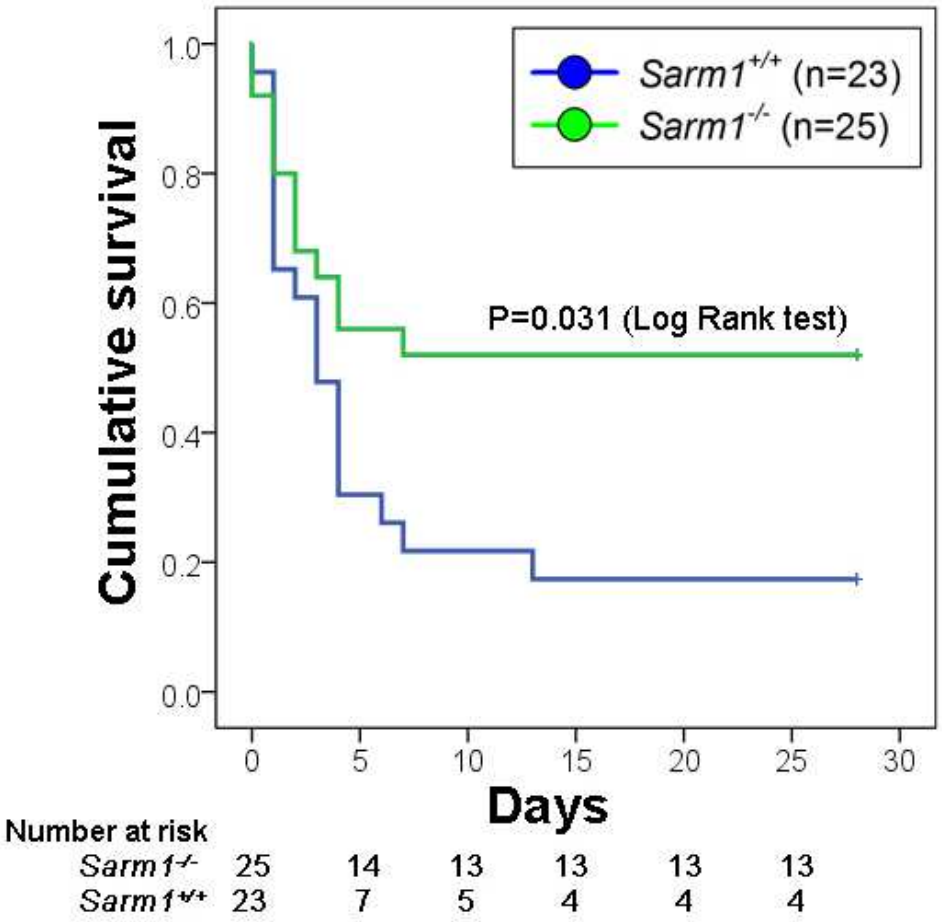

Figure A.1 Loss of *Sarm1* is associated with attenuated mortality after repetitive TBI. *Sarm1*$^{-/-}$ mice (n=25) had significantly improved survival (*P*=0.031) as compared to *Sarm1*$^{+/+}$ mice (n=23).

Loss of *Sarm1* relates to improved functional outcome repetitive TBI

Serial evaluation of the NSS showed increasing neurological deficits with repeat TBI in both wild type and *Sarm1* knockout mice (Figure A.2). Importantly, neurological deficit severity was significantly attenuated in mice lacking *Sarm1*. Furthermore, *Sarm1 wild type* mice were found to recover approximately 10 days after the last TBI (2 weeks after the first TBI) whereas *Sarm1*$^{-/-}$ animals displayed no signficant functional impairment only 3 days after the last TBI (7 days after the first TBI; Figure A.2).

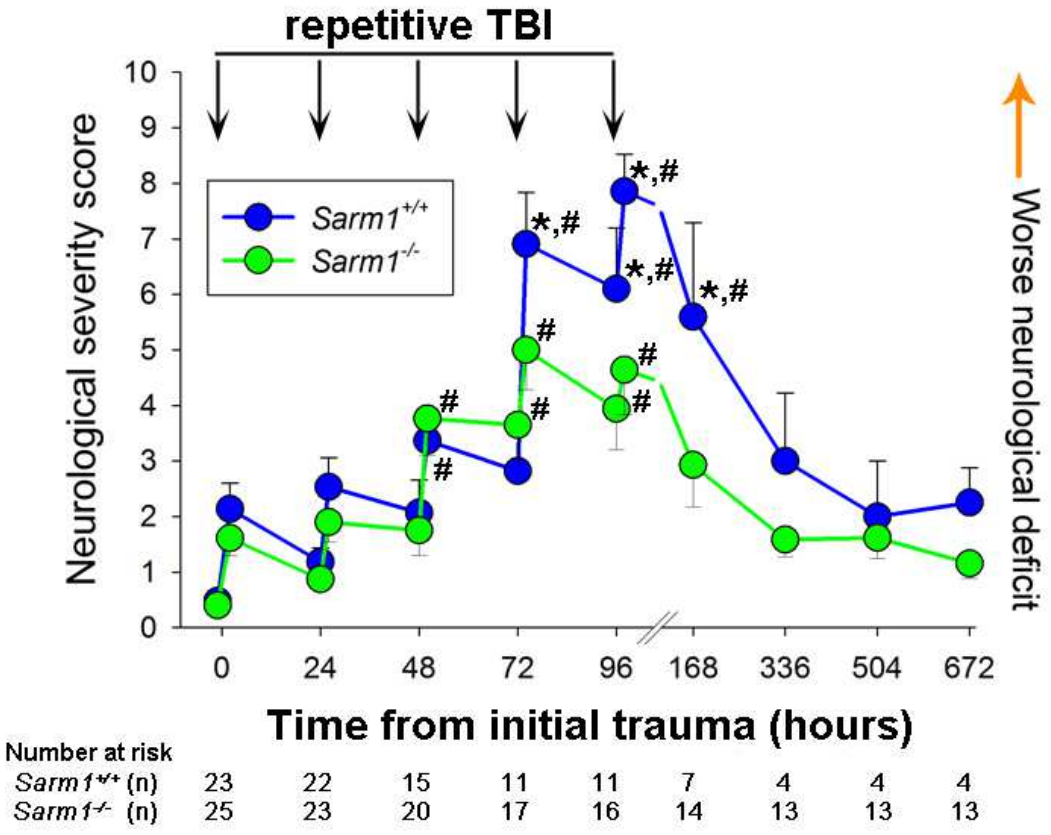

Figure A.2 Loss of *Sarm1* is associated with attenuated neurological deficits after repetitive TBI. Composite neurological severity score in the intention-to-treat analysis (i.e., all neurological severity scores were considered up to the animals' death; $^{\#}P<0.05$ versus pre-Trauma; $^{*}P<0.05$ versus *Sarm1* wild type; two-way RM ANOVA with post hoc Dunnett's test). Overall, there were significant group ($P<0.01$) and time ($P<0.001$) effects as well as presence of a significant group x time interaction ($P<0.01$). For clarity in the figure only significant results are indicated.

Similar to the single TBI experiment (see chapter III), the recovery time from anesthesia (defined as the time to spontaneously right from a supine to prone position after discontinuation of anesthesia) was similar between *Sarm1* wild type and *Sarm1* knockout groups (median [25^{th}-75^{th} percentile] 141 s [90 s - 305 s] versus 163 s [73 s – 227 s]; P=0.838; data not shown). Likewise, although there was a trend towards fewer impact seizures in *Sarm1* knockout (29%) versus wild type (55%) mice after the first TBI, this did not reach significance (P=0.134; not shown).

Notably, in contrast to the single TBI experiments (compare also with Figure 3.3), there was no significant difference in NSS between wild type and *Sarm1* knockout mice immediately after the first trauma. In particular, wild type animals appeared to have a lower than expected NSS at 2 h (2.1±0.5 [repetitive TBI] versus 3.0±0.4 [single TBI]).

To better understand this apparent inconsistency, I examined the NSS of surviving versus non-surviving mice. Overall, non-surviving animals had a worse NSS after the first TBI than survivors (P=0.027, not shown). When further stratified by genotype, surviving wild type mice had significantly lower 2 h NSS than non-survivors, whereas there was no significant difference in *Sarm1* knockout mice (P=0.29; Figure A.3, P<0.05).

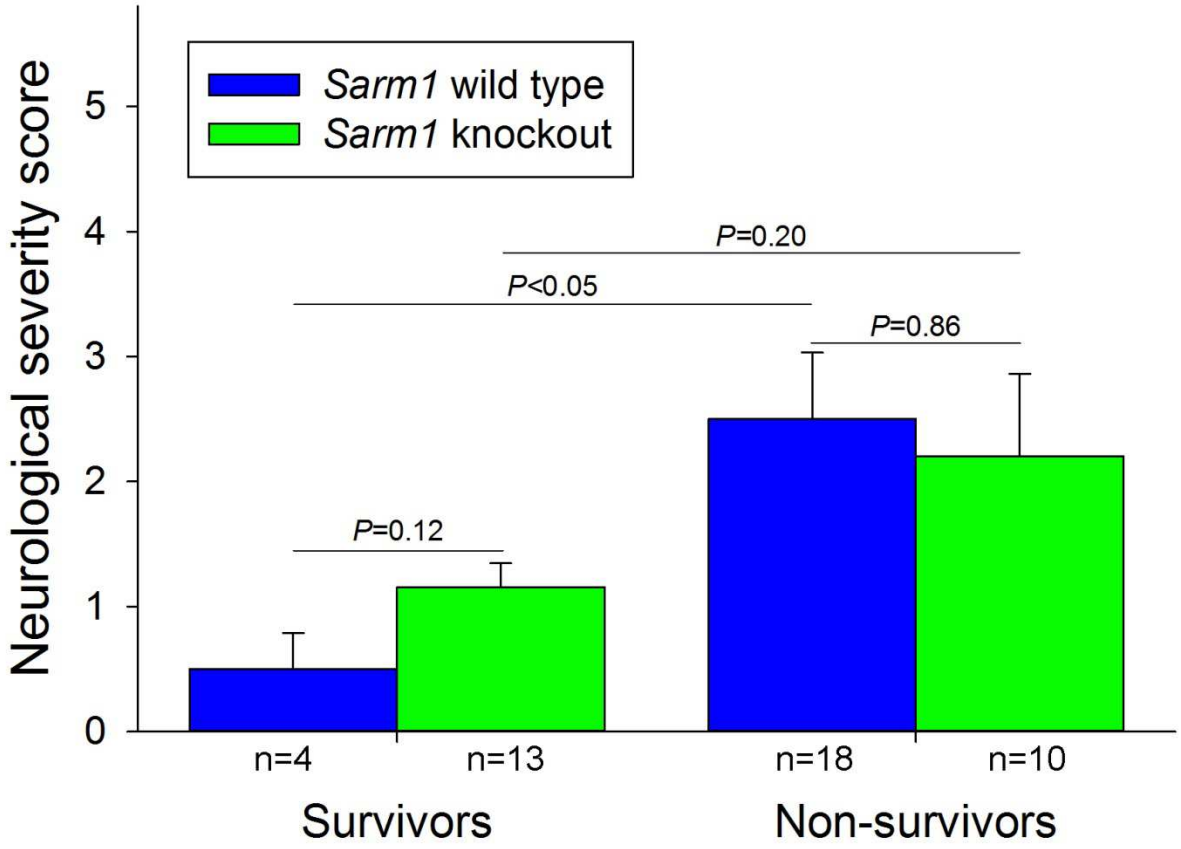

Figure A.3 Association between initial neurological deficit severity and survival to day 28. There was a significant difference in the 2 h composite neurological severity score between survivors and non-survivors among *Sarm1* wild type (P<0.05), but not *Sarm1* knockout (P=0.29) mice (two-way ANOVA). Overall, there were significant survival effects (*P*=0.019) but the analysis was underpowered for valid interaction analyses.

To gain additional insight into the association of survival status with neurological outcome, I conducted a sensitivity analysis that only included data from mice that survived for the entire 28 day observation period (complete-case analysis). Overall, the results gained from this analysis were in line with the intention-to-treat analysis. Despite initially lower composite NSS of *Sarm1* knockout versus wild type mice, neurological deficit severity was significantly greater in wild type mice after the 5th TBI up to 72 h follow up (Figure A.4). Together, these results add to the notion that absence of SARM1

mitigates TBI related neurological deficits. However, because of the limited number of included animals in the complete-case analyses, statistical tests were underpowered, and results should be considered hypothesis generating only.

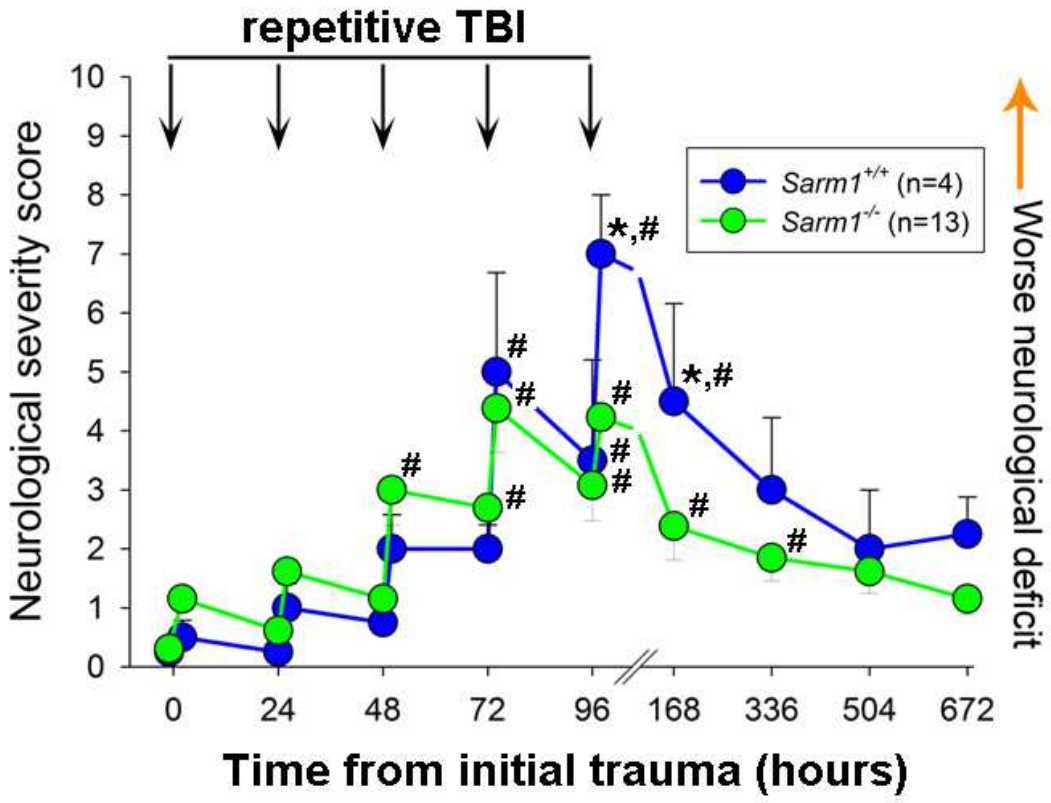

Figure A.4 Sensitivity analysis of the neurological deficits in surviving mice. Composite neurological severity score in the complete-case analysis (i.e., only surviving animals were included; $^{\#}P<0.05$ versus pre-Trauma; $^{*}P<0.05$ versus *Sarm1* wild type; two-way RM ANOVA post-hoc Holm-Šidák test). Overall, there were significant time ($P<0.001$) effects as well as presence of a significant group x time interaction ($P<0.01$).

Discussion

In summary, in this preliminary experiment I introduce a repetitive mild closed head TBI model in the mouse. This is an important extension of the single TBI model because epidemiologic studies have demonstrated that TBI increases the risk for dementia and other chronic neurodegenerative diseases.[351,354-357] However, while this association has been consistently shown even with a single moderate to severe TBI, data regarding such an association with single mild TBI is less convincing.[358] This has led to the hypothesis that there exists a “dose-response” relationship between TBI and the risk for chronic cognitive decline and dementia: the risk increases with both trauma severity and the number of injuries.[358] Under this concept multiple mild brain traumas can cause neurological injury and deficits that extend well beyond the initial impact and may manifest as CTE.[354,359] However, it is important to note that CTE likely represents a disease spectrum and not all patients will develop pathology after multiple brain injuries.[216,359] My model may help elucidate the complex pathophysiology of repeat head trauma.

Most importantly, my preliminary data indicates that loss of *Sarm1* remarkably attenuates morbidity and mortality after repetitive TBI. Although further characterization of this model, particularly with respect to chronic histological brain pathology, is needed, these data provide a strong foundation for future studies designed to determine the role of the *Sarm1* pathway in repeat head injury and possibly CTE pathophysiology. This is an important step forward in the field because CTE, unlike most other neurodegenerative diseases, can affect healthy adults as early as in their teenage years and because there is presently no treatment available for this devastating disease.[216]

Impact of the brain ventricles on traumatic axonal injury: A biomechanical hypothesis

The following work has been published in the *Journal of Neurotrauma* article published as:

Bouley J, Henninger N. Lateral ventricle attenuates underlying traumatic axonal injury after closed head injury in the mouse. *J. Neurotrauma* 2017. doi: 10.1089/neu.2017.5005. (*epub*)

Author contributions: J.B. conducted animal surgery, behavioral testing, and genotyping. N.H. designed the study, conducted animal surgery, histology analyses, statistical analyses, and wrote the paper.

Using model systems it has been suggested that the lateral ventricles could act as strain relievers and thereby mitigate TAI in adjacent tissues by absorbing energy; yet biological evidence for this hypothesis from *in vivo* studies has been lacking.[360,361] In this study, attenuated TAI was noted at 48 hours after TBI within the corpus callosum overlying the lateral ventricle of wild-type C57BL/6 mice.

Figure A.5 summarizes the spatial distribution of βAPP positive axons within the corpus callosum and indicates conspicuous TAI attenuation beneath the lateral ventricle under the impact center. This observation supports the notion that the lateral ventricle may indeed attenuate TAI through its proposed energy absorbing capacity. In extension of this data, any larger CSF space within the brain may mitigate TAI in adjacent white matter tracts in a similar fashion, which may in part explain attenuated TAI in rats with ventriculomegaly.[362] Nevertheless, although this previous rat study and the mouse model used in this dissertation share several features (both models employ a weight drop device to produce a closed head impact with associated head acceleration), there are also important differences including the use of different rodent species, presence versus absence of ventriculomegaly, use of a protective steel disc, as well as impact severity and degree of post-traumatic head acceleration.[362] Likewise, both models can only mimic certain aspects of the heterogeneous human TBI pathophysiology, which is influenced by the injury mechanism and proportion of impact and acceleration–deceleration type forces evoking TAI. Accordingly, the amount and location of axonal injury, and thus the extent by which ventricular size can affect it, will be dependent on the actual model utilized / the circumstances of the accident. Therefore, a one-to-one extrapolation of the results presented in this thesis work to other models and human TBI

may not be possible. Future studies seeking to unravel the complex interaction between the cerebral ventricles, specifically in the setting of ventriculomegaly, and TAI should include detailed assessment of the brain biomechanics during and after TBI to help assess the specific contribution of the biological (e.g., inflammation)[360-362] versus biomechanical (e.g., energy distribution and transfer) tissue response to trauma.

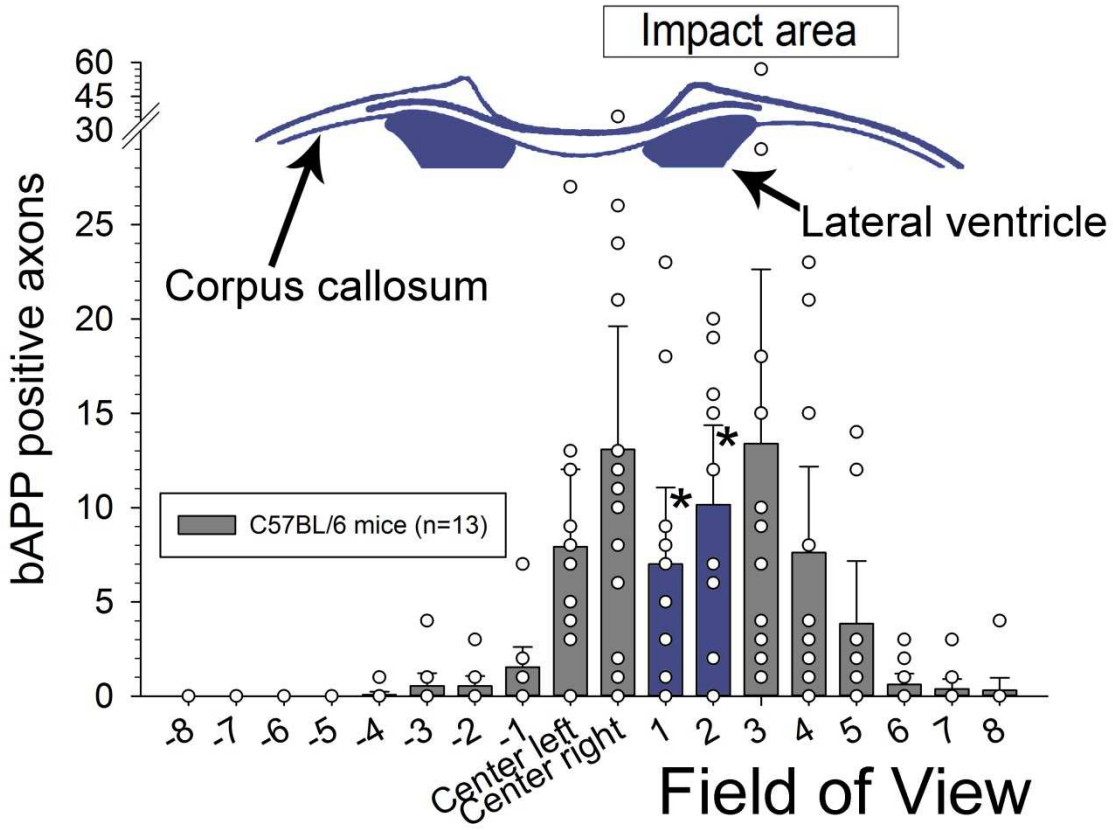

Figure A.5 Brain ventricular system and traumatic axonal injury. At 48 h after TBI significantly fewer beta amyloid precursor protein (βAPP) stained axon profiles were counted in the corpus callosum directly overlying the lateral ventricles (blue bars) as compared to immediately adjoining fields of view (FOVs). *indicates *P*<0.05 versus FOV3. There was no significant difference in the βAPP counts between FOVs 1 and 2 compared to FOV center right after adjustment (for clarity, additional pairwise comparisons are omitted). Analyses were done using repeated measures ANOVA on ranks with *post-hoc* Student-Newman-Keuls method. Bars indicate mean ± 95% confidence interval. For details regarding the experimental methods see chapter III. Figure adapted from[219] with permission (compare also with Figure 3.2).

BIBLIOGRAPHY

1. Hyder AA, Wunderlich CA, Puvanachandra P, Gururaj G, Kobusingye OC. The impact of traumatic brain injuries: a global perspective. *NeuroRehabilitation*. 2007;22:341-353.
2. Feigin VL, Theadom A, Barker-Collo S, Starkey NJ, McPherson K, Kahan M, et al. Incidence of traumatic brain injury in New Zealand: a population-based study. *Lancet Neurol*. 2013;12:53-64.
3. Fleminger S, Ponsford J. Long term outcome after traumatic brain injury. *BMJ*. 2005;331:1419-1420.
4. Traumatic brain injury: time to end the silence. *Lancet Neurol*. 2010;9:331.
5. Maas AI, Stocchetti N, Bullock R. Moderate and severe traumatic brain injury in adults. *Lancet Neurol*. 2008;7:728-741.
6. Faul MD, Xu L, Wald MM, Coronado VG. Traumatic Brain Injury in the United States: Emergency Department Visits, Hospitalizations and Deaths 2002–2006. 2010
7. Coronado VG, McGuire LC, Sarmiento K, Bell J, Lionbarger MR, Jones CD, et al. Trends in Traumatic Brain Injury in the U.S. and the public health response: 1995-2009. *J Safety Res*. 2012;43:299-307.
8. Langlois JA, Rutland-Brown W, Wald MM. The epidemiology and impact of traumatic brain injury: a brief overview. *J Head Trauma Rehabil*. 2006;21:375-378.

9. Thurman DJ, Alverson C, Dunn KA, Guerrero J, Sniezek JE. Traumatic brain injury in the United States: A public health perspective. *J Head Trauma Rehabil*. 1999;14:602-615.

10. Peeters W, van den Brande R, Polinder S, Brazinova A, Steyerberg EW, Lingsma HF, et al. Epidemiology of traumatic brain injury in Europe. *Acta Neurochir (Wien)*. 2015;157:1683-1696.

11. Hillier SL, Hiller JE, Metzer J. Epidemiology of traumatic brain injury in South Australia. *Brain Inj*. 1997;11:649-659.

12. Corso P, Finkelstein E, Miller T, Fiebelkorn I, Zaloshnja E. Incidence and lifetime costs of injuries in the United States. *Inj Prev*. 2015;21:434-440.

13. McAllister TW, Sparling MB, Flashman LA, Guerin SJ, Mamourian AC, Saykin AJ. Differential working memory load effects after mild traumatic brain injury. *Neuroimage*. 2001;14:1004-1012.

14. Englander J, Hall K, Stimpson T, Chaffin S. Mild traumatic brain injury in an insured population: subjective complaints and return to employment. *Brain Inj*. 1992;6:161-166.

15. Stalnacke BM, Elgh E, Sojka P. One-year follow-up of mild traumatic brain injury: cognition, disability and life satisfaction of patients seeking consultation. *J Rehabil Med*. 2007;39:405-411.

16. Hoge CW, McGurk D, Thomas JL, Cox AL, Engel CC, Castro CA. Mild traumatic brain injury in U.S. Soldiers returning from Iraq. *N Engl J Med*. 2008;358:453-463.

17. Annegers JF, Hauser WA, Coan SP, Rocca WA. A population-based study of seizures after traumatic brain injuries. *N Engl J Med*. 1998;338:20-24.

18. Consensus conference. Rehabilitation of persons with traumatic brain injury. NIH Consensus Development Panel on Rehabilitation of Persons With Traumatic Brain Injury. *JAMA*. 1999;282:974-983.

19. Teasdale G, Jennett B. Assessment of coma and impaired consciousness. A practical scale. *Lancet*. 1974;2:81-84.

20. Baker SP, O'Neill B, Haddon W, Jr., Long WB. The injury severity score: a method for describing patients with multiple injuries and evaluating emergency care. *J Trauma*. 1974;14:187-196.

21. Marshall LF, Marshall SB, Klauber MR, Van Berkum Clark M, Eisenberg H, Jane JA, et al. The diagnosis of head injury requires a classification based on computed axial tomography. *J Neurotrauma*. 1992;9 Suppl 1:S287-292.

22. Maas AI, Hukkelhoven CW, Marshall LF, Steyerberg EW. Prediction of outcome in traumatic brain injury with computed tomographic characteristics: a comparison between the computed tomographic classification and combinations of computed tomographic predictors. *Neurosurgery*. 2005;57:1173-1182; discussion 1173-1182.

23. Collaborators MCT, Perel P, Arango M, Clayton T, Edwards P, Komolafe E, et al. Predicting outcome after traumatic brain injury: practical prognostic models based on large cohort of international patients. *BMJ*. 2008;336:425-429.

24. Steyerberg EW, Mushkudiani N, Perel P, Butcher I, Lu J, McHugh GS, et al. Predicting outcome after traumatic brain injury: development and international

validation of prognostic scores based on admission characteristics. *PLoS Med*. 2008;5:e165; discussion e165.

25. Aarabi B, Tofighi B, Kufera JA, Hadley J, Ahn ES, Cooper C, et al. Predictors of outcome in civilian gunshot wounds to the head. *J Neurosurg*. 2014;120:1138-1146.

26. Muehlschlegel S, Ayturk D, Ahlawat A, Izzy S, Scalea TM, Stein DM, et al. Predicting survival after acute civilian penetrating brain injuries: The SPIN score. *Neurology*. 2016;87:2244-2253.

27. Mehta AI, Grant GA, Marshall LF. Blast-induced traumatic brain injury and post-traumatic stress disorder. In: Morganti-Kossman C, Raghupathi R, Maas A, eds. *Traumatic Brain and Spinal Cord Injury. Challenges and Developments.* Cambridge: Cambridge University Press; 2012:30-42.

28. Teasdale G, Jennett B. Assessment and prognosis of coma after head injury. *Acta Neurochir (Wien)*. 1976;34:45-55.

29. Levin HS, Diaz-Arrastia RR. Diagnosis, prognosis, and clinical management of mild traumatic brain injury. *Lancet Neurol*. 2015;14:506-517.

30. Kornbluth J, Bhardwaj A. Evaluation of coma: a critical appraisal of popular scoring systems. *Neurocrit Care*. 2011;14:134-143.

31. Wijdicks EF, Bamlet WR, Maramattom BV, Manno EM, McClelland RL. Validation of a new coma scale: The FOUR score. *Ann Neurol*. 2005;58:585-593.

32. Krainin BM, Forsten RD, Kotwal RS, Lutz RH, Guskiewicz KM. Mild traumatic brain injury literature review and proposed changes to classification. *J Spec Oper Med*. 2011;11:38-47.

33. Joseph B, Pandit V, Aziz H, Kulvatunyou N, Zangbar B, Green DJ, et al. Mild traumatic brain injury defined by Glasgow Coma Scale: Is it really mild? *Brain Inj*. 2015;29:11-16.

34. Provenzale JM. Imaging of traumatic brain injury: a review of the recent medical literature. *AJR Am J Roentgenol*. 2010;194:16-19.

35. Johnson VE, Stewart W, Smith DH. Axonal pathology in traumatic brain injury. *Exp Neurol*. 2013;246:35-43.

36. Jones NR, Blumbergs PC, Brown CJ, McLean AJ, Manavis J, Perrett LV, et al. Correlation of postmortem MRI and CT appearances with neuropathology in brain trauma: a comparison of two methods. *J Clin Neurosci*. 1998;5:73-79.

37. Tu TW, Williams RA, Lescher JD, Jikaria N, Turtzo LC, Frank JA. Radiological-pathological correlation of diffusion tensor and magnetization transfer imaging in a closed head traumatic brain injury model. *Ann Neurol*. 2016;79:907-920.

38. Haberg AK, Olsen A, Moen KG, Schirmer-Mikalsen K, Visser E, Finnanger TG, et al. White matter microstructure in chronic moderate-to-severe traumatic brain injury: Impact of acute-phase injury-related variables and associations with outcome measures. *J Neurosci Res*. 2015;93:1109-1126.

39. Moen KG, Brezova V, Skandsen T, Haberg AK, Folvik M, Vik A. Traumatic axonal injury: the prognostic value of lesion load in corpus callosum, brain stem, and thalamus in different magnetic resonance imaging sequences. *J Neurotrauma*. 2014;31:1486-1496.

40. Moen KG, Skandsen T, Folvik M, Brezova V, Kvistad KA, Rydland J, et al. A longitudinal MRI study of traumatic axonal injury in patients with moderate and

severe traumatic brain injury. *J Neurol Neurosurg Psychiatry*. 2012;83:1193-1200.

41. Ommaya AK, Grubb RL, Jr., Naumann RA. Coup and contre-coup injury: observations on the mechanics of visible brain injuries in the rhesus monkey. *J Neurosurg*. 1971;35:503-516.
42. Ommaya AK, Goldsmith W, Thibault L. Biomechanics and neuropathology of adult and paediatric head injury. *Br J Neurosurg*. 2002;16:220-242.
43. Hemphill MA, Dauth S, Yu CJ, Dabiri BE, Parker KK. Traumatic brain injury and the neuronal microenvironment: a potential role for neuropathological mechanotransduction. *Neuron*. 2015;85:1177-1192.
44. Martin G. Traumatic brain injury: The first 15 milliseconds. *Brain Inj*. 2016;30:1517-1524.
45. Cepeda S, Gomez PA, Castano-Leon AM, Munarriz PM, Paredes I, Lagares A. Contrecoup Traumatic Intracerebral Hemorrhage: A Geometric Study of the Impact Site and Association with Hemorrhagic Progression. *J Neurotrauma*. 2016;33:1034-1046.
46. Blennow K, Hardy J, Zetterberg H. The neuropathology and neurobiology of traumatic brain injury. *Neuron*. 2012;76:886-899.
47. Cantu RC. Head injuries in sport. *Br J Sports Med*. 1996;30:289-296.
48. Gennarelli TA, Thibault LE, Adams JH, Graham DI, Thompson CJ, Marcincin RP. Diffuse axonal injury and traumatic coma in the primate. *Ann Neurol*. 1982;12:564-574.

49. Bauman RA, Ling G, Tong L, Januszkiewicz A, Agoston D, Delanerolle N, et al. An introductory characterization of a combat-casualty-care relevant swine model of closed head injury resulting from exposure to explosive blast. *J Neurotrauma*. 2009;26:841-860.

50. Lee H, Wintermark M, Gean AD, Ghajar J, Manley GT, Mukherjee P. Focal lesions in acute mild traumatic brain injury and neurocognitive outcome: CT versus 3T MRI. *J Neurotrauma*. 2008;25:1049-1056.

51. Bergsneider M, Hovda DA, Lee SM, Kelly DF, McArthur DL, Vespa PM, et al. Dissociation of cerebral glucose metabolism and level of consciousness during the period of metabolic depression following human traumatic brain injury. *J Neurotrauma*. 2000;17:389-401.

52. Vagnozzi R, Signoretti S, Cristofori L, Alessandrini F, Floris R, Isgro E, et al. Assessment of metabolic brain damage and recovery following mild traumatic brain injury: a multicentre, proton magnetic resonance spectroscopic study in concussed patients. *Brain*. 2010;133:3232-3242.

53. Vespa P, Bergsneider M, Hattori N, Wu HM, Huang SC, Martin NA, et al. Metabolic crisis without brain ischemia is common after traumatic brain injury: a combined microdialysis and positron emission tomography study. *J Cereb Blood Flow Metab*. 2005;25:763-774.

54. Adams JH, Graham DI, Murray LS, Scott G. Diffuse axonal injury due to nonmissile head injury in humans: an analysis of 45 cases. *Ann Neurol*. 1982;12:557-563.

55. Chodobski A, Zink BJ, Szmydynger-Chodobska J. Blood-brain barrier pathophysiology in traumatic brain injury. *Transl Stroke Res*. 2011;2:492-516.

56. Bouma GJ, Muizelaar JP, Stringer WA, Choi SC, Fatouros P, Young HF. Ultra-early evaluation of regional cerebral blood flow in severely head-injured patients using xenon-enhanced computerized tomography. *J Neurosurg*. 1992;77:360-368.

57. Henninger N, Sicard KM, Li Z, Kulkarni P, Dutzmann S, Urbanek C, et al. Differential recovery of behavioral status and brain function assessed with functional magnetic resonance imaging after mild traumatic brain injury in the rat. *Crit Care Med*. 2007;35:2607-2614.

58. DeWitt DS, Prough DS. Traumatic cerebral vascular injury: the effects of concussive brain injury on the cerebral vasculature. *J Neurotrauma*. 2003;20:795-825.

59. Bramlett HM, Dietrich WD, Green EJ. Secondary hypoxia following moderate fluid percussion brain injury in rats exacerbates sensorimotor and cognitive deficits. *J Neurotrauma*. 1999;16:1035-1047.

60. Long JA, Watts LT, Li W, Shen Q, Muir ER, Huang S, et al. The effects of perturbed cerebral blood flow and cerebrovascular reactivity on structural MRI and behavioral readouts in mild traumatic brain injury. *J Cereb Blood Flow Metab*. 2015;35:1852-1861.

61. Ostergaard L, Engedal TS, Aamand R, Mikkelsen R, Iversen NK, Anzabi M, et al. Capillary transit time heterogeneity and flow-metabolism coupling after traumatic brain injury. *J Cereb Blood Flow Metab*. 2014;34:1585-1598.

62. Bouma GJ, Muizelaar JP, Choi SC, Newlon PG, Young HF. Cerebral circulation and metabolism after severe traumatic brain injury: the elusive role of ischemia. *J Neurosurg*. 1991;75:685-693.

63. Bouma GJ, Muizelaar JP. Relationship between cardiac output and cerebral blood flow in patients with intact and with impaired autoregulation. *J Neurosurg*. 1990;73:368-374.

64. Overgaard J, Tweed WA. Cerebral circulation after head injury. 1. Cerebral blood flow and its regulation after closed head injury with emphasis on clinical correlations. *J Neurosurg*. 1974;41:531-541.

65. Golding EM, Steenberg ML, Contant CF, Jr., Krishnappa I, Robertson CS, Bryan RM, Jr. Cerebrovascular reactivity to CO(2) and hypotension after mild cortical impact injury. *Am J Physiol*. 1999;277:H1457-1466.

66. Junger EC, Newell DW, Grant GA, Avellino AM, Ghatan S, Douville CM, et al. Cerebral autoregulation following minor head injury. *J Neurosurg*. 1997;86:425-432.

67. Kontos HA, Wei EP, Navari RM, Levasseur JE, Rosenblum WI, Patterson JL, Jr. Responses of cerebral arteries and arterioles to acute hypotension and hypertension. *Am J Physiol*. 1978;234:H371-383.

68. Peppiatt CM, Howarth C, Mobbs P, Attwell D. Bidirectional control of CNS capillary diameter by pericytes. *Nature*. 2006;443:700-704.

69. Hill RA, Tong L, Yuan P, Murikinati S, Gupta S, Grutzendler J. Regional Blood Flow in the Normal and Ischemic Brain Is Controlled by Arteriolar Smooth Muscle Cell Contractility and Not by Capillary Pericytes. *Neuron*. 2015;87:95-110.

70. Czosnyka M, Balestreri M, Steiner L, Smielewski P, Hutchinson PJ, Matta B, et al. Age, intracranial pressure, autoregulation, and outcome after brain trauma. *J Neurosurg*. 2005;102:450-454.

71. Cold GE, Jensen FT. Cerebral autoregulation in unconscious patients with brain injury. *Acta Anaesthesiol Scand*. 1978;22:270-280.

72. Czosnyka M, Smielewski P, Kirkpatrick P, Menon DK, Pickard JD. Monitoring of cerebral autoregulation in head-injured patients. *Stroke*. 1996;27:1829-1834.

73. Czosnyka M, Smielewski P, Piechnik S, Steiner LA, Pickard JD. Cerebral autoregulation following head injury. *J Neurosurg*. 2001;95:756-763.

74. Enevoldsen EM, Jensen FT. Autoregulation and CO2 responses of cerebral blood flow in patients with acute severe head injury. *J Neurosurg*. 1978;48:689-703.

75. Muizelaar JP, Ward JD, Marmarou A, Newlon PG, Wachi A. Cerebral blood flow and metabolism in severely head-injured children. Part 2: Autoregulation. *J Neurosurg*. 1989;71:72-76.

76. Powers WJ. Cerebral blood flow and metabolism: Regulation and pathophysiology in cerebrovascular disease. In: Grotta JC, Albers GW, Broderick JP, Kasner SE, Lo EH, Medelow AD, Sacco RL, Wong LKS, eds. *Stroke. Pathophysiology, Diagnosis, and Management*. Elsevier; 2016.

77. Len TK, Neary JP. Cerebrovascular pathophysiology following mild traumatic brain injury. *Clin Physiol Funct Imaging*. 2011;31:85-93.

78. Toth P, Szarka N, Farkas E, Ezer E, Czeiter E, Amrein K, et al. Traumatic brain injury-induced autoregulatory dysfunction and spreading depression-related

neurovascular uncoupling: Pathomechanisms, perspectives, and therapeutic implications. *Am J Physiol Heart Circ Physiol*. 2016;311:H1118-H1131.

79. Rangel-Castilla L, Gasco J, Nauta HJ, Okonkwo DO, Robertson CS. Cerebral pressure autoregulation in traumatic brain injury. *Neurosurg Focus*. 2008;25:E7.

80. Bailey DM, Jones DW, Sinnott A, Brugniaux JV, New KJ, Hodson D, et al. Impaired cerebral haemodynamic function associated with chronic traumatic brain injury in professional boxers. *Clin Sci (Lond)*. 2013;124:177-189.

81. Bartnik-Olson BL, Holshouser B, Wang H, Grube M, Tong K, Wong V, et al. Impaired neurovascular unit function contributes to persistent symptoms after concussion: a pilot study. *J Neurotrauma*. 2014;31:1497-1506.

82. Golding EM, Robertson CS, Bryan RM, Jr. The consequences of traumatic brain injury on cerebral blood flow and autoregulation: a review. *Clin Exp Hypertens*. 1999;21:299-332.

83. Lee JH, Kelly DF, Oertel M, McArthur DL, Glenn TC, Vespa P, et al. Carbon dioxide reactivity, pressure autoregulation, and metabolic suppression reactivity after head injury: a transcranial Doppler study. *J Neurosurg*. 2001;95:222-232.

84. Girouard H, Iadecola C. Neurovascular coupling in the normal brain and in hypertension, stroke, and Alzheimer disease. *J Appl Physiol (1985)*. 2006;100:328-335.

85. Obrist WD, Gennarelli TA, Segawa H, Dolinskas CA, Langfitt TW. Relation of cerebral blood flow to neurological status and outcome in head-injured patients. *J Neurosurg*. 1979;51:292-300.

86. Coles JP, Fryer TD, Smielewski P, Chatfield DA, Steiner LA, Johnston AJ, et al. Incidence and mechanisms of cerebral ischemia in early clinical head injury. *J Cereb Blood Flow Metab*. 2004;24:202-211.

87. Kelly DF, Kordestani RK, Martin NA, Nguyen T, Hovda DA, Bergsneider M, et al. Hyperemia following traumatic brain injury: relationship to intracranial hypertension and outcome. *J Neurosurg*. 1996;85:762-771.

88. Martin NA, Patwardhan RV, Alexander MJ, Africk CZ, Lee JH, Shalmon E, et al. Characterization of cerebral hemodynamic phases following severe head trauma: hypoperfusion, hyperemia, and vasospasm. *J Neurosurg*. 1997;87:9-19.

89. Bruce DA, Langfitt TW, Miller JD, Schutz H, Vapalahti MP, Stanek A, et al. Regional cerebral blood flow, intracranial pressure, and brain metabolism in comatose patients. *J Neurosurg*. 1973;38:131-144.

90. Tarantini S, Hertelendy P, Tucsek Z, Valcarcel-Ares MN, Smith N, Menyhart A, et al. Pharmacologically-induced neurovascular uncoupling is associated with cognitive impairment in mice. *J Cereb Blood Flow Metab*. 2015;35:1871-1881.

91. Wei EP, Dietrich WD, Povlishock JT, Navari RM, Kontos HA. Functional, morphological, and metabolic abnormalities of the cerebral microcirculation after concussive brain injury in cats. *Circ Res*. 1980;46:37-47.

92. Leao AAP. Spreading depression of activity in the cerebral cortex. *J Neurophysiol*. 1944;7:359-390.

93. Leao AAP. Pial circulation and spreading depression of activity in the cerebral cortex. *J Neurophysiol*. 1944;7:391-396.

94. Ayata C, Lauritzen M. Spreading Depression, Spreading Depolarizations, and the Cerebral Vasculature. *Physiol Rev*. 2015;95:953-993.

95. Lauritzen M, Dreier JP, Fabricius M, Hartings JA, Graf R, Strong AJ. Clinical relevance of cortical spreading depression in neurological disorders: migraine, malignant stroke, subarachnoid and intracranial hemorrhage, and traumatic brain injury. *J Cereb Blood Flow Metab*. 2011;31:17-35.

96. Dreier JP. The role of spreading depression, spreading depolarization and spreading ischemia in neurological disease. *Nat Med*. 2011;17:439-447.

97. Dreier JP, Major S, Manning A, Woitzik J, Drenckhahn C, Steinbrink J, et al. Cortical spreading ischaemia is a novel process involved in ischaemic damage in patients with aneurysmal subarachnoid haemorrhage. *Brain*. 2009;132:1866-1881.

98. Dreier JP, Woitzik J, Fabricius M, Bhatia R, Major S, Drenckhahn C, et al. Delayed ischaemic neurological deficits after subarachnoid haemorrhage are associated with clusters of spreading depolarizations. *Brain*. 2006;129:3224-3237.

99. Nakamura H, Strong AJ, Dohmen C, Sakowitz OW, Vollmar S, Sue M, et al. Spreading depolarizations cycle around and enlarge focal ischaemic brain lesions. *Brain*. 2010;133:1994-2006.

100. Hinzman JM, Wilson JA, Mazzeo AT, Bullock MR, Hartings JA. Excitotoxicity and Metabolic Crisis Are Associated with Spreading Depolarizations in Severe Traumatic Brain Injury Patients. *J Neurotrauma*. 2016;33:1775-1783.

101. Hartings JA, Bullock MR, Okonkwo DO, Murray LS, Murray GD, Fabricius M, et al. Spreading depolarisations and outcome after traumatic brain injury: a prospective observational study. *Lancet Neurol*. 2011;10:1058-1064.

102. Hartings JA, Watanabe T, Bullock MR, Okonkwo DO, Fabricius M, Woitzik J, et al. Spreading depolarizations have prolonged direct current shifts and are associated with poor outcome in brain trauma. *Brain*. 2011;134:1529-1540.

103. Hartings JA, Wilson JA, Hinzman JM, Pollandt S, Dreier JP, DiNapoli V, et al. Spreading depression in continuous electroencephalography of brain trauma. *Ann Neurol*. 2014;76:681-694.

104. Takahashi H, Nakazawa S. Specific type of head injury in children. Report of 5 cases. *Childs Brain*. 1980;7:124-131.

105. Sato S, Kawauchi S, Okuda W, Nishidate I, Nawashiro H, Tsumatori G. Real-time optical diagnosis of the rat brain exposed to a laser-induced shock wave: observation of spreading depolarization, vasoconstriction and hypoxemia-oligemia. *PLoS One*. 2014;9:e82891.

106. Wang JT, Medress ZA, Barres BA. Axon degeneration: molecular mechanisms of a self-destruction pathway. *J Cell Biol*. 2012;196:7-18.

107. Warner MA, Marquez de la Plata C, Spence J, Wang JY, Harper C, Moore C, et al. Assessing spatial relationships between axonal integrity, regional brain volumes, and neuropsychological outcomes after traumatic axonal injury. *J Neurotrauma*. 2010;27:2121-2130.

108. Adams JH, Doyle D, Ford I, Gennarelli TA, Graham DI, McLellan DR. Diffuse axonal injury in head injury: definition, diagnosis and grading. *Histopathology*. 1989;15:49-59.

109. Povlishock JT. Traumatically induced axonal injury: pathogenesis and pathobiological implications. *Brain Pathol*. 1992;2:1-12.

110. Smith DH, Meaney DF, Shull WH. Diffuse axonal injury in head trauma. *J Head Trauma Rehabil*. 2003;18:307-316.

111. Smith DH, Hicks R, Povlishock JT. Therapy development for diffuse axonal injury. *J Neurotrauma*. 2013;30:307-323.

112. Johnson VE, Stewart W, Smith DH. Axonal pathology in traumatic brain injury. *Exp Neurol*. 2012

113. Rosenblath W. Über einen bemerkenswerten Fall von Hirnerschütterung (aus dem Landeskrankenhaus Cassel). *Dtsch. Arch. klin. Med.* 1899;64:406-422.

114. Rand CW, Courville CB. Histologic changes in the brain in cases of fatal injury to the head; alterations in nerve cells. *Arch Neurol Psychiatry*. 1946;55:79-110.

115. Strich SJ. Diffuse degeneration of the cerebral white matter in severe dementia following head injury. *J Neurol Neurosurg Psychiatry*. 1956;19:163-185.

116. Strich SJ. Shearing of nerve fibers as a cause of brain damage due to head injury. A Pathological Study of Twenty Cases. *Lancet*. 1961;278:443–448.

117. Nevin NC. Neuropathological changes in the white matter following head injury. *J Neuropathol Exp Neurol*. 1967;26:77-84.

118. Oppenheimer DR. Microscopic lesions in the brain following head injury. *J Neurol Neurosurg Psychiatry*. 1968;31:299-306.

119. Peerless SJ, Rewcastle NB. Shear injuries of the brain. *Can Med Assoc J*. 1967;96:577-582.

120. Adams JH, Doyle D, Graham DI, Lawrence AE, McLellan DR. Diffuse axonal injury in head injuries caused by a fall. *Lancet*. 1984;2:1420-1422.

121. Sherriff FE, Bridges LR, Sivaloganathan S. Early detection of axonal injury after human head trauma using immunocytochemistry for beta-amyloid precursor protein. *Acta Neuropathol*. 1994;87:55-62.

122. Gentleman SM, Nash MJ, Sweeting CJ, Graham DI, Roberts GW. Beta-amyloid precursor protein (beta APP) as a marker for axonal injury after head injury. *Neurosci Lett*. 1993;160:139-144.

123. Graham DI, Smith C, Reichard R, Leclercq PD, Gentleman SM. Trials and tribulations of using beta-amyloid precursor protein immunohistochemistry to evaluate traumatic brain injury in adults. *Forensic Sci Int*. 2004;146:89-96.

124. Gentleman SM, Roberts GW, Gennarelli TA, Maxwell WL, Adams JH, Kerr S, et al. Axonal injury: a universal consequence of fatal closed head injury? *Acta Neuropathol*. 1995;89:537-543.

125. Chen XH, Johnson VE, Uryu K, Trojanowski JQ, Smith DH. A lack of amyloid beta plaques despite persistent accumulation of amyloid beta in axons of long-term survivors of traumatic brain injury. *Brain Pathol*. 2009;19:214-223.

126. Stone JR, Singleton RH, Povlishock JT. Antibodies to the C-terminus of the beta-amyloid precursor protein (APP): a site specific marker for the detection of traumatic axonal injury. *Brain Res*. 2000;871:288-302.

127. Hortobagyi T, Wise S, Hunt N, Cary N, Djurovic V, Fegan-Earl A, et al. Traumatic axonal damage in the brain can be detected using beta-APP immunohistochemistry within 35 min after head injury to human adults. *Neuropathol Appl Neurobiol*. 2007;33:226-237.

128. Geddes JF, Whitwell HL, Graham DI. Traumatic axonal injury: practical issues for diagnosis in medicolegal cases. *Neuropathol Appl Neurobiol*. 2000;26:105-116.

129. Yaghmai A, Povlishock J. Traumatically induced reactive change as visualized through the use of monoclonal antibodies targeted to neurofilament subunits. *J Neuropathol Exp Neurol*. 1992;51:158-176.

130. Grady MS, McLaughlin MR, Christman CW, Valadka AB, Fligner CL, Povlishock JT. The use of antibodies targeted against the neurofilament subunits for the detection of diffuse axonal injury in humans. *J Neuropathol Exp Neurol*. 1993;52:143-152.

131. Schweitzer JB, Park MR, Einhaus SL, Robertson JT. Ubiquitin marks the reactive swellings of diffuse axonal injury. *Acta Neuropathol*. 1993;85:503-507.

132. Uryu K, Chen XH, Martinez D, Browne KD, Johnson VE, Graham DI, et al. Multiple proteins implicated in neurodegenerative diseases accumulate in axons after brain trauma in humans. *Exp Neurol*. 2007;208:185-192.

133. Stone JR, Singleton RH, Povlishock JT. Intra-axonal neurofilament compaction does not evoke local axonal swelling in all traumatically injured axons. *Exp Neurol*. 2001;172:320-331.

134. Buki A, Okonkwo DO, Wang KK, Povlishock JT. Cytochrome c release and caspase activation in traumatic axonal injury. *J Neurosci*. 2000;20:2825-2834.

135. Buki A, Siman R, Trojanowski JQ, Povlishock JT. The role of calpain-mediated spectrin proteolysis in traumatically induced axonal injury. *J Neuropathol Exp Neurol*. 1999;58:365-375.

136. Povlishock JT, Becker DP, Cheng CL, Vaughan GW. Axonal change in minor head injury. *J Neuropathol Exp Neurol*. 1983;42:225-242.

137. Tang-Schomer MD, Johnson VE, Baas PW, Stewart W, Smith DH. Partial interruption of axonal transport due to microtubule breakage accounts for the formation of periodic varicosities after traumatic axonal injury. *Exp Neurol*. 2012;233:364-372.

138. Li S, Sun Y, Shan D, Feng B, Xing J, Duan Y, et al. Temporal profiles of axonal injury following impact acceleration traumatic brain injury in rats--a comparative study with diffusion tensor imaging and morphological analysis. *Int J Legal Med*. 2013;127:159-167.

139. Christman CW, Grady MS, Walker SA, Holloway KL, Povlishock JT. Ultrastructural studies of diffuse axonal injury in humans. *J Neurotrauma*. 1994;11:173-186.

140. Tang-Schomer MD, Patel AR, Baas PW, Smith DH. Mechanical breaking of microtubules in axons during dynamic stretch injury underlies delayed elasticity, microtubule disassembly, and axon degeneration. *FASEB J*. 2010;24:1401-1410.

141. Smith DH, Wolf JA, Lusardi TA, Lee VM, Meaney DF. High tolerance and delayed elastic response of cultured axons to dynamic stretch injury. *J Neurosci*. 1999;19:4263-4269.

142. Greer JE, Hanell A, McGinn MJ, Povlishock JT. Mild traumatic brain injury in the mouse induces axotomy primarily within the axon initial segment. *Acta Neuropathol*. 2013;126:59-74.

143. Perrot R, Berges R, Bocquet A, Eyer J. Review of the multiple aspects of neurofilament functions, and their possible contribution to neurodegeneration. *Mol Neurobiol*. 2008;38:27-65.

144. Siedler DG, Chuah MI, Kirkcaldie MT, Vickers JC, King AE. Diffuse axonal injury in brain trauma: insights from alterations in neurofilaments. *Front Cell Neurosci*. 2014;8:429.

145. Fournier AJ, Rajbhandari L, Shrestha S, Venkatesan A, Ramesh KT. In vitro and in situ visualization of cytoskeletal deformation under load: traumatic axonal injury. *FASEB J*. 2014;28:5277-5287.

146. Povlishock JT, Marmarou A, McIntosh T, Trojanowski JQ, Moroi J. Impact acceleration injury in the rat: evidence for focal axolemmal change and related neurofilament sidearm alteration. *J Neuropathol Exp Neurol*. 1997;56:347-359.

147. Okonkwo DO, Pettus EH, Moroi J, Povlishock JT. Alteration of the neurofilament sidearm and its relation to neurofilament compaction occurring with traumatic axonal injury. *Brain Res*. 1998;784:1-6.

148. Pettus EH, Povlishock JT. Characterization of a distinct set of intra-axonal ultrastructural changes associated with traumatically induced alteration in axolemmal permeability. *Brain Res*. 1996;722:1-11.

149. DiLeonardi AM, Huh JW, Raghupathi R. Impaired axonal transport and neurofilament compaction occur in separate populations of injured axons following diffuse brain injury in the immature rat. *Brain Res*. 2009;1263:174-182.

150. Rostami E, Davidsson J, Ng KC, Lu J, Gyorgy A, Walker J, et al. A Model for Mild Traumatic Brain Injury that Induces Limited Transient Memory Impairment and Increased Levels of Axon Related Serum Biomarkers. *Front Neurol*. 2012;3:115.

151. Zetterberg H, Blennow K. Fluid biomarkers for mild traumatic brain injury and related conditions. *Nat Rev Neurol*. 2016;12:563-574.

152. Anderson KJ, Scheff SW, Miller KM, Roberts KN, Gilmer LK, Yang C, et al. The phosphorylated axonal form of the neurofilament subunit NF-H (pNF-H) as a blood biomarker of traumatic brain injury. *J Neurotrauma*. 2008;25:1079-1085.

153. Zurek J, Bartlova L, Fedora M. Hyperphosphorylated neurofilament NF-H as a predictor of mortality after brain injury in children. *Brain Inj*. 2011;25:221-226.

154. Yokobori S, Hosein K, Burks S, Sharma I, Gajavelli S, Bullock R. Biomarkers for the clinical differential diagnosis in traumatic brain injury--a systematic review. *CNS Neurosci Ther*. 2013;19:556-565.

155. Wolf JA, Stys PK, Lusardi T, Meaney D, Smith DH. Traumatic axonal injury induces calcium influx modulated by tetrodotoxin-sensitive sodium channels. *J Neurosci*. 2001;21:1923-1930.

156. Maxwell WL, Watt C, Pediani JD, Graham DI, Adams JH, Gennarelli TA. Localisation of calcium ions and calcium-ATPase activity within myelinated nerve fibres of the adult guinea-pig optic nerve. *J Anat*. 1991;176:71-79.

157. Maxwell WL, McCreath BJ, Graham DI, Gennarelli TA. Cytochemical evidence for redistribution of membrane pump calcium-ATPase and ecto-Ca-ATPase activity, and calcium influx in myelinated nerve fibres of the optic nerve after stretch injury. *J Neurocytol*. 1995;24:925-942.

158. Maxwell WL, Kosanlavit R, McCreath BJ, Reid O, Graham DI. Freeze-fracture and cytochemical evidence for structural and functional alteration in the axolemma and myelin sheath of adult guinea pig optic nerve fibers after stretch injury. *J Neurotrauma*. 1999;16:273-284.

159. Iwata A, Stys PK, Wolf JA, Chen XH, Taylor AG, Meaney DF, et al. Traumatic axonal injury induces proteolytic cleavage of the voltage-gated sodium channels modulated by tetrodotoxin and protease inhibitors. *J Neurosci*. 2004;24:4605-4613.

160. Staal JA, Dickson TC, Gasperini R, Liu Y, Foa L, Vickers JC. Initial calcium release from intracellular stores followed by calcium dysregulation is linked to secondary axotomy following transient axonal stretch injury. *J Neurochem*. 2010;112:1147-1155.

161. Johnson GV, Litersky JM, Jope RS. Degradation of microtubule-associated protein 2 and brain spectrin by calpain: a comparative study. *J Neurochem*. 1991;56:1630-1638.

162. Billger M, Wallin M, Karlsson JO. Proteolysis of tubulin and microtubule-associated proteins 1 and 2 by calpain I and II. Difference in sensitivity of assembled and disassembled microtubules. *Cell Calcium*. 1988;9:33-44.

163. Huh JW, Franklin MA, Widing AG, Raghupathi R. Regionally distinct patterns of calpain activation and traumatic axonal injury following contusive brain injury in immature rats. *Dev Neurosci*. 2006;28:466-476.

164. Kupina NC, Nath R, Bernath EE, Inoue J, Mitsuyoshi A, Yuen PW, et al. The novel calpain inhibitor SJA6017 improves functional outcome after delayed administration in a mouse model of diffuse brain injury. *J Neurotrauma*. 2001;18:1229-1240.

165. McGinn MJ, Kelley BJ, Akinyi L, Oli MW, Liu MC, Hayes RL, et al. Biochemical, structural, and biomarker evidence for calpain-mediated cytoskeletal change after diffuse brain injury uncomplicated by contusion. *J Neuropathol Exp Neurol*. 2009;68:241-249.

166. Saatman KE, Murai H, Bartus RT, Smith DH, Hayward NJ, Perri BR, et al. Calpain inhibitor AK295 attenuates motor and cognitive deficits following experimental brain injury in the rat. *Proc Natl Acad Sci U S A*. 1996;93:3428-3433.

167. Saatman KE, Abai B, Grosvenor A, Vorwerk CK, Smith DH, Meaney DF. Traumatic axonal injury results in biphasic calpain activation and retrograde transport impairment in mice. *J Cereb Blood Flow Metab*. 2003;23:34-42.

168. von Reyn CR, Spaethling JM, Mesfin MN, Ma M, Neumar RW, Smith DH, et al. Calpain mediates proteolysis of the voltage-gated sodium channel alpha-subunit. *J Neurosci*. 2009;29:10350-10356.

169. Saatman KE, Zhang C, Bartus RT, McIntosh TK. Behavioral efficacy of posttraumatic calpain inhibition is not accompanied by reduced spectrin

proteolysis, cortical lesion, or apoptosis. *J Cereb Blood Flow Metab*. 2000;20:66-73.

170. Coleman MP, Freeman MR. Wallerian degeneration, wld(s), and nmnat. *Annu Rev Neurosci*. 2010;33:245-267.

171. Beirowski B, Adalbert R, Wagner D, Grumme DS, Addicks K, Ribchester RR, et al. The progressive nature of Wallerian degeneration in wild-type and slow Wallerian degeneration (WldS) nerves. *BMC Neurosci*. 2005;6:6.

172. Kerschensteiner M, Schwab ME, Lichtman JW, Misgeld T. In vivo imaging of axonal degeneration and regeneration in the injured spinal cord. *Nat Med*. 2005;11:572-577.

173. Waller AV. Experiments on the section of the glossopharyngeal and hypoglossal nerves of the frog, and observations of the alterations produced thereby in the structure of their primitive fibres. *Philos. Trans. R. Soc. Lond.* 1850;140:423–429.

174. Maxwell WL, Bartlett E, Morgan H. Wallerian degeneration in the optic nerve stretch-injury model of traumatic brain injury: a stereological analysis. *J Neurotrauma*. 2015;32:780-790.

175. Coleman M. Axon degeneration mechanisms: commonality amid diversity. *Nat Rev Neurosci*. 2005;6:889-898.

176. Avery MA, Rooney TM, Pandya JD, Wishart TM, Gillingwater TH, Geddes JW, et al. WldS prevents axon degeneration through increased mitochondrial flux and enhanced mitochondrial Ca2+ buffering. *Curr Biol*. 2012;22:596-600.

177. Lunn ER, Perry VH, Brown MC, Rosen H, Gordon S. Absence of Wallerian Degeneration does not Hinder Regeneration in Peripheral Nerve. *Eur J Neurosci*. 1989;1:27-33.

178. Fox GB, Faden AI. Traumatic brain injury causes delayed motor and cognitive impairment in a mutant mouse strain known to exhibit delayed Wallerian degeneration. *J Neurosci Res*. 1998;53:718-727.

179. Conforti L, Gilley J, Coleman MP. Wallerian degeneration: an emerging axon death pathway linking injury and disease. *Nat Rev Neurosci*. 2014;15:394-409.

180. Osterloh JM, Yang J, Rooney TM, Fox AN, Adalbert R, Powell EH, et al. dSarm/Sarm1 is required for activation of an injury-induced axon death pathway. *Science*. 2012;337:481-484.

181. Gerdts J, Summers DW, Milbrandt J, DiAntonio A. Axon Self-Destruction: New Links among SARM1, MAPKs, and NAD+ Metabolism. *Neuron*. 2016;89:449-460.

182. Mink M, Fogelgren B, Olszewski K, Maroy P, Csiszar K. A novel human gene (SARM) at chromosome 17q11 encodes a protein with a SAM motif and structural similarity to Armadillo/beta-catenin that is conserved in mouse, Drosophila, and Caenorhabditis elegans. *Genomics*. 2001;74:234-244.

183. Kim Y, Zhou P, Qian L, Chuang JZ, Lee J, Li C, et al. MyD88-5 links mitochondria, microtubules, and JNK3 in neurons and regulates neuronal survival. *J Exp Med*. 2007;204:2063-2074.

184. Lin CW, Liu HY, Chen CY, Hsueh YP. Neuronally-expressed Sarm1 regulates expression of inflammatory and antiviral cytokines in brains. *Innate Immun*. 2014;20:161-172.

185. Chen CY, Lin CW, Chang CY, Jiang ST, Hsueh YP. Sarm1, a negative regulator of innate immunity, interacts with syndecan-2 and regulates neuronal morphology. *J Cell Biol*. 2011;193:769-784.

186. Geisler S, Doan RA, Strickland A, Huang X, Milbrandt J, DiAntonio A. Prevention of vincristine-induced peripheral neuropathy by genetic deletion of SARM1 in mice. *Brain*. 2016;139:3092-3108.

187. Massoll C, Mando W, Chintala SK. Excitotoxicity upregulates SARM1 protein expression and promotes Wallerian-like degeneration of retinal ganglion cells and their axons. *Invest Ophthalmol Vis Sci*. 2013;54:2771-2780.

188. Xiong Y, Mahmood A, Chopp M. Animal models of traumatic brain injury. *Nat Rev Neurosci*. 2013;14:128-142.

189. Marklund N, Hillered L. Animal modelling of traumatic brain injury in preclinical drug development: where do we go from here? *Br J Pharmacol*. 2011;164:1207-1229.

190. Morales DM, Marklund N, Lebold D, Thompson HJ, Pitkanen A, Maxwell WL, et al. Experimental models of traumatic brain injury: do we really need to build a better mousetrap? *Neuroscience*. 2005;136:971-989.

191. Flierl MA, Stahel PF, Beauchamp KM, Morgan SJ, Smith WR, Shohami E. Mouse closed head injury model induced by a weight-drop device. *Nat Protoc*. 2009;4:1328-1337.

192. Wang HC, Duan ZX, Wu FF, Xie L, Zhang H, Ma YB. A new rat model for diffuse axonal injury using a combination of linear acceleration and angular acceleration. *J Neurotrauma*. 2010;27:707-719.

193. Marmarou A, Foda MA, van den Brink W, Campbell J, Kita H, Demetriadou K. A new model of diffuse brain injury in rats. Part I: Pathophysiology and biomechanics. *J Neurosurg*. 1994;80:291-300.

194. Greer JE, McGinn MJ, Povlishock JT. Diffuse traumatic axonal injury in the mouse induces atrophy, c-Jun activation, and axonal outgrowth in the axotomized neuronal population. *J Neurosci*. 2011;31:5089-5105.

195. Smith DH, Soares HD, Pierce JS, Perlman KG, Saatman KE, Meaney DF, et al. A model of parasagittal controlled cortical impact in the mouse: cognitive and histopathologic effects. *J Neurotrauma*. 1995;12:169-178.

196. Sullivan PG, Bruce-Keller AJ, Rabchevsky AG, Christakos S, Clair DK, Mattson MP, et al. Exacerbation of damage and altered NF-kappaB activation in mice lacking tumor necrosis factor receptors after traumatic brain injury. *J Neurosci*. 1999;19:6248-6256.

197. Hunt RF, Boychuk JA, Smith BN. Neural circuit mechanisms of post-traumatic epilepsy. *Front Cell Neurosci*. 2013;7:89.

198. Hunt RF, Scheff SW, Smith BN. Regionally localized recurrent excitation in the dentate gyrus of a cortical contusion model of posttraumatic epilepsy. *J Neurophysiol*. 2010;103:1490-1500.

199. Goldstein LE, Fisher AM, Tagge CA, Zhang XL, Velisek L, Sullivan JA, et al. Chronic traumatic encephalopathy in blast-exposed military veterans and a blast neurotrauma mouse model. *Sci Transl Med*. 2012;4:134ra160.

200. Heldt SA, Elberger AJ, Deng Y, Guley NH, Del Mar N, Rogers J, et al. A novel closed-head model of mild traumatic brain injury caused by primary overpressure blast to the cranium produces sustained emotional deficits in mice. *Front Neurol*. 2014;5:2.

201. Wang Y, Wei Y, Oguntayo S, Wilkins W, Arun P, Valiyaveettil M, et al. Tightly coupled repetitive blast-induced traumatic brain injury: development and characterization in mice. *J Neurotrauma*. 2011;28:2171-2183.

202. Chen Y, Constantini S, Trembovler V, Weinstock M, Shohami E. An experimental model of closed head injury in mice: pathophysiology, histopathology, and cognitive deficits. *J Neurotrauma*. 1996;13:557-568.

203. Hall ED. High-dose glucocorticoid treatment improves neurological recovery in head-injured mice. *J Neurosurg*. 1985;62:882-887.

204. Zohar O, Schreiber S, Getslev V, Schwartz JP, Mullins PG, Pick CG. Closed-head minimal traumatic brain injury produces long-term cognitive deficits in mice. *Neuroscience*. 2003;118:949-955.

205. Tang YP, Noda Y, Hasegawa T, Nabeshima T. A concussive-like brain injury model in mice (II): selective neuronal loss in the cortex and hippocampus. *J Neurotrauma*. 1997;14:863-873.

206. Tang YP, Noda Y, Hasegawa T, Nabeshima T. A concussive-like brain injury model in mice (I): impairment in learning and memory. *J Neurotrauma*. 1997;14:851-862.

207. Yatsiv I, Morganti-Kossmann MC, Perez D, Dinarello CA, Novick D, Rubinstein M, et al. Elevated intracranial IL-18 in humans and mice after traumatic brain injury and evidence of neuroprotective effects of IL-18-binding protein after experimental closed head injury. *J Cereb Blood Flow Metab*. 2002;22:971-978.

208. Albert-Weissenberger C, Varrallyay C, Raslan F, Kleinschnitz C, Siren AL. An experimental protocol for mimicking pathomechanisms of traumatic brain injury in mice. *Exp Transl Stroke Med*. 2012;4:1.

209. Tsenter J, Beni-Adani L, Assaf Y, Alexandrovich AG, Trembovler V, Shohami E. Dynamic changes in the recovery after traumatic brain injury in mice: effect of injury severity on T2-weighted MRI abnormalities, and motor and cognitive functions. *J Neurotrauma*. 2008;25:324-333.

210. Beni-Adani L, Gozes I, Cohen Y, Assaf Y, Steingart RA, Brenneman DE, et al. A peptide derived from activity-dependent neuroprotective protein (ADNP) ameliorates injury response in closed head injury in mice. *J Pharmacol Exp Ther*. 2001;296:57-63.

211. Creeley CE, Wozniak DF, Bayly PV, Olney JW, Lewis LM. Multiple episodes of mild traumatic brain injury result in impaired cognitive performance in mice. *Acad Emerg Med*. 2004;11:809-819.

212. DeFord SM, Wilson MS, Rice AC, Clausen T, Rice LK, Barabnova A, et al. Repeated mild brain injuries result in cognitive impairment in B6C3F1 mice. *J Neurotrauma*. 2002;19:427-438.

213. Ojo JO, Mouzon B, Greenberg MB, Bachmeier C, Mullan M, Crawford F. Repetitive mild traumatic brain injury augments tau pathology and glial activation in aged hTau mice. *J Neuropathol Exp Neurol*. 2013;72:137-151.

214. Ojo JO, Mouzon BC, Crawford F. Repetitive head trauma, chronic traumatic encephalopathy and tau: Challenges in translating from mice to men. *Exp Neurol*. 2015

215. Mouzon BC, Bachmeier C, Ferro A, Ojo JO, Crynen G, Acker CM, et al. Chronic neuropathological and neurobehavioral changes in a repetitive mild traumatic brain injury model. *Ann Neurol*. 2014;75:241-254.

216. McKee AC, Stern RA, Nowinski CJ, Stein TD, Alvarez VE, Daneshvar DH, et al. The spectrum of disease in chronic traumatic encephalopathy. *Brain*. 2013;136:43-64.

217. Henninger N, Dutzmann S, Sicard KM, Kollmar R, Bardutzky J, Schwab S. Impaired spatial learning in a novel rat model of mild cerebral concussion injury. *Exp Neurol*. 2005;195:447-457.

218. Paxinos G, Franklin KBJ. *The Mouse Brain in Stereotaxic Coordinates*. Amsterdam: Elsevier Academic Press; 2013.

219. Henninger N, Bouley J, Sikoglu EM, An J, Moore CM, King JA, et al. Attenuated traumatic axonal injury and improved functional outcome after traumatic brain injury in mice lacking Sarm1. *Brain*. 2016;139:1094-1105.

220. Henninger N, Bouley J, Bratane BT, Bastan B, Shea M, Fisher M. Laser Doppler flowmetry predicts occlusion but not tPA-mediated reperfusion success after rat embolic stroke. *Exp Neurol*. 2009;215:290-297.

221. Samoriski GM, Applegate CD. Repeated generalized seizures induce time-dependent changes in the behavioral seizure response independent of continued seizure induction. *J Neurosci*. 1997;17:5581-5590.

222. Wang J, Hamm RJ, Povlishock JT. Traumatic axonal injury in the optic nerve: evidence for axonal swelling, disconnection, dieback, and reorganization. *J Neurotrauma*. 2011;28:1185-1198.

223. Kenney K, Amyot F, Haber M, Pronger A, Bogoslovsky T, Moore C, et al. Cerebral Vascular Injury in Traumatic Brain Injury. *Exp Neurol*. 2016;275 Pt 3:353-366.

224. Ayata C, Shin HK, Salomone S, Ozdemir-Gursoy Y, Boas DA, Dunn AK, et al. Pronounced hypoperfusion during spreading depression in mouse cortex. *J Cereb Blood Flow Metab*. 2004;24:1172-1182.

225. Woitzik J, Hecht N, Pinczolits A, Sandow N, Major S, Winkler MK, et al. Propagation of cortical spreading depolarization in the human cortex after malignant stroke. *Neurology*. 2013;80:1095-1102.

226. Kaufmann D, Theriot JJ, Zyuzin J, Service CA, Chang JC, Tang YT, et al. Heterogeneous incidence and propagation of spreading depolarizations. *J Cereb Blood Flow Metab*. 2016:271678X16659496.

227. Matsuura T, Bures J. The minimum volume of depolarized neural tissue required for triggering cortical spreading depression in rat. *Exp Brain Res*. 1971;12:238-249.

228. Bayly PV, Black EE, Pedersen RC, Leister EP, Genin GM. In vivo imaging of rapid deformation and strain in an animal model of traumatic brain injury. *J Biomech*. 2006;39:1086-1095.

229. Levchakov A, Linder-Ganz E, Raghupathi R, Margulies SS, Gefen A. Computational studies of strain exposures in neonate and mature rat brains during closed head impact. *J Neurotrauma*. 2006;23:1570-1580.

230. Altamura C, Dell'Acqua ML, Moessner R, Murphy DL, Lesch KP, Persico AM. Altered neocortical cell density and layer thickness in serotonin transporter knockout mice: a quantitation study. *Cereb Cortex*. 2007;17:1394-1401.

231. Dreier JP, Reiffurth C. The stroke-migraine depolarization continuum. *Neuron*. 2015;86:902-922.

232. Schott GD. Exploring the visual hallucinations of migraine aura: the tacit contribution of illustration. *Brain*. 2007;130:1690-1703.

233. Hansen JM, Baca SM, Vanvalkenburgh P, Charles A. Distinctive anatomical and physiological features of migraine aura revealed by 18 years of recording. *Brain*. 2013;136:3589-3595.

234. von Baumgarten L, Trabold R, Thal S, Back T, Plesnila N. Role of cortical spreading depressions for secondary brain damage after traumatic brain injury in mice. *J Cereb Blood Flow Metab*. 2008;28:1353-1360.

235. Kager H, Wadman WJ, Somjen GG. Conditions for the triggering of spreading depression studied with computer simulations. *J Neurophysiol*. 2002;88:2700-2712.

236. Back T, Nedergaard M, Ginsberg MD. The ischemic penumbra. Pathophysiology and relevance of spreading depression-like phenomena. In: Ginsberg MD, Bogousslavsky J, eds. *Cerebrovascular disease: Pathophysiology, Diagnosis, and Management.*: Blackwell Science; 1998:276-286.

237. Lauritzen M, Rice ME, Okada Y, Nicholson C. Quisqualate, kainate and NMDA can initiate spreading depression in the turtle cerebellum. *Brain Res*. 1988;475:317-327.

238. Grafstein B. Mechanism of spreading cortical depression. *J Neurophysiol*. 1956;19:154-171.

239. Largo C, Ibarz JM, Herreras O. Effects of the gliotoxin fluorocitrate on spreading depression and glial membrane potential in rat brain in situ. *J Neurophysiol*. 1997;78:295-307.

240. De Fusco M, Marconi R, Silvestri L, Atorino L, Rampoldi L, Morgante L, et al. Haploinsufficiency of ATP1A2 encoding the Na+/K+ pump alpha2 subunit associated with familial hemiplegic migraine type 2. *Nat Genet*. 2003;33:192-196.

241. Rossi DJ, Oshima T, Attwell D. Glutamate release in severe brain ischaemia is mainly by reversed uptake. *Nature*. 2000;403:316-321.

242. Strong AJ, Fabricius M, Boutelle MG, Hibbins SJ, Hopwood SE, Jones R, et al. Spreading and synchronous depressions of cortical activity in acutely injured human brain. *Stroke*. 2002;33:2738-2743.

243. Hartings JA, Strong AJ, Fabricius M, Manning A, Bhatia R, Dreier JP, et al. Spreading depolarizations and late secondary insults after traumatic brain injury. *J Neurotrauma*. 2009;26:1857-1866.

244. Henninger N, Heimann A, Kempski O. Electrophysiology and neuronal integrity following systemic arterial hypotension in a rat model of unilateral carotid artery occlusion. *Brain Res*. 2007;1163:119-129.

245. Somjen GG. Mechanisms of spreading depression and hypoxic spreading depression-like depolarization. *Physiol Rev*. 2001;81:1065-1096.

246. Maxwell WL, Domleo A, McColl G, Jafari SS, Graham DI. Post-acute alterations in the axonal cytoskeleton after traumatic axonal injury. *J Neurotrauma*. 2003;20:151-168.

247. Kelley BJ, Farkas O, Lifshitz J, Povlishock JT. Traumatic axonal injury in the perisomatic domain triggers ultrarapid secondary axotomy and Wallerian degeneration. *Exp Neurol*. 2006;198:350-360.

248. Faul F, Erdfelder E, Buchner A, Lang AG. Statistical power analyses using G*Power 3.1: tests for correlation and regression analyses. *Behav Res Methods*. 2009;41:1149-1160.

249. Faul F, Erdfelder E, Lang AG, Buchner A. G*Power 3: a flexible statistical power analysis program for the social, behavioral, and biomedical sciences. *Behav Res Methods*. 2007;39:175-191.

250. Lamprecht MR, Sabatini DM, Carpenter AE. CellProfiler: free, versatile software for automated biological image analysis. *Biotechniques*. 2007;42:71-75.

251. Provencher SW. Automatic quantitation of localized in vivo 1H spectra with LCModel. *NMR Biomed*. 2001;14:260-264.

252. Provencher SW. Estimation of metabolite concentrations from localized in vivo proton NMR spectra. *Magn Reson Med*. 1993;30:672-679.

253. Siman R, Toraskar N, Dang A, McNeil E, McGarvey M, Plaum J, et al. A panel of neuron-enriched proteins as markers for traumatic brain injury in humans. *J Neurotrauma*. 2009;26:1867-1877.

254. Gatson JW, Barillas J, Hynan LS, Diaz-Arrastia R, Wolf SE, Minei JP. Detection of neurofilament-H in serum as a diagnostic tool to predict injury severity in patients who have suffered mild traumatic brain injury. *J Neurosurg*. 2014;121:1232-1238.

255. McCrea M, Guskiewicz KM, Marshall SW, Barr W, Randolph C, Cantu RC, et al. Acute effects and recovery time following concussion in collegiate football players: the NCAA Concussion Study. *JAMA*. 2003;290:2556-2563.

256. Kirov, II, Tal A, Babb JS, Reaume J, Bushnik T, Ashman TA, et al. Proton MR spectroscopy correlates diffuse axonal abnormalities with post-concussive symptoms in mild traumatic brain injury. *J Neurotrauma*. 2013;30:1200-1204.

257. Duarte JM, Lei H, Mlynarik V, Gruetter R. The neurochemical profile quantified by in vivo 1H NMR spectroscopy. *Neuroimage*. 2012;61:342-362.

258. Harris JL, Yeh HW, Choi IY, Lee P, Berman NE, Swerdlow RH, et al. Altered neurochemical profile after traumatic brain injury: (1)H-MRS biomarkers of pathological mechanisms. *J Cereb Blood Flow Metab*. 2012;32:2122-2134.

259. Schuhmann MU, Stiller D, Skardelly M, Bernarding J, Klinge PM, Samii A, et al. Metabolic changes in the vicinity of brain contusions: a proton magnetic resonance spectroscopy and histology study. *J Neurotrauma*. 2003;20:725-743.

260. Gardner A, Iverson GL, Stanwell P. A systematic review of proton magnetic resonance spectroscopy findings in sport-related concussion. *J Neurotrauma*. 2014;31:1-18.

261. Gilley J, Coleman MP. Endogenous Nmnat2 is an essential survival factor for maintenance of healthy axons. *PLoS Biol*. 2010;8:e1000300.

262. O'Neill LA, Fitzgerald KA, Bowie AG. The Toll-IL-1 receptor adaptor family grows to five members. *Trends Immunol*. 2003;24:286-290.

263. Gerdts J, Summers DW, Sasaki Y, DiAntonio A, Milbrandt J. Sarm1-mediated axon degeneration requires both SAM and TIR interactions. *J Neurosci*. 2013;33:13569-13580.

264. Gerdts J, Brace EJ, Sasaki Y, DiAntonio A, Milbrandt J. Neurobiology. SARM1 activation triggers axon degeneration locally via NAD(+) destruction. *Science*. 2015;348:453-457.

265. Freeman MR. Signaling mechanisms regulating Wallerian degeneration. *Curr Opin Neurobiol*. 2014;27:224-231.

266. Chuang CF, Bargmann CI. A Toll-interleukin 1 repeat protein at the synapse specifies asymmetric odorant receptor expression via ASK1 MAPKKK signaling. *Genes Dev*. 2005;19:270-281.

267. Knoferle J, Koch JC, Ostendorf T, Michel U, Planchamp V, Vutova P, et al. Mechanisms of acute axonal degeneration in the optic nerve in vivo. *Proc Natl Acad Sci U S A*. 2010;107:6064-6069.

268. Yang J, Weimer RM, Kallop D, Olsen O, Wu Z, Renier N, et al. Regulation of axon degeneration after injury and in development by the endogenous calpain inhibitor calpastatin. *Neuron*. 2013;80:1175-1189.

269. Kilinc D, Gallo G, Barbee KA. Mechanical membrane injury induces axonal beading through localized activation of calpain. *Exp Neurol*. 2009;219:553-561.

270. Ma M, Ferguson TA, Schoch KM, Li J, Qian Y, Shofer FS, et al. Calpains mediate axonal cytoskeleton disintegration during Wallerian degeneration. *Neurobiol Dis*. 2013;56:34-46.

271. Penkowa M, Camats J, Giralt M, Molinero A, Hernandez J, Carrasco J, et al. Metallothionein-I overexpression alters brain inflammation and stimulates brain repair in transgenic mice with astrocyte-targeted interleukin-6 expression. *Glia*. 2003;42:287-306.

272. Walker PA, Harting MT, Jimenez F, Shah SK, Pati S, Dash PK, et al. Direct intrathecal implantation of mesenchymal stromal cells leads to enhanced neuroprotection via an NFkappaB-mediated increase in interleukin-6 production. *Stem Cells Dev*. 2010;19:867-876.

273. Longhi L, Gesuete R, Perego C, Ortolano F, Sacchi N, Villa P, et al. Long-lasting protection in brain trauma by endotoxin preconditioning. *J Cereb Blood Flow Metab*. 2011;31:1919-1929.

274. Philip S, Udomphorn Y, Kirkham FJ, Vavilala MS. Cerebrovascular pathophysiology in pediatric traumatic brain injury. *J Trauma*. 2009;67:S128-134.

275. Godzik K, Coleman MP. The axon-protective WLD(S) protein partially rescues mitochondrial respiration and glycolysis after axonal injury. *J Mol Neurosci*. 2015;55:865-871.

276. Yin TC, Britt JK, De Jesus-Cortes H, Lu Y, Genova RM, Khan MZ, et al. P7C3 neuroprotective chemicals block axonal degeneration and preserve function after traumatic brain injury. *Cell Rep*. 2014;8:1731-1740.

277. Brown MC, Perry VH, Hunt SP, Lapper SR. Further studies on motor and sensory nerve regeneration in mice with delayed Wallerian degeneration. *Eur J Neurosci*. 1994;6:420-428.

278. Martin SM, O'Brien GS, Portera-Cailliau C, Sagasti A. Wallerian degeneration of zebrafish trigeminal axons in the skin is required for regeneration and developmental pruning. *Development*. 2010;137:3985-3994.

279. Gowda NK, Agrawal D, Bal C, Chandrashekar N, Tripati M, Bandopadhyaya GP, et al. Technetium Tc-99m ethyl cysteinate dimer brain single-photon emission CT in mild traumatic brain injury: a prospective study. *AJNR Am J Neuroradiol*. 2006;27:447-451.

280. Wang Y, Nelson LD, LaRoche AA, Pfaller AY, Nencka AS, Koch KM, et al. Cerebral Blood Flow Alterations in Acute Sport-Related Concussion. *J Neurotrauma*. 2016;33:1227-1236.

281. Metting Z, Spikman JM, Rodiger LA, van der Naalt J. Cerebral perfusion and neuropsychological follow up in mild traumatic brain injury: acute versus chronic disturbances? *Brain Cogn*. 2014;86:24-31.

282. Audenaert K, Jansen HM, Otte A, Peremans K, Vervaet M, Crombez R, et al. Imaging of mild traumatic brain injury using 57Co and 99mTc HMPAO SPECT as compared to other diagnostic procedures. *Med Sci Monit*. 2003;9:MT112-117.

283. Lorberboym M, Lampl Y, Gerzon I, Sadeh M. Brain SPECT evaluation of amnestic ED patients after mild head trauma. *Am J Emerg Med*. 2002;20:310-313.

284. Villapol S, Byrnes KR, Symes AJ. Temporal dynamics of cerebral blood flow, cortical damage, apoptosis, astrocyte-vasculature interaction and astrogliosis in the pericontusional region after traumatic brain injury. *Front Neurol*. 2014;5:82.

285. Navarro JC, Pillai S, Cherian L, Garcia R, Grill RJ, Robertson CS. Histopathological and behavioral effects of immediate and delayed hemorrhagic shock after mild traumatic brain injury in rats. *J Neurotrauma*. 2012;29:322-334.

286. Namiranian K, Brink CD, Goodman JC, Robertson CS, Bryan RM, Jr. Traumatic brain injury in mice lacking the K channel, TREK-1. *J Cereb Blood Flow Metab*. 2011;31:e1-6.

287. Ozawa Y, Nakamura T, Sunami K, Kubota M, Ito C, Murai H, et al. Study of regional cerebral blood flow in experimental head injury: changes following cerebral contusion and during spreading depression. *Neurol Med Chir (Tokyo)*. 1991;31:685-690.

288. Garnett MR, Blamire AM, Rajagopalan B, Styles P, Cadoux-Hudson TA. Evidence for cellular damage in normal-appearing white matter correlates with injury severity in patients following traumatic brain injury: A magnetic resonance spectroscopy study. *Brain*. 2000;123 (Pt 7):1403-1409.

289. Garnett MR, Blamire AM, Corkill RG, Cadoux-Hudson TA, Rajagopalan B, Styles P. Early proton magnetic resonance spectroscopy in normal-appearing brain correlates with outcome in patients following traumatic brain injury. *Brain*. 2000;123 (Pt 10):2046-2054.

290. Tremblay S, De Beaumont L, Henry LC, Boulanger Y, Evans AC, Bourgouin P, et al. Sports concussions and aging: a neuroimaging investigation. *Cereb Cortex*. 2013;23:1159-1166.

291. Koerte IK, Lin AP, Muehlmann M, Merugumala S, Liao H, Starr T, et al. Altered Neurochemistry in Former Professional Soccer Players without a History of Concussion. *J Neurotrauma*. 2015;32:1287-1293.

292. Poole VN, Abbas K, Shenk TE, Breedlove EL, Breedlove KM, Robinson ME, et al. MR spectroscopic evidence of brain injury in the non-diagnosed collision sport athlete. *Dev Neuropsychol*. 2014;39:459-473.

293. Maudsley AA, Govind V, Levin B, Saigal G, Harris L, Sheriff S. Distributions of Magnetic Resonance Diffusion and Spectroscopy Measures with Traumatic Brain Injury. *J Neurotrauma*. 2015;32:1056-1063.

294. Kochanek PM, Bramlett H, Dietrich WD, Dixon CE, Hayes RL, Povlishock J, et al. A novel multicenter preclinical drug screening and biomarker consortium for

experimental traumatic brain injury: operation brain trauma therapy. *J Trauma*. 2011;71:S15-24.

295. Kochanek PM, Bramlett HM, Shear DA, Dixon CE, Mondello S, Dietrich WD, et al. Synthesis of Findings, Current Investigations, and Future Directions: Operation Brain Trauma Therapy. *J Neurotrauma*. 2016;33:606-614.

296. Dixon CE, Bramlett HM, Dietrich WD, Shear DA, Yan HQ, Deng-Bryant Y, et al. Cyclosporine Treatment in Traumatic Brain Injury: Operation Brain Trauma Therapy. *J Neurotrauma*. 2016;33:553-566.

297. Piilgaard H, Witgen BM, Rasmussen P, Lauritzen M. Cyclosporine A, FK506, and NIM811 ameliorate prolonged CBF reduction and impaired neurovascular coupling after cortical spreading depression. *J Cereb Blood Flow Metab*. 2011;31:1588-1598.

298. Meehan WP, 3rd, Mannix R, Monuteaux MC, Stein CJ, Bachur RG. Early symptom burden predicts recovery after sport-related concussion. *Neurology*. 2014;83:2204-2210.

299. McCrory P, Meeuwisse W, Johnston K, Dvorak J, Aubry M, Molloy M, et al. Consensus Statement on Concussion in Sport: the 3rd International Conference on Concussion in Sport held in Zurich, November 2008. *Br J Sports Med*. 2009;43 Suppl 1:i76-90.

300. Russell MB, Olesen J. A nosographic analysis of the migraine aura in a general population. *Brain*. 1996;119 (Pt 2):355-361.

301. Saver JL, Starkman S, Eckstein M, Stratton SJ, Pratt FD, Hamilton S, et al. Prehospital use of magnesium sulfate as neuroprotection in acute stroke. *N Engl J Med*. 2015;372:528-536.

302. van der Hel WS, van den Bergh WM, Nicolay K, Tulleken KA, Dijkhuizen RM. Suppression of cortical spreading depressions after magnesium treatment in the rat. *Neuroreport*. 1998;9:2179-2182.

303. Hall RC, Hall RC, Chapman MJ. Definition, diagnosis, and forensic implications of postconcussional syndrome. *Psychosomatics*. 2005;46:195-202.

304. Sterr A, Herron KA, Hayward C, Montaldi D. Are mild head injuries as mild as we think? Neurobehavioral concomitants of chronic post-concussion syndrome. *BMC Neurol*. 2006;6:7.

305. Carroll LJ, Cassidy JD, Cancelliere C, Cote P, Hincapie CA, Kristman VL, et al. Systematic review of the prognosis after mild traumatic brain injury in adults: cognitive, psychiatric, and mortality outcomes: results of the International Collaboration on Mild Traumatic Brain Injury Prognosis. *Arch Phys Med Rehabil*. 2014;95:S152-173.

306. Ponsford J, Cameron P, Fitzgerald M, Grant M, Mikocka-Walus A. Long-term outcomes after uncomplicated mild traumatic brain injury: a comparison with trauma controls. *J Neurotrauma*. 2011;28:937-946.

307. Meares S, Shores EA, Taylor AJ, Batchelor J, Bryant RA, Baguley IJ, et al. The prospective course of postconcussion syndrome: the role of mild traumatic brain injury. *Neuropsychology*. 2011;25:454-465.

308. Shahim P, Tegner Y, Wilson DH, Randall J, Skillback T, Pazooki D, et al. Blood biomarkers for brain injury in concussed professional ice hockey players. *JAMA Neurol*. 2014;71:684-692.

309. Medana IM, Esiri MM. Axonal damage: a key predictor of outcome in human CNS diseases. *Brain*. 2003;126:515-530.

310. Hellyer PJ, Leech R, Ham TE, Bonnelle V, Sharp DJ. Individual prediction of white matter injury following traumatic brain injury. *Ann Neurol*. 2013;73:489-499.

311. Zetterberg H, Hietala MA, Jonsson M, Andreasen N, Styrud E, Karlsson I, et al. Neurochemical aftermath of amateur boxing. *Arch Neurol*. 2006;63:1277-1280.

312. Neselius S, Zetterberg H, Blennow K, Marcusson J, Brisby H. Increased CSF levels of phosphorylated neurofilament heavy protein following bout in amateur boxers. *PLoS One*. 2013;8:e81249.

313. Gyorgy A, Ling G, Wingo D, Walker J, Tong L, Parks S, et al. Time-dependent changes in serum biomarker levels after blast traumatic brain injury. *J Neurotrauma*. 2011;28:1121-1126.

314. Panneerselvam P, Singh LP, Ho B, Chen J, Ding JL. Targeting of pro-apoptotic TLR adaptor SARM to mitochondria: definition of the critical region and residues in the signal sequence. *Biochem J*. 2012;442:263-271.

315. O'Neill LA, Bowie AG. The family of five: TIR-domain-containing adaptors in Toll-like receptor signalling. *Nat Rev Immunol*. 2007;7:353-364.

316. Mukherjee P, Woods TA, Moore RA, Peterson KE. Activation of the innate signaling molecule MAVS by bunyavirus infection upregulates the adaptor protein SARM1, leading to neuronal death. *Immunity*. 2013;38:705-716.

317. Yang J, Wu Z, Renier N, Simon DJ, Uryu K, Park DS, et al. Pathological axonal death through a MAPK cascade that triggers a local energy deficit. *Cell*. 2015;160:161-176.

318. Qiao F, Bowie JU. The many faces of SAM. *Sci STKE*. 2005;2005:re7.

319. Wang J, Zhai Q, Chen Y, Lin E, Gu W, McBurney MW, et al. A local mechanism mediates NAD-dependent protection of axon degeneration. *J Cell Biol*. 2005;170:349-355.

320. Goldner R, Yaron A. TIR Axons Apart: Unpredicted NADase Controls Axonal Degeneration. *Neuron*. 2017;93:1239-1241.

321. Essuman K, Summers DW, Sasaki Y, Mao X, DiAntonio A, Milbrandt J. The SARM1 Toll/Interleukin-1 Receptor Domain Possesses Intrinsic NAD+ Cleavage Activity that Promotes Pathological Axonal Degeneration. *Neuron*. 2017;93:1334-1343 e1335.

322. Yan T, Feng Y, Zheng J, Ge X, Zhang Y, Wu D, et al. Nmnat2 delays axon degeneration in superior cervical ganglia dependent on its NAD synthesis activity. *Neurochem Int*. 2010;56:101-106.

323. Gilley J, Orsomando G, Nascimento-Ferreira I, Coleman MP. Absence of SARM1 rescues development and survival of NMNAT2-deficient axons. *Cell Rep*. 2015;10:1974-1981.

324. Sasaki Y, Nakagawa T, Mao X, DiAntonio A, Milbrandt J. NMNAT1 inhibits axon degeneration via blockade of SARM1-mediated NAD+ depletion. *Elife*. 2016;5

325. Miller BR, Press C, Daniels RW, Sasaki Y, Milbrandt J, DiAntonio A. A dual leucine kinase-dependent axon self-destruction program promotes Wallerian degeneration. *Nat Neurosci*. 2009;12:387-389.

326. Walker LJ, Summers DW, Sasaki Y, Brace EJ, Milbrandt J, DiAntonio A. MAPK signaling promotes axonal degeneration by speeding the turnover of the axonal maintenance factor NMNAT2. *Elife*. 2017;6

327. Kou Z, Vandevord PJ. Traumatic white matter injury and glial activation: From basic science to clinics. *Glia*. 2014

328. Szretter KJ, Samuel MA, Gilfillan S, Fuchs A, Colonna M, Diamond MS. The immune adaptor molecule SARM modulates tumor necrosis factor alpha production and microglia activation in the brainstem and restricts West Nile Virus pathogenesis. *J Virol*. 2009;83:9329-9338.

329. Parkhurst CN, Yang G, Ninan I, Savas JN, Yates JR, 3rd, Lafaille JJ, et al. Microglia promote learning-dependent synapse formation through brain-derived neurotrophic factor. *Cell*. 2013;155:1596-1609.

330. Doerflinger NH, Macklin WB, Popko B. Inducible site-specific recombination in myelinating cells. *Genesis*. 2003;35:63-72.

331. Ganat YM, Silbereis J, Cave C, Ngu H, Anderson GM, Ohkubo Y, et al. Early postnatal astroglial cells produce multilineage precursors and neural stem cells in vivo. *J Neurosci*. 2006;26:8609-8621.

332. Madisen L, Zwingman TA, Sunkin SM, Oh SW, Zariwala HA, Gu H, et al. A robust and high-throughput Cre reporting and characterization system for the whole mouse brain. *Nat Neurosci*. 2010;13:133-140.

333. Popp MW, Maquat LE. Organizing principles of mammalian nonsense-mediated mRNA decay. *Annu Rev Genet*. 2013;47:139-165.

334. Requardt RP, Kaczmarczyk L, Dublin P, Wallraff-Beck A, Mikeska T, Degen J, et al. Quality control of astrocyte-directed Cre transgenic mice: the benefits of a direct link between loss of gene expression and reporter activation. *Glia*. 2009;57:680-692.

335. Muzumdar MD, Tasic B, Miyamichi K, Li L, Luo L. A global double-fluorescent Cre reporter mouse. *Genesis*. 2007;45:593-605.

336. Lin CW, Liu HY, Chen CY, Hsueh YP. Neuronally-expressed Sarm1 regulates expression of inflammatory and antiviral cytokines in brains. *Innate Immun*. 2013

337. Feil S, Valtcheva N, Feil R. Inducible Cre mice. *Methods Mol Biol*. 2009;530:343-363.

338. Fricker FR, Antunes-Martins A, Galino J, Paramsothy R, La Russa F, Perkins J, et al. Axonal neuregulin 1 is a rate limiting but not essential factor for nerve remyelination. *Brain*. 2013;136:2279-2297.

339. Yang G, Chen L, Grant GR, Paschos G, Song WL, Musiek ES, et al. Timing of expression of the core clock gene Bmal1 influences its effects on aging and survival. *Sci Transl Med*. 2016;8:324ra316.

340. Monvoisin A, Alva JA, Hofmann JJ, Zovein AC, Lane TF, Iruela-Arispe ML. VE-cadherin-CreERT2 transgenic mouse: a model for inducible recombination in the endothelium. *Dev Dyn*. 2006;235:3413-3422.

341. Ma M, Li L, Wang X, Bull DL, Shofer FS, Meaney DF, et al. Short-duration treatment with the calpain inhibitor MDL-28170 does not protect axonal transport in an in vivo model of traumatic axonal injury. *J Neurotrauma*. 2012;29:445-451.

342. Reeves TM, Phillips LL, Povlishock JT. Myelinated and unmyelinated axons of the corpus callosum differ in vulnerability and functional recovery following traumatic brain injury. *Exp Neurol*. 2005;196:126-137.

343. Baker AJ, Phan N, Moulton RJ, Fehlings MG, Yucel Y, Zhao M, et al. Attenuation of the electrophysiological function of the corpus callosum after fluid percussion injury in the rat. *J Neurotrauma*. 2002;19:587-599.

344. Crawford DK, Mangiardi M, Tiwari-Woodruff SK. Assaying the functional effects of demyelination and remyelination: revisiting field potential recordings. *J Neurosci Methods*. 2009;182:25-33.

345. van den Heuvel MP, Hulshoff Pol HE. Exploring the brain network: a review on resting-state fMRI functional connectivity. *Eur Neuropsychopharmacol*. 2010;20:519-534.

346. Heffernan ME, Huang W, Sicard KM, Bratane BT, Sikoglu EM, Zhang N, et al. Multi-modal approach for investigating brain and behavior changes in an animal model of traumatic brain injury. *J Neurotrauma*. 2013;30:1007-1012.

347. White BR, Bauer AQ, Snyder AZ, Schlaggar BL, Lee JM, Culver JP. Imaging of functional connectivity in the mouse brain. *PLoS One*. 2011;6:e16322.

348. Bauer AQ, Kraft AW, Wright PW, Snyder AZ, Lee JM, Culver JP. Optical imaging of disrupted functional connectivity following ischemic stroke in mice. *Neuroimage*. 2014;99:388-401.

349. Bero AW, Bauer AQ, Stewart FR, White BR, Cirrito JR, Raichle ME, et al. Bidirectional relationship between functional connectivity and amyloid-beta deposition in mouse brain. *J Neurosci*. 2012;32:4334-4340.

350. Critchley M. Medical aspects of boxing, particularly from a neurological standpoint. *Br Med J*. 1957;1:357-362.

351. Martland HS. Punch drunk. *JAMA*. 1928;91:1103–1107.

352. Millspaugh JA. Dementia pugilistica. *U S Nav Med Bull*. 1937;35:297–303.

353. Parker HL. Traumatic Encephalopathy (`Punch Drunk') of Professional Pugilists. *J Neurol Psychopathol*. 1934;15:20-28.

354. Gavett BE, Stern RA, McKee AC. Chronic traumatic encephalopathy: a potential late effect of sport-related concussive and subconcussive head trauma. *Clin Sports Med*. 2011;30:179-188, xi.

355. McKee AC, Cantu RC, Nowinski CJ, Hedley-Whyte ET, Gavett BE, Budson AE, et al. Chronic traumatic encephalopathy in athletes: progressive tauopathy after repetitive head injury. *J Neuropathol Exp Neurol*. 2009;68:709-735.

356. Goldman SM, Tanner CM, Oakes D, Bhudhikanok GS, Gupta A, Langston JW. Head injury and Parkinson's disease risk in twins. *Ann Neurol*. 2006;60:65-72.

357. May S, Martin G, Wellington C. Brain injury and dementia: Is there a connection? *Journal of Neurology and Neuroscience*. 2011;2:1-7.

358. Smith DH, Johnson VE, Stewart W. Chronic neuropathologies of single and repetitive TBI: substrates of dementia? *Nat Rev Neurol*. 2013;9:211-221.

359. Petraglia AL, Plog BA, Dayawansa S, Chen M, Dashnaw ML, Czerniecka K, et al. The spectrum of neurobehavioral sequelae after repetitive mild traumatic brain

injury: a novel mouse model of chronic traumatic encephalopathy. *J Neurotrauma*. 2014;31:1211-1224.

360. Ivarsson J, Viano DC, Lovsund P, Aldman B. Strain relief from the cerebral ventricles during head impact: experimental studies on natural protection of the brain. *J Biomech*. 2000;33:181-189.

361. Szczyrba I, Burtscher M. (2003). On the role of ventricles in diffuse axonal injuries. 2003 Summer Bioengineering Conference. 147-148.

362. Tu TW, Lescher JD, Williams RA, Jikaria N, Turtzo LC, Frank JA. Abnormal Injury Response in Spontaneous Mild Ventriculomegaly Wistar Rat Brains: A Pathological Correlation Study of Diffusion Tensor and Magnetization Transfer Imaging in Mild Traumatic Brain Injury. *J Neurotrauma*. 2017;34:248-256.